SPATIOTEMPORAL PARTITIONING OF MAMMALIAN MESOPREDATORS IN RESPONSE TO URBANIZATION AND DROUGHT IN CALIFORNIA'S CENTRAL VALLEY

By

Chad Weston Moura

A Thesis Presented to

The Faculty of Humboldt State University

In Partial Fulfillment of the Requirements for the Degree

Master of Science in Natural Resources: Wildlife

Committee Membership

Dr. Barbara A. Clucas, Committee Chair

Dr. Angela D. Baker, Committee Member

Dr. Brett J. Furnas, Committee Member

Dr. Daniel C. Barton, Committee Member

Dr. Erin Kelly, Graduate Coordinator

December 2020

ABSTRACT

SPATIOTEMPORAL PARTITIONING OF MAMMALIAN MESOPREDATORS IN RESPONSE TO URBANIZATION AND DROUGHT IN CALIFORNIA'S CENTRAL VALLEY

Chad Weston Moura

Mammalian mesopredators commonly associated with human dominated landscapes often exhibit generalist diets, behavioral plasticity, and relatively high reproductive rates. Because of this wide range of adaptive traits, ecologists have been speculative of what conditions may drive species to change their activity and behavior to avoid or mitigate against resource competition, intraguild predation, and human disturbance. I investigated a community of common mesopredators within the Sacramento Metropolitan Area of California's Central Valley to address whether species are spatially and/or temporally partitioning due to a defacto apex predator, coyotes (*Canis latrans*), and humans alongside large landscape altering disturbances: urbanization and drought. I used single species occupancy models and temporal overlap analyses to evaluate raccoon (*Procyon lotor*), opossum (*Didelphis virginiana*), striped skunk (*Mephitis mephitis*), domestic cat (*Felis catus*), and coyote spatiotemporal activity following drought and recovery across 2016, 2017, and 2019 as well as their response to varying scales of urban intensity post drought. Coyote activity was more diurnal and varied during the drought, with coyotes overlapping with nocturnal mesopredators near water sources following drought recovery. Coyotes and skunks avoided humans and

increased temporal overlap post drought. Opossums and raccoons were associated to wetlands during the drought but were the most wide-ranging species across urban intensities. Cats were the most urban tolerant, while coyotes were least urban tolerant. My results suggest mesopredators avoid humans across urban intensities while still benefiting from urban resources. Coyotes may influence mesopredators primarily in non-urban areas, while drought and urban residences may lessen mesopredator fear of intraguild predation.

ACKNOWLEDGEMENTS

I would like to thank California Department of Fish and Wildlife for funding and providing support for this project. Special thanks to Misty Nelson for providing me with contacts and support for resurveying and finding new camera sites. I am especially appreciative of the field technicians and team members who sorted and collected thousands of photos, and who left me the necessary breadcrumbs to reestablish my survey sites. Thank you to the many agencies, trusts, managers, and staff who supported me and let me put cameras out on in the working lands that they manage and love, including Brannan Island State Recreation Area, California Department of Water Resources, Citrona Farms, City of Sacramento Department of Parks and Recreation, City of West Sacramento, Cordova Recreation and Parks District, Cosumnes River Preserve, Effie Yeaw Nature Center, Grizzly Island Wildlife Area, Jim and Sally Barrett, Lockeford Plant Materials Center, Sacramento Bypass Wildlife Area, Sacramento County Parks Department, Sacramento Valley Conservancy, San Joaquin County Parks Department, Stone Lakes National Wildlife Refuge, Sutter National Wildlife Refuge, The Nature Conservancy, University of California Cooperative Extensions, University of California Davis, White Slough Wildlife Area, Yolo Bypass Wildlife Area, and Yolo Land Trust. Thank you to Harry McQuillen of Cosumnes River Preserve for letting me stay on site in my home away from home on the Preserve during my field season. Thank you to all of the Acampo, Carmichael Davis, Elk Grove, Fair Oaks, Galt, Knights Landing, Oakley, Rancho Cordova, Rocklin, Sacramento, Winters, and Woodland

wildlife loving residents who let a stranger with a camera into your yards, as you all have been instrumental to this project becoming a reality.

I would like to thank my committee members Dr. Brett Furnas and Dr. Ange Baker for supporting me logistically in and around Sacramento as well as for their invaluable advice on statistical analysis and study design. Thank you to my committee member Dr. Dan Barton for teaching me the foundational knowledge of occupancy models both in class and over a drink at Rita's. Thank you to my field technicians Anjelica Yee, Sara Moriarty-Graves, and Trevor McDowell for assisting me in placing out and collecting cameras, and the hours you spent in the heat prying scorching T-posts from the concrete-like soil of the Valley, as well as the hours you spent looking over thousands of photos of grass waving in the wind. Thank you to the founding matriarchs of the Clucas lab, Trinity Smith and Molly Parren, whose work, laughter, and willingness to let a "Chad" become their friend and colleague helped me infinitely. Thank you also to my current labmates, Leigh Douglas, whose insight and passion is a guiding light, Travis Farwell, whose wit and candor and love of smoked meats is a treasure, Sydney McCluskey, whose kindness and spirit are unbreaking, and Janelle Chojnaki, whose determination is inspiring. I would also like to thank the whole body of Wildlife, Fisheries, and Biology graduate students I have come to know and befriend, your work and drive for change from the status quo inspires and comforts me daily.

I especially want to thank my amazing advisor, committee lead, mentor, and friend Barbara Clucas for her willingness to take me on as a graduate student and the generous support and advice she has given to me throughout this whole process. You

have made this journey through grad school such a rewarding and fun experience, your insight and passion for teaching and mentoring is a treat for everyone who has the honor of taking one of your classes or getting to know you. I am beyond lucky to have gotten to be your student and part of your lab, and you have made my experience here at Humboldt one that I will cherish and love forever.

Thank you to my friends and family who have been a major support in keeping me sane throughout my work and life. I would not be here if not for my mom and dad, Michele Moura and Eduardo Moura, who both cultivated my love for nature and the outdoors in the heart of the Silicon Valley. Thank you to my sister, Anethra Rhodes for always checking in on me and making sure I am supported and loved. To my nieces Dusty and Zoe, I hope I will inspire you both to love the parks and creek trails I grew up in and you are growing up in now. Thank you to my brother Anthony Moura for lending an ear whenever I try to talk about weird animal facts. Thank you to my Santa Barbara, Humboldt, and Bay Area friends for your laughter and wit and willingness to always pick up and play a game or watch a terrible movie with me. Thank you to my friend Chan Fin Saeteurn for always being willing to help me with a wildlife project, and for your late-night musings on the world.

And finally, to my fiancée and the love of my life, Ximena Gil, I am so lucky to have met you and so grateful for everything you do daily to make our lives the best they can be. I wouldn't have been able to survive through a pandemic and quarantine without driving anyone else absolutely insane, so thank you for putting up with all of my weirdness, singing, and late hours working on this thesis. I love you, mi bonbon.

TABLE OF CONTENTS

LIST OF TABLES

LIST OF FIGURES

LIST OF APPENDICES

GENERAL INTRODUCTION

Anthropogenic land-use and climate change are two of the most prominent contributors to global biodiversity loss and ecosystem function, especially in terrestrial environments (Sala et al. 2000, Pereira et al. 2004, Smith and Zollner 2005, Mawdsley et al. 2009). The interaction of these two large scale environmental transformations may drive plant and animal populations to expand or contract in abundance and range, leading to modified species assemblages across ecosystems and potentially novel species interactions (Traill et al. 2010, Thorne et al. 2012, Ancillotto et al. 2016, Kowarik and Lippe 2018). Range restricted specialist species may suffer the most from increasing climatic and human disturbance (Schneider et al. 2002, Travis 2003, Clavel et al. 2011), while generalist mid-trophic level mammals, or mesopredators, are one group that may benefit from a changing world (Prugh et al. 2009). In fact, many mammalian mesopredators are expanding their ranges as climates become warmer and are exploiting more widely available anthropogenic food sources as human development increases (Lewis et al. 1999, Gompper 2002, Larivière 2004, Beatty et al. 2013). However, as climate instability and anthropogenic land-use increase, expanding populations of mammalian mesopredators may come into more conflict with each other as they colonize previously occupied niches (Ritchie and Johnson 2009, Schuette et al. 2013, Terborgh and Estes 2013). Thus, conflict between sympatric mesopredators may be a result of negative interactions such as resource competition (Durant 1998, Shamoon et al. 2017, Smith et al. 2018) and intraguild predation (Kitchen et al. 1999, Fedriani et al. 2000,

Magle et al. 2014). These negative interspecies interactions are often the most severe when resource availability and biodiversity is low (Holt and Huxel 2007, Prugh et al., 2009, Terborgh and Estes 2013) and external risk factors such as human disturbance and climatic extremes are present (Brawata and Neeman 2011, Beatty et al. 2013). Understanding how mesopredators change and respond to one another in the face of increasing climatic and anthropogenic disturbances may be key to understanding the form and function of future ecosystems.

One way mesopredators mitigate negative species interactions is through resource partitioning. Resource partitioning, or the division of shared food and habitat resources, can occur both spatially and temporally. This allows mesopredators to differentially exploit resources, such as prey species (Rosenzweig 1966, Terborgh and Estes 2013, Smith et al. 2018), anthropogenic food sources (Theimer et al. 2015), foraging sites (Durant 1998), watering holes (Brawata and Neeman 2011), refugia from predation (Lesmeister et al. 2015), and terrain (Kozlowski et al. 2008). The strength of spatiotemporal partitioning depends upon mesopredator response to habitat features, seasonality, intensity of external disturbances, and heterogeneity in individual response (Wang et al. 2015). Generally, spatiotemporal partitioning is most often observed when there is a dominant (usually apex) predator that imposes a high risk of intraguild predation or interference competition on a subordinate mesopredator in a low productivity environment (Johnson and Franklin 1994, Holt and Huxel 2007).

In North America, where many traditional apex predators have been locally extirpated, the coyote (*Canis latrans*) is often reported to be a major contributor to

interference competition and intraguild predation or intimidation (Gompper 2002). While coyotes may induce spatial and temporal partitioning in canids like foxes (Kitchen et al. 1999, Gehring and Swihart 2003, Atwood et al. 2011, Lesmeister et al. 2015), increased anthropogenic stress from urbanization may facilitate coexistence (Mueller et al. 2018). Additionally, coyote dominance over non-canid mesopredators has come into question. For instance, there is evidence that raccoons may not spatially or temporally avoid coyotes in human dominated landscapes; however, raccoons may be negatively influenced by coyote presence at water sites during the drought (Gehrt and Clark 2003, Gehrt and Prange 2007, Parren 2019). Thus, while the importance of mesopredator species interactions can depend on the species and habitat features present on the landscape, external disturbance factors can play an equally important role in either strengthening or weakening these influences.

I investigated two subsets of these disturbance types - drought and urbanization – in the mammalian mesopredator communities of California's Central Valley. Specifically, I addressed how the intensity of drought and urbanization may influence spatiotemporal partitioning of mesopredators at multiple spatial and temporal scales. I examined mammalian mesopredator responses across two chapters: the first evaluating the impacts of drought and the second evaluating the impacts of urbanization.

CHAPTER 1: SPATIOTEMPORAL RESPONSES OF MAMMALIAN MESOPREDATORS TO DROUGHT AND SUBSEQUENT RECOVERY IN CALIFORNIA'S CENTRAL VALLEY

Abstract

During 2012–2016, California was afflicted with an extensive and severe statewide drought. In response to this drought in 2016, California's Department of Fish and Wildlife's (CDFW) Terrestrial Species Stressor Monitoring program (TSM) sought to determine baseline vertebrate distributions in the Central Valley. The TSM surveys ran for two years; however, between 2016 and 2017, record winter rainfall returned to California, bringing much of the state out of drought. I analyzed 45 TSM camera sites to assess changes in mammalian mesopredator spatiotemporal activity patterns during 2016 (drought), 2017 (drought recovery) and 2019 as a post-drought year. I hypothesized that during the drought, mesopredators would take risks to find adequate resources, thus increasing their activity overlap and potential for conflict between a potential intraguild predator (coyotes, *Canis latrans*) and humans. I used multi-season single species occupancy models and temporal overlap analyses to predict spatial and temporal overlap across three study years for four wild mesopredator species including coyotes and one domestic mesopredator. Mesopredator detection and occupancy were most influenced by wetland and riparian habitats and drought year regardless of water availability. Wild mesopredator spatial and temporal overlap as well as avoidance of humans increased

following drought recovery. My results suggest drought impacts mesopredator activity, yet mesopredators are able to quickly recover and adapt to post drought conditions. Further, drought may reduce the influence of coyote and human presence on mesopredator activity. More work is needed to understand the influence drought has on specific behaviors and microhabitat movements of mesopredators.

Introduction

Prolonged periods of drought are predicted to increase around the world due to anthropogenic climate change (Dai 2013). Rising temperatures and drier climatic conditions can have cumulative increases in evapotranspiration rates as well as drying out soils in the plains, deserts, and valleys of the western United States, transforming plant and animal communities in the process (Cook et al. 2015). Regionally, California's drought sensitive landscapes are a prime model for studying wildlife community dynamics in the face of climate change (Griffin and Anchukaitis 2014, Swain 2015). The effects of these stressors can have community wide impacts on wildlife range expansions and collapses, changing species interactions as they move in response to climatic shifts (Walther et al. 2002).

During 2012 through 2016, California experienced an exceptionally severe drought not seen in the last 1,200 years, with evidence that drought severity and length were exacerbated by anthropogenic warming (Griffin and Anchukaitis 2014, Williams et al. 2015). Increases in temperatures during drought conditions have been shown to induce tree mortality in forests (Adams et al. 2009, Asner et al. 2016) and vegetation die-offs in

grassland and shrublands leading to declines in plant and animal communities at all trophic levels (Prugh et al. 2018). While the effects of increased global warming have been investigated for small mammals and birds throughout California using historical data to detect changes in occupancy and local extinction, little is known about the effects climate change and drought have on common mammalian mesopredator communities (Moritz et al. 2008, Iknayan and Beissinger 2018, MacLean et al. 2018).

While species with small geographic ranges may experience range collapses and local extinctions (e.g., small mammals in desert and high elevation areas, Brown et al. 1997, Moritz et al. 2008), mammalian mesopredators may have more flexible responses to climate change due to their dispersal abilities and widespread habitat use (Schloss et al. 2012). For instance, as once dominant prey items become rare due to drought, mesopredators might be able to acquire more varied food sources to sustain themselves (Catling 1988). However, climatic shifts may be driving sympatric mesopredators to increase competition and intraguild predation due to scarcity of shared resources, which can negatively impact the overall fitness of already stressed species (Tylianakis et al. 2008).

More severe droughts may force mesopredator into spending more energy searching for scarce food and water resources, which may in turn shift mesopredator activity and community composition. Increased temperatures and dwindling rodent populations in agricultural areas may impact scavenging mesopredators that rely on rodent carcasses and carrion, potentially decreasing foraging activity ranges and increasing competition (Pereira 2010, DeVault et al. 2011, Olson et al. 2012). If dominant

intraguild predators are negatively impacted as a result of lower prey species populations during drought conditions, they may lose their competitive edge over subordinate species with more varied diets (Carroll 2007). Droughts and increased temperatures may also cause mesopredators to expand their ranges into areas with more water availability, or less extreme temperatures, increasing the potential for competitive interactions and predation (Brawata and Neeman 2011, Schuette et al. 2013). Mesopredators that are able to expand their ranges as a result of climate change may also be more attracted to areas with widely available anthropogenic resources, which may influence competitive advantages for more disturbance tolerant species (Larivière 2004, Jannett et al. 2007). Additionally, mammals with obligate nocturnal or diurnal behavior may be at risk of population extirpation and range contraction as the effects of climate change intensify (McCain and King 2014). Therefore, drought may impact mesopredator species differently depending on their ability to spatiotemporal partition or mitigate against a variety of complex environmental and biotic interactions. Investigating how California's mesopredator communities are responding to drought and subsequent recovery in human dominated landscapes can elucidate patterns of shifting community interactions, and their potential impacts on mesopredator community composition and resilience.

In 2014, California was declared as being in a state of emergency due to exceptional and severe drought conditions statewide. In response, the California Department of Fish and Wildlife (CDFW) created the Terrestrial Species Stressor Monitoring (TSM) project to collect baseline species data for two of California's most drought sensitive ecoregions, the Great Valley (hereafter: Central Valley) and Mojave

Desert (Rich et al. 2018). While TSM was originally designed to monitor species abundance and activity during the drought for two years (2016 and 2017), winter rains between 2016 and 2017 slowly brought much of the state out of the extreme drought conditions (Lund et al. 2018). As a result of this change in climatic conditions, TSM was able to capture mesopredator responses to drought (2016) and drought recovery (2017) conditions. The analysis of the spatial distribution and co-occurrence of mesopredators in both ecoregions during and following the drought suggest that coyotes (which represent a de-facto apex predator in the Central Valley) and human disturbance may be important drivers of species habitat use and coexistence; however, further investigation into how humans and coyotes effect the spatiotemporal activity of mesopredators during and following drought may inform future trends in community composition and resilience (Parren 2019).

To address the influence of drought on the spatial and temporal activity of mesopredators, I compared camera trap data from sites across California's Central Valley from 2016 and 2017 (drought and immediately post drought) to data from sites I resurveyed in 2019 (post-drought). In addition, I also examined how human and coyote presence influenced mesopredators during and following this historic drought. I investigated the spatiotemporal activity of a defacto apex predator, coyotes, and four mammalian mesopredator species, raccoon (*Procyon lotor*), opossum (*Didelphis virginiana*), striped skunk (*Mephitis mephitis*), and domestic cat (*Felis catus*), across the three years: 2016 (drought), 2017 (recovery), and 2019 (post-drought). I hypothesized that during the drought mesopredators would take increased risks to find adequate

resources. Thus, I predicted that mesopredators would have greater spatiotemporal overlap with humans and coyotes during the drought (2016), with declines in overlap starting immediately post-drought (2017) and becoming most apparent two years post-drought (2019).

Methods

Study Area

My 2019 study and the previous 2016-2017 California Department of Fish and Wildlife's Terrestrial Species Stressor (TSM) study were conducted in the Great Valley ecoregion (Central Valley) in California. While the TSM study spanned the entire Central Valley, I focused my main survey efforts around the south Sacramento Valley and Sacramento Metropolitan Area (SMA) with the perimeter of the survey area extending from Stockton in the south to the southern edge of Yuba City to the north and from Citrus Heights in the east stretching to Fairfield in the west (Figure 1).

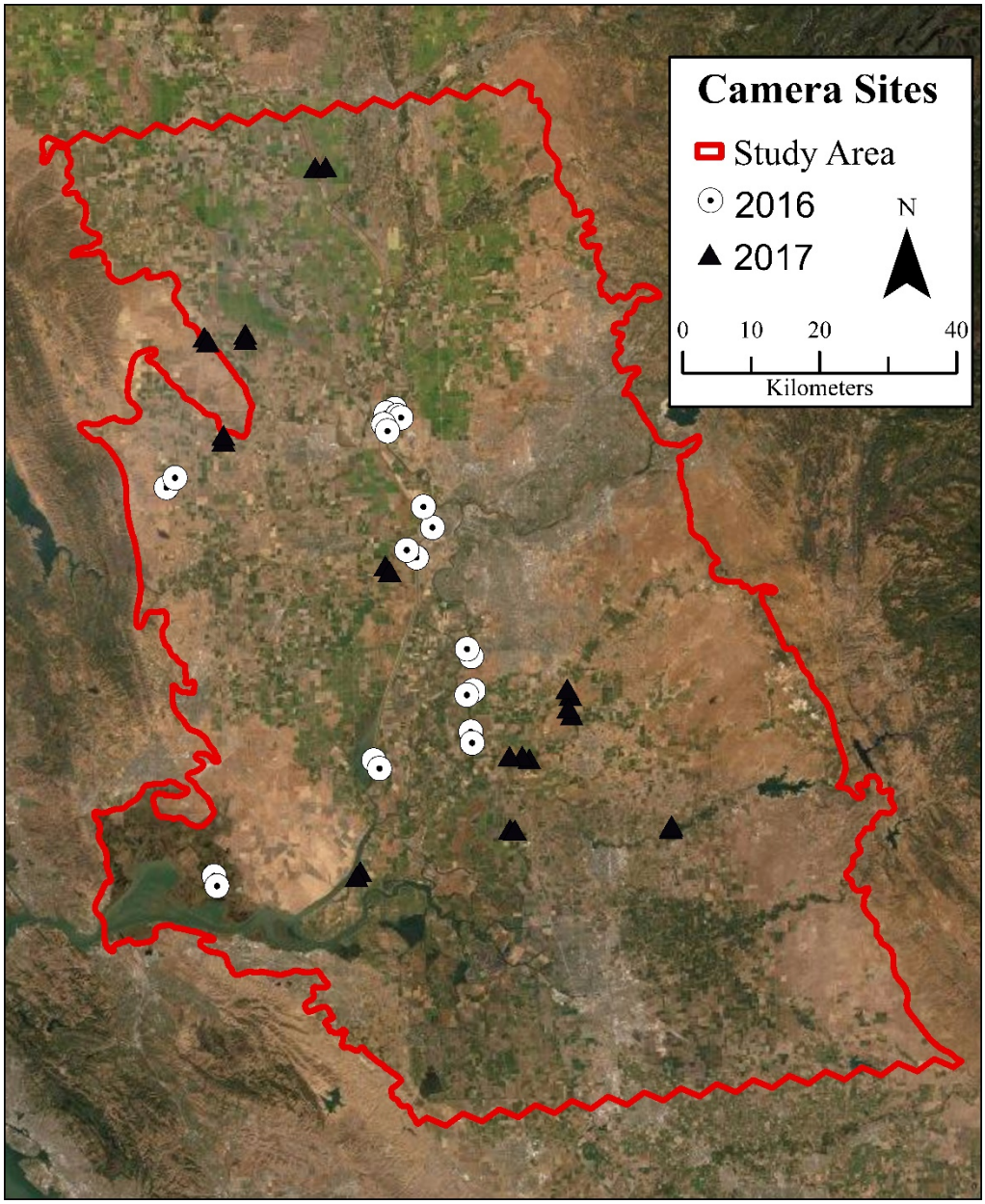

Figure 1. Terrestrial Species Stressor Monitoring (TSM) sites for 2016 (white circles) and 2017 (black triangles). Study area (red outline) is based on a 20 x 20 USDA Forest Inventory and Analysis Program Hexagon grid for the Central Valley based around the

Sacramento Metropolitan Area. All camera sites are independent by initial survey year (2016/2017) and were resurveyed in 2019.

California's Central Valley covers more than 48,909 km^2 of area in the middle of California, stretching from the Sierra Nevada Mountains to the east and the Coastal Ranges to the west (McNab et al. 2007). The Central Valley ecoregion is characterized by its flat and expansive mosaic of agriculture in the form of expansive orchards, row crops, vineyards, ranching, and many roads that facilitate the transportation and distribution of these products to both local and global cities (Soulard and Wilson 2015). A majority of the Central Valley is privately owned and operated while the remnant protected riparian and wetland habitats are mostly on public lands (Garone 2011).

Much of the Central Valley's hydrology relies on runoff from the Sierras, which flows into the Sacramento River to the north and San Joaquin River to the south (McNab et al. 2007). However, much of the vernal hydrology and alluvial wetlands of the Central Valley has been dramatically changed due to diversion of water to crops and urban areas (Bailey 1980, Garone 2011). Annual rainfall comes primarily from winter rains and can range from 15 cm in the south to 75 cm near the Sacramento delta, while average temperatures hover around 15ºC to 19ºC with summer extremes often reaching into the high 30's in many parts of the valley (Bailey 1980). Because of limited precipitation and high evapotranspiration during summer months, overexploitation of available wetland and groundwater resources is especially common in the Central Valley during times of drought, and can be detrimental to both ecosystem function and long term agricultural production (Scanlon et al. 2012, Howitt et al. 2014).

The Central Valley hosts a variety of mammalian mesopredator species including American badger (*Taxidea taxus*), American mink (*Neovison vison*), bobcat (*Lynx rufus*), coyote, gray fox (*Urocyon cinereoargenteus*), opossum, raccoon, red fox (*Vulpes* vulpes), river otter (*Lontra canadensis*), and striped skunk as well as feral and domestic populations of cats and dogs (*Canis lupus familiaris*; Rich et al. 2018). Large carnivores such as American black bear (*Ursus americanus*) and mountain lion (*Puma concolor*) are rare visitors to the Valley due to historic persecution and habitat loss and, therefore, occur mainly along the foothills and riparian corridors when present.

Study Design

My study was designed to evaluate whether mesopredators were spatiotemporally responding to a dominant predator, the coyote, and humans during and following drought conditions. I used presence and absence data of mesopredators collected from wildlife cameras traps to compare species occupancy and detection during a post-drought year (2019) to both a drought year (2016) and a year immediately after the drought (2017). Additionally, I compared species temporal activity from all three years in order to address if species were temporally partitioning. My study covers the Sacramento Metro Area and surrounding areas as these 2019 sites were selected in order to maximize the number of available drought response resurvey sites with a limited crew and to meet the objectives of my other study focusing on the influence of urbanization (see Chapter 2).

Terrestrial species stressor monitoring design (2016, 2017)

A total of 266 functioning camera sites were surveyed in California's Central Valley as a part of the TSM project in 2016 and 2017 (Rich et al. 2018). Sites were

selected based on the USDA Forest and Inventory and Analysis Program hexagon (2.6 km radius) grid used to describe the Central Valley ecoregion (Bechtold and Patterson 2005). A random site selection occurred for 75 (2016) and 100 (2017) sites in the Central Valley, with hexagons being opportunistically sampled due to private land constraints. Within each hexagon, a fine scale grid of 2,400 points spaced 100 meters apart were generated and categorized based on key vegetative lifeforms. From the 2,400 points in each hexagon, 1 to 3 points were selected as study sites by assigning random values to each point and selecting the lowest 3 numbers which represented appropriate lifeform stratification as well as feasibility of site access. Due to limited landowner permission, some hexagons were chosen to have up to 6 sites to maximize habitat stratification.

All sites were selected to be at least 1 km away from each other to reduce spatial autocorrelation; however, some sites ended up closer to each other due to fine-scale site placement restrictions (i.e. microsite habitat characteristics and landowner restrictions). Camera sites between the two consecutive years differed and no sites were resurveyed according to initial project goals and objectives. Cameras were deployed for a total of 28 days across an approximately 3 to 4 month study period (23 March – 27 July, 2016; 3 April – 28 June, 2017) beginning in the spring to maximize species detections during the year's more stable weather conditions.

Reconyx PC900 cameras were deployed within the target vegetative lifeform/habitat type as signified by site selection at least 20 to 30 meters away from a marked centerpoint. Technicians placed cameras to face north to avoid direct sunlight and intentionally pointed them at least three meters away from game trails or other signs of

wildlife. Cameras were mounted approximately one meter above ground onto T-posts in open areas or to tree or shrub boles when available. All camera settings were uniform to ensure consistent data collection (Appendix A). Cameras were U-bolted and attached to wooden boards with a bungee cord to the T-posts or bole to allow the angle of the camera to be adjusted with wooden shims. Technicians baited cameras at the start of the survey with approximated 0.5 – 1 kg salt lick, 500 mg of peanut butter- oat mixture (grain), and 150 g of fishy cat food in order to attract a wide variety of carnivores, ungulates, and rodent species. The three bait items were spaced approximately 10 cm apart and covered with sticks or rocks in order to maximize capture potential by causing animals to linger. Technicians tested camera triggering by walking in front of cameras and checking camera activation before final deployment, and all foliage and potential obstructions were cleared out of the cameras view to decrease false triggers. Cameras were outfitted with desiccant packets to prevent water damage, were powered by 12 AA lithium-ion batteries, and were locked with cable locks to prevent tampering and theft. Cameras were set to have a high motion/infrared beam trigger sensitivity and to take a set of 3 photos with every trigger event with no delay between trigger events. Cameras were left running for the sample period and checked at least once after two weeks of deployment to change SD cards and batteries as well as ensure camera functionality. Additional surveys were also completed at camera sites in 2016 and 2017 during which technicians were on site for over an hour, potentially influencing wildlife during that period. Camera sites in 2016 and 2017 were paired and deployed at the same time to maximize detections in the area.

Post drought resurvey design (2019)

During the summer of 2019, I resurveyed 45 of the original 266 camera sites (2016, n = 22; 2017, n = 23) throughout the Sacramento Metropolitan Area for mesopredator and human presence or absence. Sites were selected using a restricted 20 by 20 grid of the USDA Forest and Inventory and Analysis Program hexagon grid centered around the Sacramento Metropolitan Area (Bechtold and Patterson 2005). Sites were on a mixture of both private and public land representing a comparative subsample of habitat types originally selected by the initial TSM surveys. The resurvey season (20 May – 20 August 2019) coincided with a later start into the summer months due to time constraints around receiving landowner permission. I placed cameras at resurvey sites as close as possible to their 2016/2017 locations using site establishment photos and GPS coordinates from initial surveys; however, final site establishment was decided based on microsite characteristics (e.g., presence of game trails, sun position, vegetation growth, accessibility, etc.) within an approximate 50m radius around initial camera sites. I baited cameras with fishy cat food once at the beginning of the sampling period but did not include the other bait types used in TSM project because I was focusing on mesopredators. As with the initial design, cameras were left running for the sample period and checked at least once after two weeks of deployment to ensure camera functionality for both surveys; however, site visits rarely lasted more than an hour at a time. While TSM paired two or more camera sites and set at the same time within the same survey period, resurvey sites in 2019 were temporally and spatially independent, meaning paired camera sites were deployed at different times in order to maximize

temporal independence of sites and coincide with the assumptions of the urbanization survey (Chapter 2) occurring simultaneously. The protocols for camera settings and establishment were consistent across all three years of the study (Appendix A). All protocol and procedures adhere to the animal care and use policy at Humboldt State University (HSU) and were approved by the HSU Institutional Animal Care and Use Committee (IACUC), protocol # 08 16.17.W.08-A.

Camera Data Processing

After an initial review of the camera trap photos, I imported the photo files and extracted metadata using MapView Professional (MapView Professional 3.7.2.2 Version https://www.reconyx.com/software/mapview, accessed 11 Nov 2020). A trained technician or I would then review the photos again to match all species recorded with matching camera metadata, checking against the initial review for discrepancies. Species records were considered independent after 30 minutes of a previous detection. Species were included in the analysis if there were at least three (n = 3) detections for all survey years (2016, 2017, and 2019).

Data Analysis

All statistical analysis was completed using R 3.5.2 and RStudio 1.3.959 (R Core Team 2018; RStudio Team 2020). I consolidated all camera trap photos into species records and made into detection histories using the package “camptrapR” (Niedballa et al. 2016). Occupancy and detection models were created using the package “unmarked” (Fiske and Chandler 2016); while temporal overlap analyzes were run using the package overlap (Meredith and Ridout 2014).

Single species multi-season occupancy modeling

I used single-species multi-season occupancy modeling to evaluate whether mesopredators spatially and temporally responded to changes in coyote presence, human presence, and water availability during and after drought. Multi-season occupancy models use four variables to evaluate changes in species occurrence over multiple survey seasons. Initial occupancy (psi or ψ) is the probability of a species occurring at camera sites at the beginning of the first season; colonization (gamma or γ) is the probability of camera sites becoming occupied in subsequent seasons; extinction (epsilon or ε) is the probability of camera sites becoming unoccupied in subsequent seasons; and detection (p) is the probability of detecting a species at camera sites throughout the seasons (MacKenzie et al. 2017). Although camera sites were approximately a minimum distance of 1km apart, the mesopredator species I am studying have large varying home ranges and the potential to move between sampled camera sites. Thus, the assumption of closure required for true occupancy to be estimated may be violated in this study; therefore, occupancy is viewed as species "use" of sampled areas within the sample season (MacKenzie et al. 2017).

Covariates

I used environmental covariates representing both ephemeral and permanent water availability to evaluate changes in initial occupancy, colonization, and extinction probabilities of mesopredators. I used two covariates to classify mesopredator response to both types of water availability—surface water availability and water associated habitats (wetlands).

I classified surface water availability as whether surface water was visible or not within a 50 m area of the camera site based on either the identification by on-site technicians or presence of surface water in site establishment photos. Sites where surface water was apparent were scored with a "1", while sites where surface water was not readily visible were scored with a "0". Since surface water can change throughout the study period for a variety of reasons (i.e., anthropogenic irrigation, rainfall, evaporation), surface water availability was only determined at the beginning of the survey period. Thus, I used surface water as a yearly covariate, as surface water availability changed at each site from the initial season (2016 and 2017) to resurvey (2019).

While surface water availability could change from season to season as well as within the survey period of 28 days, I also sought to capture mesopredator response to areas or habitats that are known for their association with either surface or ground water. Therefore, I classified camera sites in wetlands, riparian, and rice cultivated habitats as "wetlands" (2016, n = 13; 2017, n = 13) while sites in annual croplands, orchards, and grassland/shrubland habitats were classified as "drylands" (2016, n = 9; 2017, n = 10, Appendix B). I used the "wetland" habitat covariate as a site level covariate, as wetland habitat types did not change drastically between TSM sites from year to year.

Additionally, I expected detection probability for mesopredators to change as a result of both behavioral responses and ecological conditions as well as imperfect detection of species at camera sites. A total of seven detection covariates were evaluated: wetland habitat, surface water availability, year, coyote presence, human presence, Julian date, and bait. The wetland habitat and surface water availability covariates used for

estimating occupancy, colonization, and extinction probabilities were also used for estimating detection probability. I used year to represent changes in mesopredator detection as a result of the initial survey year (2016 or 2017) and the resurvey year (2019). Coyote and human presence are observational covariates based on coyote and human detection histories for the sample period. Interactions between year and available surface water, human presence, and coyote presence were included to discern whether detection probability changed covariate relationships between initial surveys and 2019. I used Julian date as a yearly covariate to evaluate whether changes in the timing/ seasonality of camera placement influenced mesopredator detection between survey years. Lastly, I used bait as an observational covariate measuring bait presence and subsequent decay for each sample occasion until the end of the sample period. All covariates were considered uncorrelated using Pearson's correlation coefficients (Appendix B).

Candidate model sets and model selection

I created single-species multi-season occupancy models for mammalian mesopredators using the "unmarked" package in R (Fiske and Chandler 2011). After preliminary goodness of fit testing, I determined that a 3-day lag effect improved model goodness of fit for all species. To maintain covariate beta estimates and goodness of fit, I extended the sample period from one day to three days in order to account for this lag effect. Thus, for each camera site within each season there is a 27-day sample period made up of nine 3-day sample occasions. Detection histories were created for all

mesopredator species as well as humans using the package “camtrapR” in R (Niedballa 2016).

Due to sites from 2016 and 2017 being independent from one another, I created two candidate model sets for each species in order to evaluate occupancy, colonization, extinction, and detection between the initial survey (either 2016 or 2017) and the resurvey year (2019). Consequently, I cannot directly measure multi-season occupancy variables between initial survey years 2016 and 2017. Thus, comparisons made between 2016 and 2017 for each species will result from comparing the top covariates within top models for each candidate model set.

I first built models by including combinations of covariates for each variable (occupancy, colonization, extinction, and detection) individually with all other variables set with no covariates, ranking them by Akaike’s Information Criterion for small sample sizes (AICc; Anderson and Burnham 2002), and then by finding the best combination of variables and their covariates to find the top models. Global models including all appropriate covariates for each variable were created and used to run goodness of fit tests for each candidate model set; if c-hat values were greater than 1, QAICc was used to rank models. If c-hat was less than 1, c-hat was set to be 1 and AICc was used to rank models (MacKenzie and Bailey 2004).

I selected top models if they were 1) within a delta AICc of 2, 2) the most generalized (greatest number of covariates), and 3) had the most significant beta estimates of covariates. I then inspected the beta estimates for each covariate response by calculating beta estimate 95% confidence intervals. If covariate beta estimate 95%

confidence intervals overlapped with zero, the covariate's response and interpretation were considered uninformative (Arnold 2010). Thus, covariates within the top model are only considered competitive and interpretable if their beta estimates result in a significant 95% confidence interval. This process was used twice for each species; once for the 2016–2019 resurvey sites and once for 2017–2019. Candidate model set ranking and goodness of fit testing were done using the package "AICcmodavg" in R (Mazerolle 2020).

Temporal overlap

I extracted times and dates from independent species records (i.e., 30 minutes apart) to interpret the temporal activity patterns of species captured on camera. Detections were combined for each of the three sampling years, 2016 (n = 22), 2017 (n = 23), and 2019 (n = 45). In 2019, all resurveyed sites from 2016 and 2017 are included in the temporal analysis of the species to maximize differences between years rather than sites. I used the "overlap" package in R, which relies on a non-parametric kernel density analysis of species temporal data in order to estimate activity patterns and temporal overlap of each species (Meredith and Ridout 2014).

Temporal overlap is calculated as the coefficient of overlap ($\hat{\Delta}$ or D-hat) between two species' activity patterns. D-hat ranges from 0 to 1, where a value of 0 indicates no temporal overlap and a value of 1 indicates complete temporal overlap. As suggested by Ridout and Linkie (2009), I used two methods to estimate D-hat as provided by the *overlap* package; D-hat$_1$ ($\hat{\Delta}_1$) for when at least one species had a small sample size (n < 50), where $\hat{\Delta}_1$ is described by equation (1)

$$\hat{\Delta}_1 = \int_0^1 \min\{\hat{f}(t), \hat{g}(t)\}\, dt \quad (1)$$

where $\hat{\Delta}_1$ is the coeffecient of overlap for small sample sizes, which is represented as the integral of overlap between one species activity pattern, described as function $\hat{f}(t)$ and another species activity patterns, described as function $\hat{g}(t)$. I used D-hat$_4$ ($\hat{\Delta}_4$) for when both species had large sample sizes (n > 50), as described by equation (2)

$$\hat{\Delta}_4 = \frac{1}{2}\left(\frac{1}{n}\sum_{i=1}^{n} \min\left\{1, \frac{\hat{g}(x_i)}{\hat{f}(x_i)}\right\} + \frac{1}{m}\sum_{j=1}^{m} \min\left\{1, \frac{\hat{f}(y_j)}{\hat{g}(y_j)}\right\}\right) \quad (2)$$

where $\hat{\Delta}_4$ is the coeffecient of overlap for sample sizes *n* and *m* between two species, x_i represents the sample times for the first species over *i* detections, and y_j represents the sample times for the second species over *j* detections. In order to account for changing daylight hours between surveys influencing mesopredator activity, I used the sunTime function in the "overlap" package to scale temporal activity to be between sunrise and sunset across survey periods (Nouvellet et al. 2012).

I determined if activity patterns were changing within species across years by using a 2-sample Anderson Darling test using the R package "kSamples" (Scholz and Zhu 2019). To compare the changes in temporal overlap across species between all three survey years, I first compared within species overlap from year to year (intraspecies) and then compared overlap of species pairs for each survey year (interspecies). I used 95% confidence intervals for each D-hat estimate determined from 10,000 bootstrap samples to compare overlap estimates of species pairs between years. Thus, if a species pairs' confidence intervals from one year overlapped the same species pairs' confidence

intervals for another year, the change of temporal overlap of that species pairing from one year to another is considered non-significant.

Results

Cameras captured 11 mammalian mesopredator species across all three study years. Of the species, five mesopredator species had enough data to compare between all three years including four wild mesopredators (coyote, raccoon, opossum, and striped skunk), and one domestic mesopredator (domestic cat). The other five mesopredators omitted from analysis either had low detection resulting from one or two sightings (American badger, American mink), had high detection in one year but low or no detection in other years (bobcat, red fox, river otter), or could not be differentiated from their occurrence with humans (domestic dog).

Coyote, opossum, and striped skunk detections were lowest in 2016 compared to 2019 when the same sites were resurveyed, while coyote detections were consistent between sites in 2017 and 2019 (Table 1). Raccoons and domestic cats had highest detections in 2016 versus 2019, while raccoon and skunk detections increased from 2017 to 2019. Detections of both opossums and domestic cats decreased between 2017 and 2019. Human detections increased in 2019 compared to 2016 and 2017 due to more detections of technicians checking more frequently cameras in 2019 versus initial surveys, as well as increased agricultural work around certain camera sites.

Table 1. Species detections (# of independent records) across survey year (n = 45 sites total).

Camera Survey	Year	Coyote	Raccoon	Opossum	Striped Skunk	Domestic Cat	Human
Drought (n = 22)	2016	14	92	29	6	23	94
Recovery (n = 23)	2017	26	41	87	54	12	76
Resurvey 2016 (n = 22)	2019	42	79	65	42	3	149
Resurvey 2017 (n = 23)	2019	29	64	18	84	9	176
Total		111	276	199	188	47	495

Single Species Multi-Season Occupancy Models

Below I report top models by species along with their associated significant covariates. I also report β estimates along with odds ratios (OR) for significant covariates to show the magnitude of covariate effects, along with 95% confidence intervals for odds ratios obtained through the "confint" function in package "unmarked" (Fiske and Chandler 2011). Odds ratios indicate the slope or consistent change in odds (e.g., the odds of occupancy are equal to the probability of a species occupying a site divided by the probability of not occupying a site, so the OR for two sites would be the change in odds of occupancy for site 1 divided by the odds of occupancy for site 2). Thus, odds ratios can be used to determine the strength of a covariate as a percentage of increasing or decreasing odds around an unchanging OR = 1 (an OR greater than 1 indicates an

increase in odds, while an OR less than 1 indicates a decrease in odds). Odds ratios for covariates are in reference to the units of the covariate. All covariates used along with candidate model sets for both 2016–2019 and 2017–2019 appear in Appendix C.

Coyotes

Coyotes were detected at 5 sites in 2016 and 11 sites in 2019. For 2016–2019, the top model for coyotes included available surface water as a covariate for estimating initial occupancy probability and year and Julian date for detection probability (Figure 2). Available surface water had no influence over coyote initial occupancy probability in either 2016 or 2019 even though it was included in the top model. Survey year had a negative relationship with coyote detection (β = -2.287, OR = 0.102, OR 95%CI [0.013, 0.821]) indicating a decrease in the odds of coyote detection by 89.8% in 2019 sites (post drought) compared to 2016 (drought; Figure 3). Julian date had a positive effect on coyote detection (β = 0.029, OR = 1.029, OR 95% CI= [1.009, 1.050]), increasing odds of detection by 2.9% for each day into the season camera placement occurred (Figure 4).

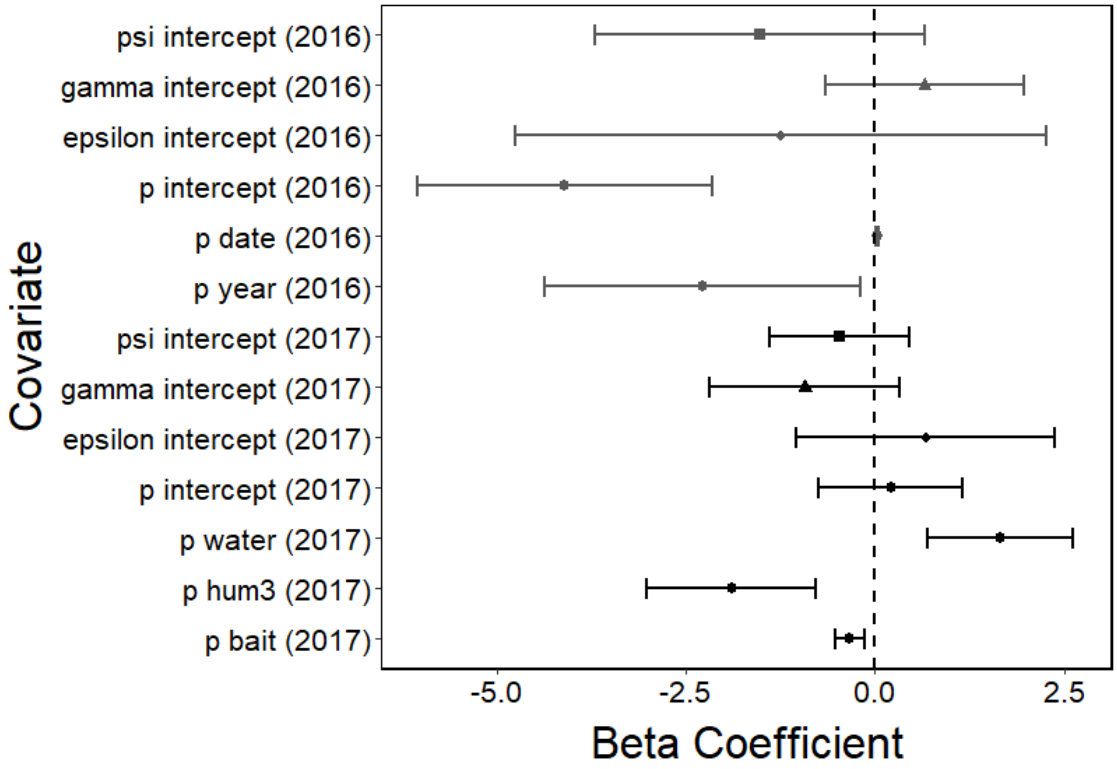

Figure 2. Beta coefficients for initial occupancy (psi, squares), colonization (gamma, triangles), extinction (epsilon, diamonds), and detection (p, circles) intercepts and covariates for both 2016–2019 (gray) and 2017–2019 (black) top coyote models. If error bars, representing 95% confidence intervals, cross the zero dashed line, the beta estimate is considered not statistically significant. Omitted beta estimates include surface water as an initial occupancy covariate in 2016–2019 and surface water as an extinction covariate in 2017–2019 due to uninterpretable beta estimates and large standard errors.

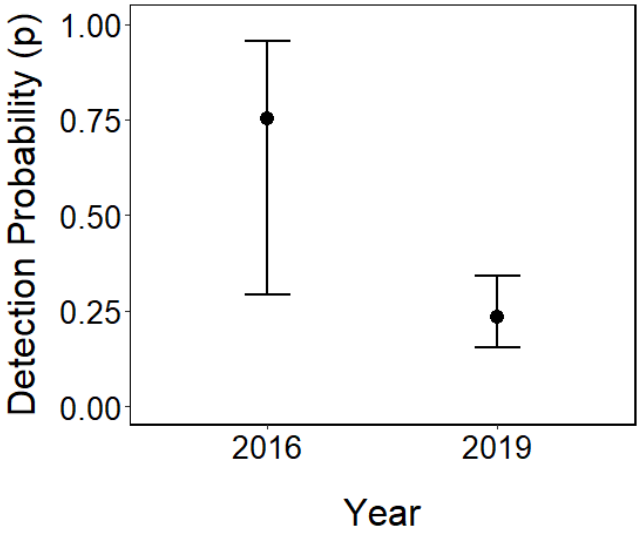

Figure 3. Detection probability (p) for coyotes in 2016 and 2019. Julian date is set at July 1st for both years.

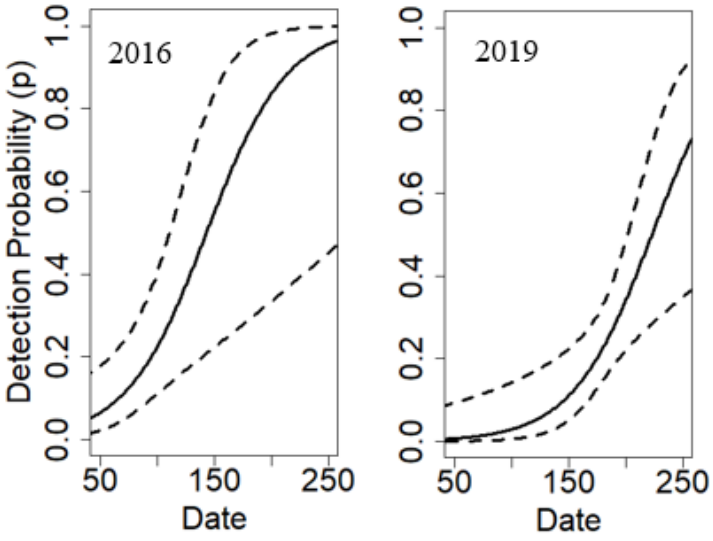

Figure 4. Detection probability (p) for coyotes in 2016 (left) and 2019 (right) in relation to the Julian date of camera placement.

In 2017–2019, coyotes were detected at 8 sites in 2017 and 8 sites in 2019. The top model included surface water for site extinction probability as well as surface water, bait, and human presence for detection probability (Figure 2). While surface water did not significantly influence extinction, it did significantly increase the odds of coyote detection by 424.9% (β =1.658, OR = 5.249, OR 95%CI = [2.020, 13.637]). Bait decay had a negative impact on coyote detection, decreasing the odds of coyote detection by 28.6% for every 3-day period since initial baiting (β = -0.337, OR = 0.714, OR 95%CI = [0.590, 0.863]). Human presence within a 3-day period also decreased the odds of coyote detection by 85.1% (β = -1.904, OR = 0.149, OR 95%CI = [0.049, 0.456]; Figure 5).

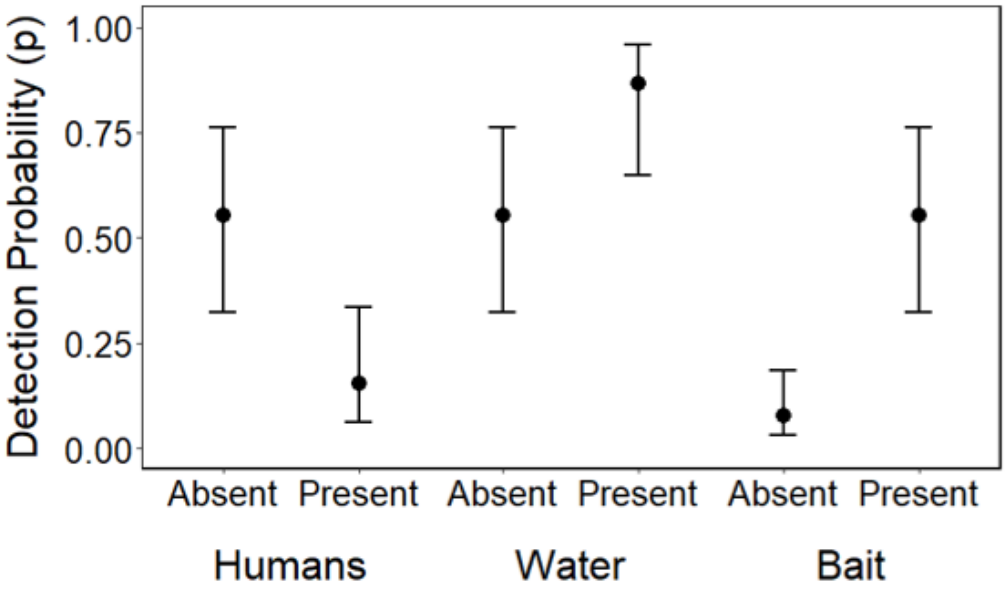

Figure 5. Detection probability (p) for coyotes from 2017 to 2019 in relation to the absence and presence of (from left to right) humans, surface water, and bait. Estimates

are calculated assuming the other detection covariates are absent, except for bait, which is assumed present.

Raccoons

Raccoons were detected at 11 sites in 2016 versus 12 sites in 2019. The top model for 2016–2019 includes wetlands for occupancy and available surface water and bait for detection (Figure 6). Raccoons were the only mesopredator to have a covariate with a significant relationship to initial occupancy. Initial occupancy probability for raccoons was greatly influenced by wetland habitat, with odds of raccoons using wetland sites versus non-wetland sites increasing by 784.6% (β =2.18, OR = 8.846, OR 95%CI = [1.105, 58.871]; Figure 6). Additionally, surface water at a site increased the odds of raccoons being detected by 197.1% (β = 1.089, OR = 2.971, OR 95%CI = [1.512, 5.840]). Conversely, bait decay decreased raccoon detection odds by 20.2% for every 3-day period (β = -0.226, OR = 0.798, OR 95%CI = [0.708, 0.898]; Figure 7).

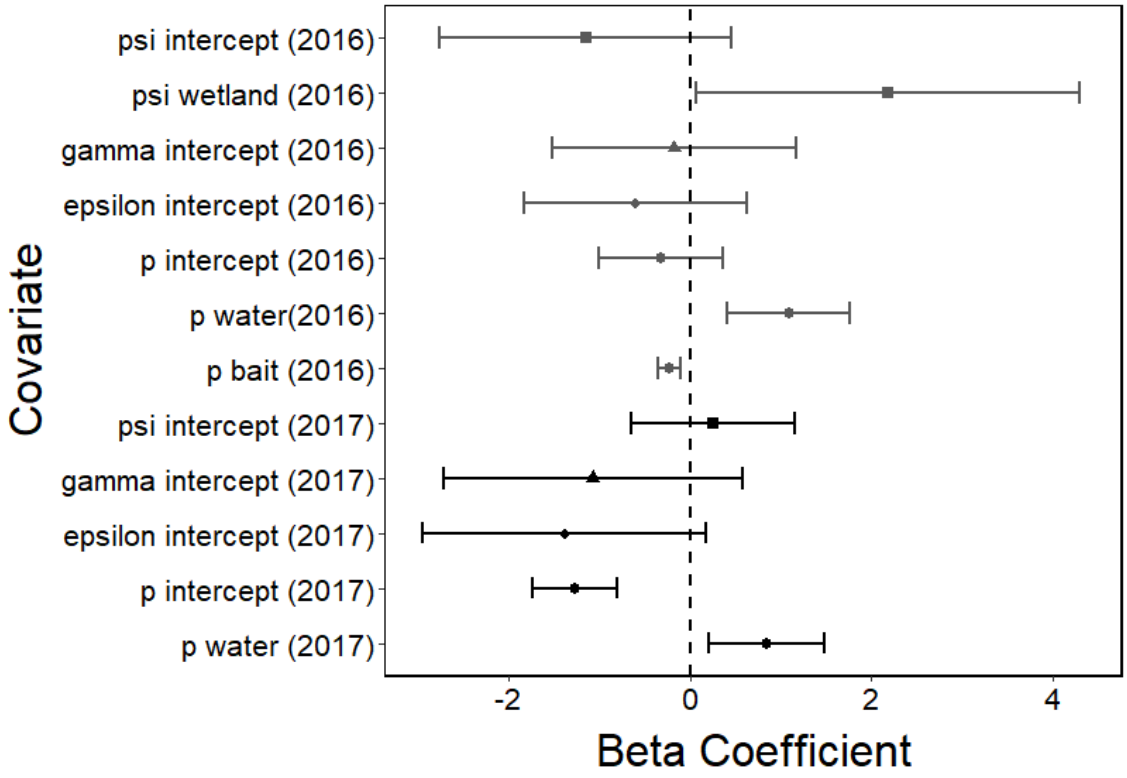

Figure 6. Beta coefficients for initial occupancy (psi, squares), colonization (gamma, triangles), extinction (epsilon, diamonds), and detection (p, circles) intercepts and covariates for both 2016–2019 (gray) and 2017–2019 (black) top raccoon models. If error bars, representing 95% confidence intervals, cross the zero dashed line, the beta estimate is considered not statistically significant.

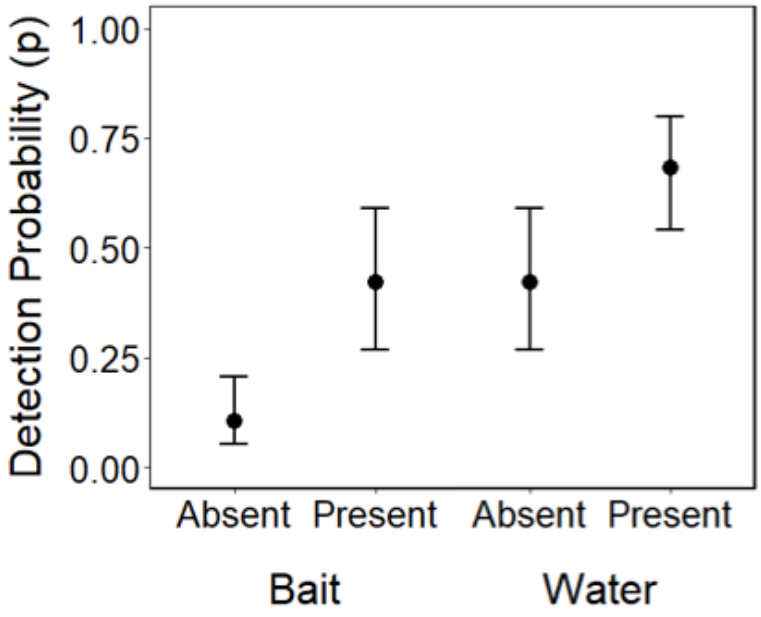

Figure 7. Detection probability (p) for raccoons from 2016 to 2019 in relation to the absence and presence of (from left to right) bait and surface water. Water estimate is calculated assuming bait is present.

Raccoon detections were similar in 2017–2019 sites, with raccoons being detected at 12 sites in 2017 and 11 sites in 2019. The top model for 2017-2019 had only one detection covariate, available surface water (Figure 6). Similar to 2016 sites, the odds of detecting a raccoon at sites with available surface water increased by 131.6% ($\beta = 0.84$, OR = 2.316, OR 95%CI = [1.223, 4.384]; Figure 8).

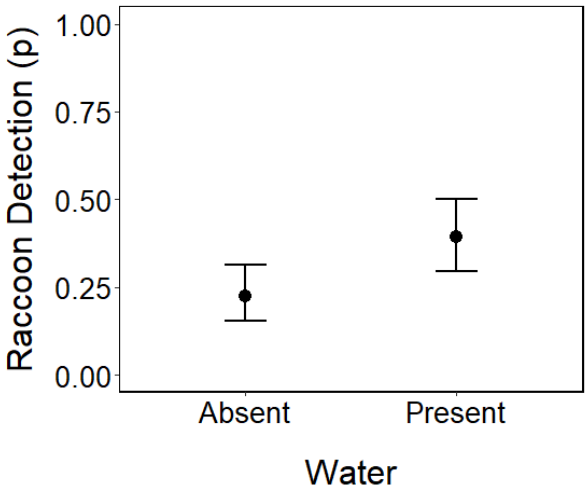

Figure 8. Detection probability (p) for raccoons from 2017 to 2019 in relation to the absence and presence of surface water.

Opossums

Opossums were detected 5 sites in 2016 and 7 sites in 2019. The top model for 2016–2019 included two detection covariates, wetland, and bait (Figure 9). Wetlands had a large positive effect on opossum detection, increasing odds by 2208.1% ($\beta = 3.139$, OR = 23.0801, OR 95%CI = [3.255, 163.619]). Opossums returned to some wetland sites during every 3-day occasion period throughout the survey period. Bait decay across the survey period decreased the odds of opossum detection by 20.8% ($\beta = -0.233$, OR = 0.792, OR 95%CI = [0.675, 0.929]; Figure 10).

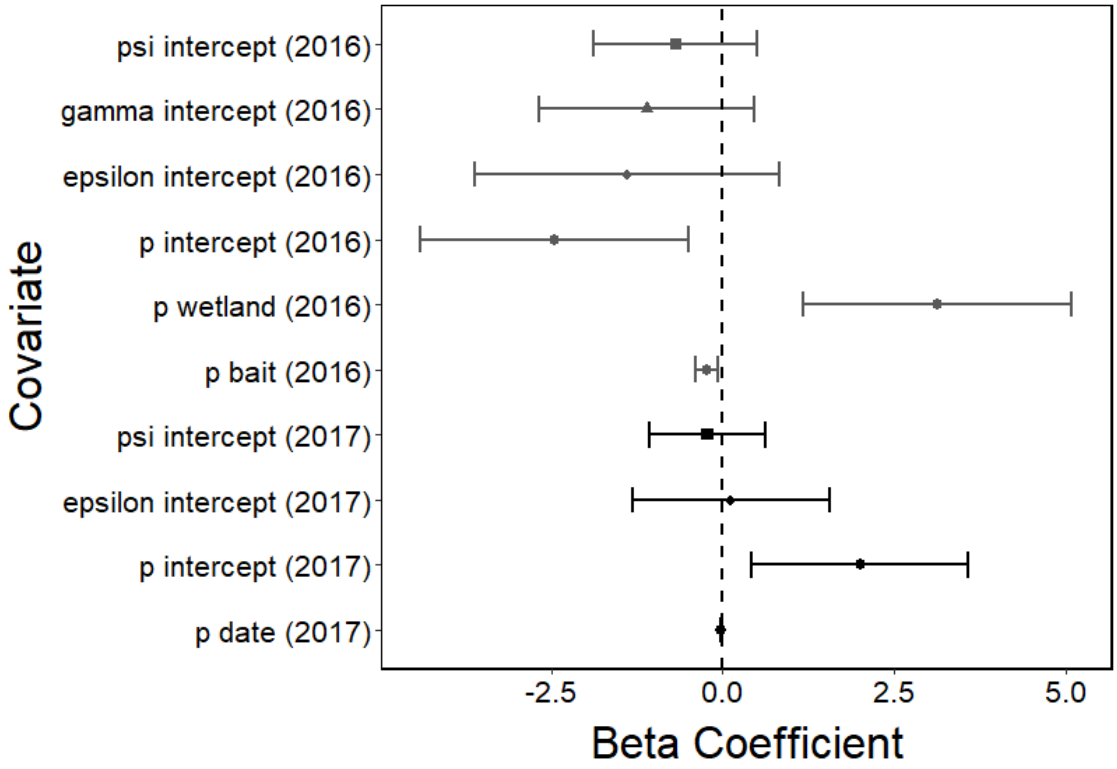

Figure 9. Beta coefficients for initial occupancy (psi, squares), colonization (gamma, triangles), extinction (epsilon, diamonds), and detection (p, circles) intercepts and covariates for both 2016–2019 (gray) and 2017–2019 (black) top opossum models. If error bars, representing 95% confidence intervals, cross the zero dashed line, the beta estimate is considered not statistically significant. Omitted beta estimates include surface water and wetland as colonization covariates and colonization intercept in 2017–2019 due to uninterpretable beta estimates and large standard errors.

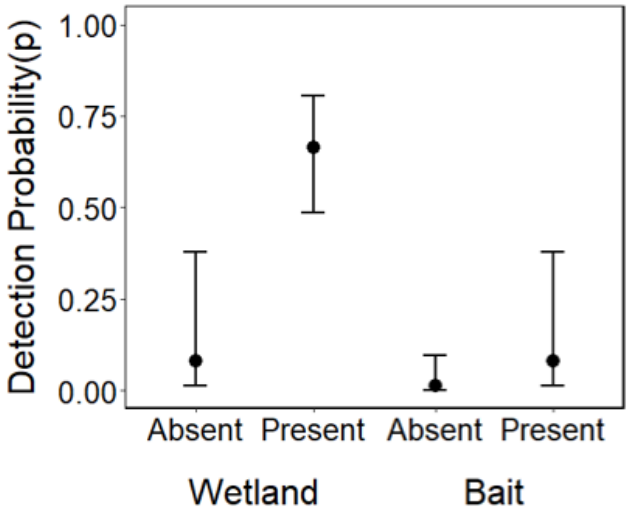

Figure 10. Detection probability (p) for opossums from 2016 to 2019 in relation to the absence and presence of wetlands and bait. Wetland estimate is calculated assuming bait is present.

In 2017, opossums were detected at 10 sites versus 7 sites in 2019. The top model for 2017–2019 included wetland and available surface water as predictors for colonization, and Julian date as a predictor for detection (Figure 9). Neither wetland nor surface water availability had interpretable relationships with opossum site colonization probabilities. Julian date decreased the odds of opossum detection by 2% for each subsequent day that cameras were placed (β = -0.0202, OR = 0.980, OR 95%CI = [0.969, 0.991]; Figure 11).

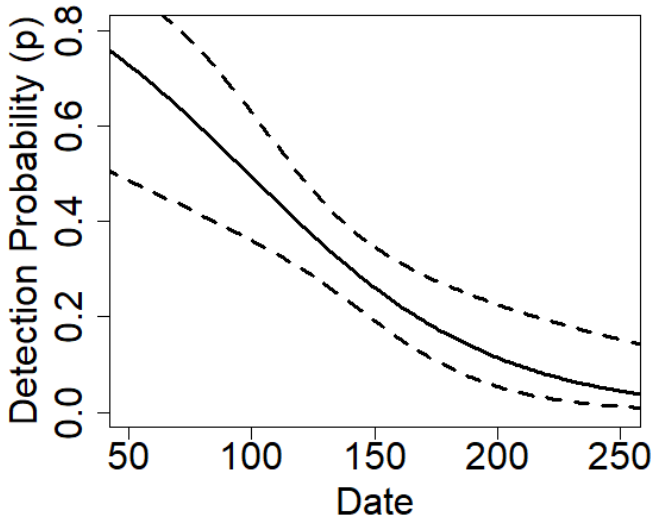

Figure 11. Detection probability (p) for opossums from 2017 to 2019 in relation to the Julian date of camera placement.

Striped skunks

Striped skunks were detected at 5 sites in 2016 and 11 sites in 2019. For 2016–2019, the top model included wetland, year, and bait as covariates for detection (Figure 12). Wetland and bait, while included in the top model, showed no relationship for estimating detection probability. Year had a positive relationship with skunk detection, increasing the odds of skunk detection by 553.4% in 2019 compared to 2016 ($\beta = 1.877$, OR = 6.534, OR 95%CI = [2.379, 17.941]; Figure 13).

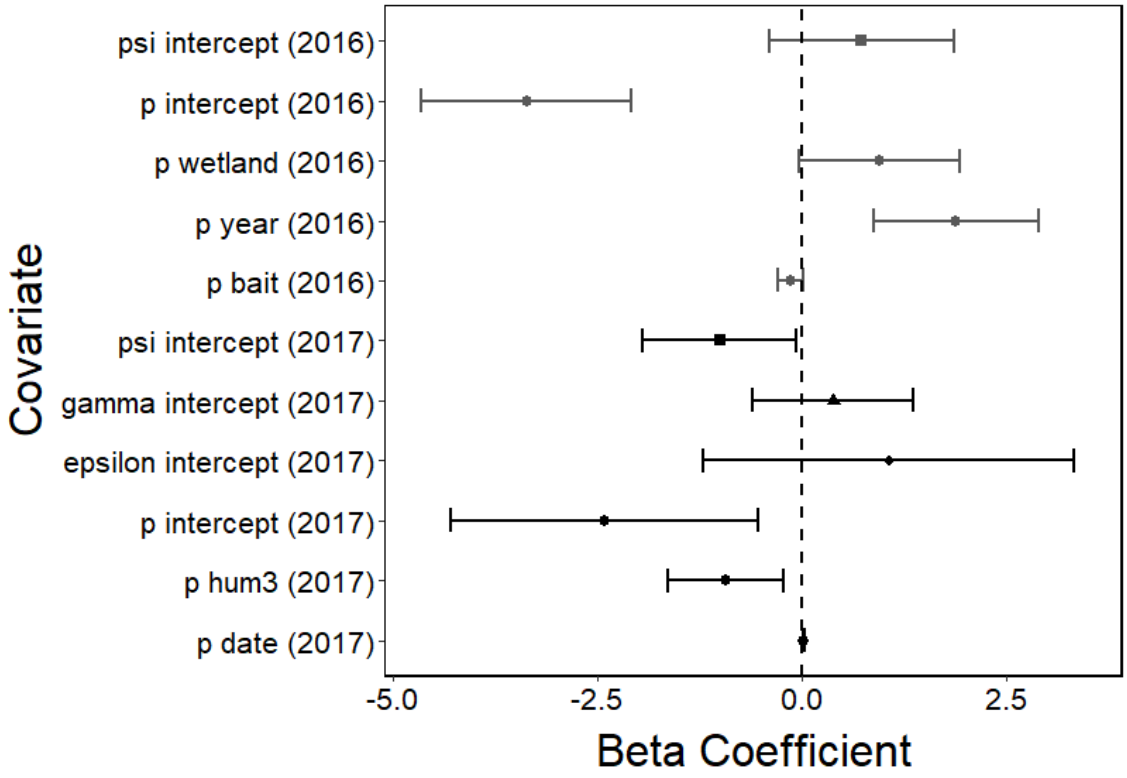

Figure 12. Beta coefficients for initial occupancy (psi, squares), colonization (gamma, triangles), extinction (epsilon, diamonds), and detection (p, circles) intercepts and covariates for both 2016–2019 (gray) and 2017–2019 (black) top striped skunk models. If error bars, representing 95% confidence intervals, cross the zero dashed line, the beta estimate is considered not statistically significant. Omitted beta estimates include colonization and extinction intercepts in 2016–2019 and surface water as an extinction covariate in 2017–2019 due to uninterpretable beta estimates and large standard errors.

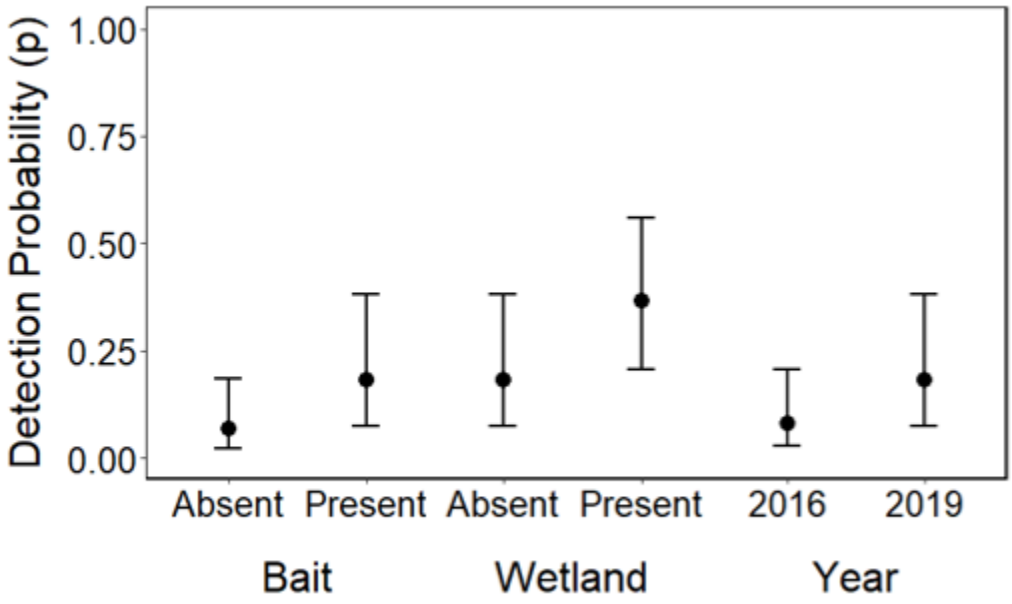

Figure 13. Detection probability (p) for skunks from 2016 to 2019 in relation to the absence and presence of bait, wetland, and year. Wetland estimate is calculated assuming bait is present. Bait and wetland estimates are calculated assuming the year is 2019. Year is the only significant covariate.

In 2017, skunks were detected at 6 sites compared to 13 sites in 2019. The top model for 2017–2019 includes available surface water as a covariate for extinction probability, while human presence and Julian date were top covariates for detection probability (Figure 12). Available surface water was uninformative in explaining extinction probability. Human presence within a 3-day period decreased the odds of skunk detection by 60.8% (β = -0.936, OR = 0.392, OR 95%CI = [0.194, 0.793]; Figure 14). Alternatively, Julian date increased the odds of skunk detection by 1.5% for every

subsequent day cameras were placed out (β = 0.015, OR =1.015, OR 95%CI = [1.003, 1.305]; Figure 15).

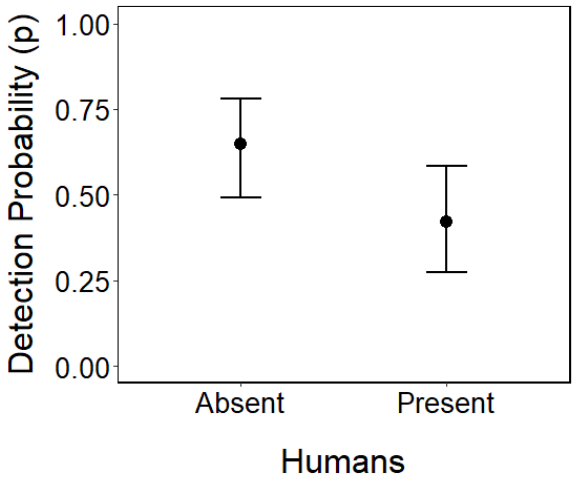

Figure 14. Detection probability (p) for skunks from 2017 to 2019 in relation to the absence and presence of humans after 3 days. Human presence estimate is calculated assuming Julian date is constant (July 21).

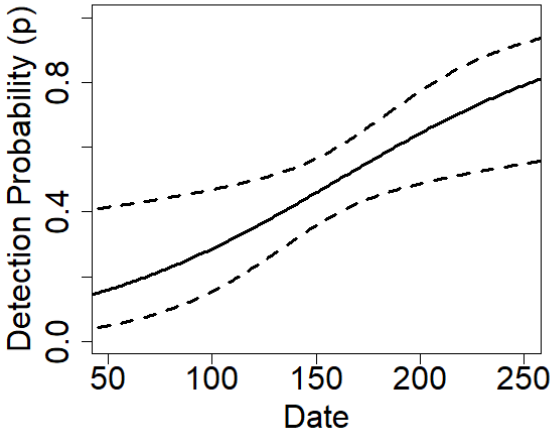

Figure 15. Detection probability (p) for skunks from 2017 to 2019 in relation to the Julian date of camera placement.

Domestic cats

Domestic cats were detected at 3 sites in 2016 and 2 sites in 2019. The top model included wetlands and bait as detection covariates (Figure 16). Wetlands had a negative relationship with cat detection, decreasing odds of detection by 98.5% (β = -4.229, OR = 0.015, OR 95%CI = [0.001, 0.165]). Bait had a negative impact on cat detection; as bait decayed over each 3-day period, odds of cat detection decreased by 28.6% (β = -0.337, OR = 0.714, OR 95%CI = [0.538, 0.948]; Figure 17).

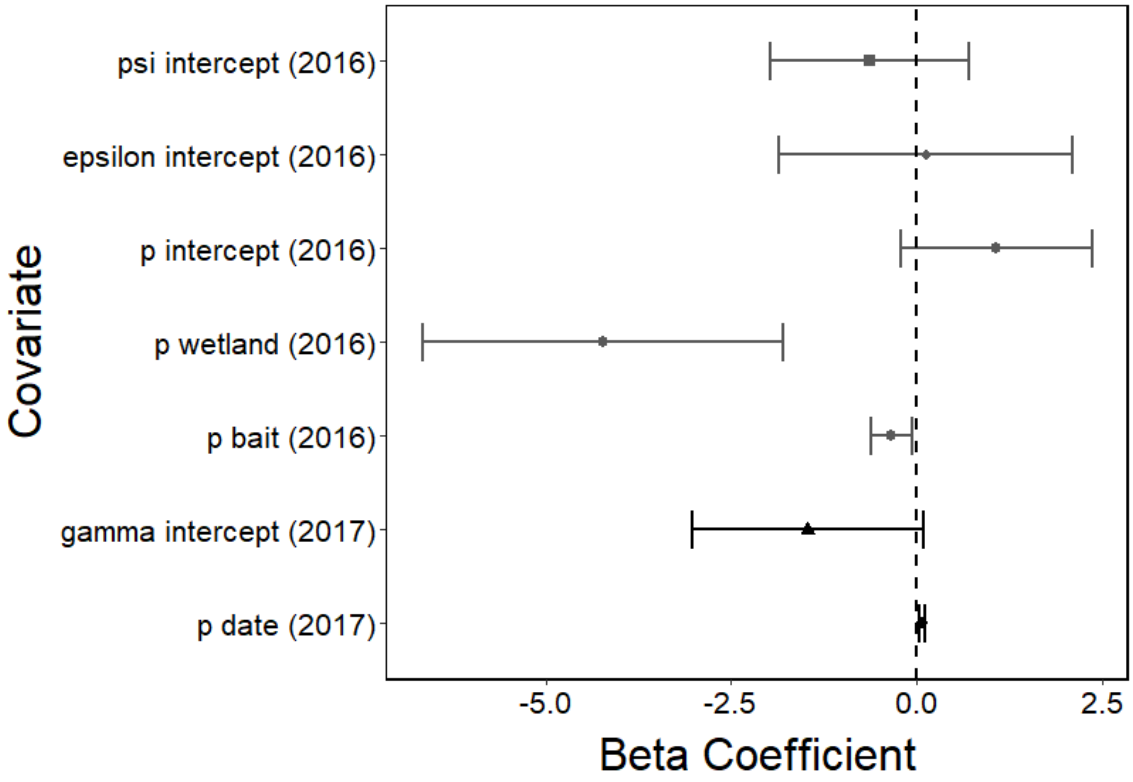

Figure 16. Beta coefficients for initial occupancy (psi, squares), colonization (gamma, triangles), extinction (epsilon, diamonds), and detection (p, circles) intercepts and covariates for both 2016–2019 (gray) and 2017–2019 (black) top domestic cat models. If error bars, representing 95% confidence intervals, cross the zero dashed line, the beta

estimate is considered not statistically significant. Omitted beta estimates include colonization intercept in 2016–2019 and wetland as an initial occupancy covariate as well as initial occupancy and extinction intercepts in 2017–2019 due to uninterpretable beta estimates and large standard errors.

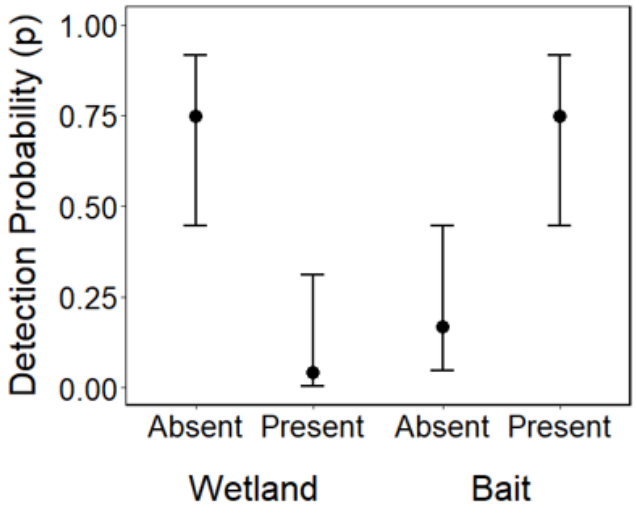

Figure 17. Detection probability (p) for domestic cats from 2016 to 2019 in relation to the absence and presence wetland, and bait. Wetland estimate is calculated assuming bait is present.

In 2017, domestic cats were detected at 4 sites while in 2019 they were detected at 2 sites. For 2017–2019, the top model included wetland as a covariate for initial occupancy, and Julian date as a covariate for detection (Figure 16). While wetland was included as a covariate in the top model, it was uninformative at estimating a relationship with initial occupancy. Julian date did increase the odds of cats being detected by 7.3% for every subsequent day a camera was placed ($\beta = 0.071$, OR = 1.073, OR 95%CI = [1.033, 1.115]; Figure 18).

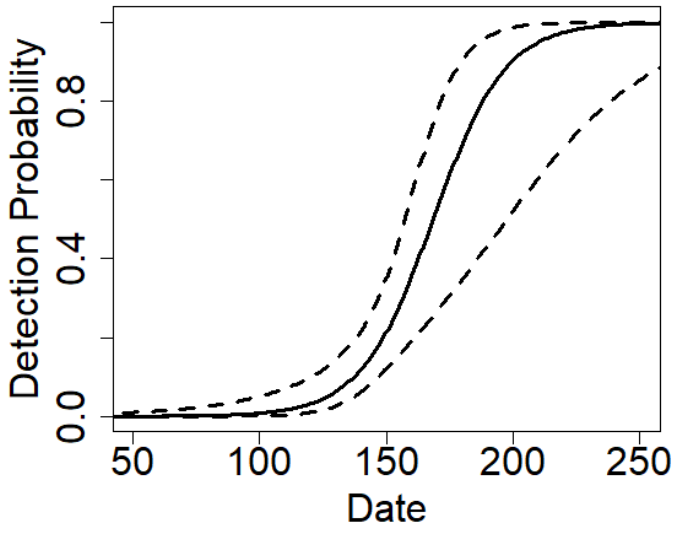

Figure 18. Detection probability (p) for domestic cats from 2017 to 2019 in relation to the Julian date of camera placement.

Temporal Overlap

Mesopredator species exhibited mainly crepuscular and nocturnal activity while humans were strongly diurnal (Appendix D). Intraspecies temporal overlap across all three years ranged widely; however, species overlap did not seem to change significantly from year to year (Figure 19). Interspecies overlap across all three years tended to be the highest in 2019 versus 2016 for all wild mesopredator species; however, this overlap was mostly non-significant and wide ranging for a majority of species pairs across years. I combined species detections from both sets of resurvey sites, therefore, mesopredator activity in 2019 is informed by almost double the number of sites compared to species activity in 2016 and 2017 (Table 1).

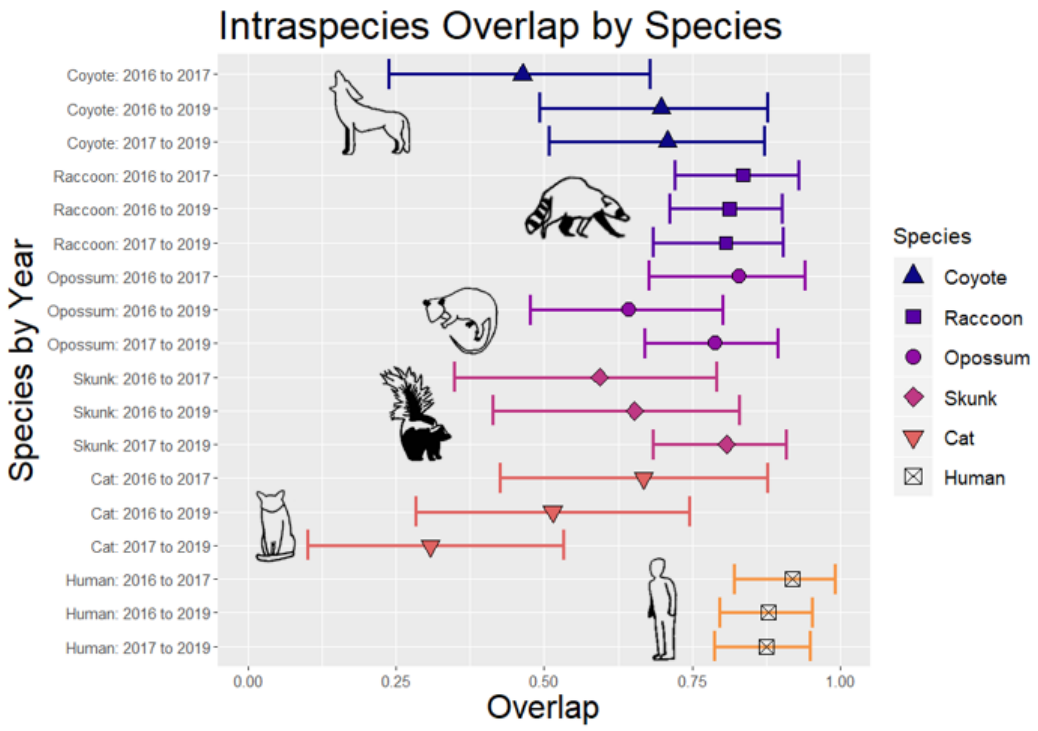

Figure 19. Temporal overlap within species across all survey years (2016, 2017, and 2019). Points represent temporal overlap value (D-hat) for the same species between two different survey years. Error bars are 95% confidence intervals are given from calculating D-hat from bootstrapping (n = 10,000).

Humans

Humans were more active in the hours before sunrise and after sunset in 2019 compared to human activity in 2016 and 2017 (Appendix D). This change in human activity in 2019 was significant compared to both 2016 (AD = 3.642, T.AD = 3.484, p = 0.01292, $\alpha = 0.05$) and 2017 (AD = 3.746, T.AD = 3.622, p = 0.01148, $\alpha = 0.05$). However, human temporal overlap remained consistently across all three years (Figure

20). Most mesopredators had moderate to low overlap with humans with no significant change from year to year.

Coyotes

Coyote activity, while variable, did not change significantly from year to year. (Appendix D). Coyotes had the lowest temporal overlap range from 2016 to 2017, but intraspecies overlap did not significantly change across years (Figure 19). Coyotes overlap with wild mesopredators increased from 2016 to 2019. This trend was most apparent for coyotes and striped skunks, as temporal overlap increased significantly from 2016 ($\Delta\text{-hat}_1 = 0.38616$, 95% CI = [0.133, 0.638]) to 2019 ($\Delta\text{-hat}_4 = 0.853$, 95% CI = [0.769, 0.925]). Coyote temporal overlap with domestic cats as well as humans was the highest in 2016, and the lowest in 2019, although non-significant (Figure 20).

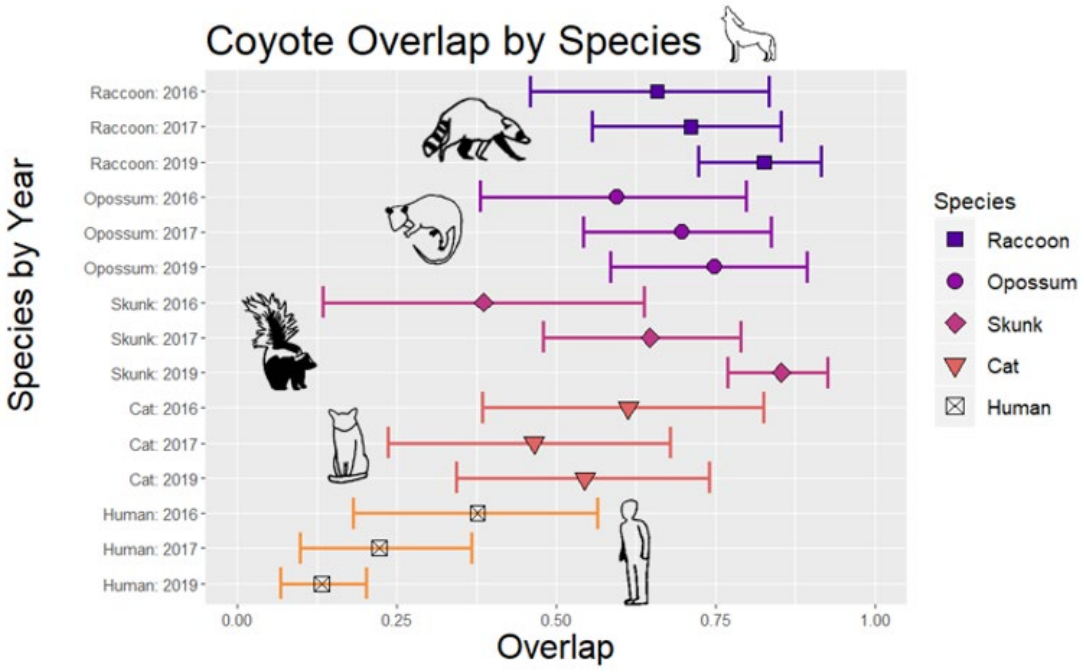

Figure 20. Temporal overlap between coyotes and all other species across all survey years (2016, 2017, and 2019).

Raccoons

Raccoon activity did not change significantly across all three years, showing strong nocturnality with some minimal diurnal activity (Appendix D). Because of this, intraspecies temporal overlap was consistently high across all years (Figure 19). Raccoons generally had high overlap with all wild mesopredator species across all years. Only domestic cats exhibited lowest temporal overlap with raccoons in 2019 compared to 2016 and 2017; however, confidence intervals show overlap across years within similar ranges. Raccoons and humans consistently had low temporal overlap between all three years (Figure 21).

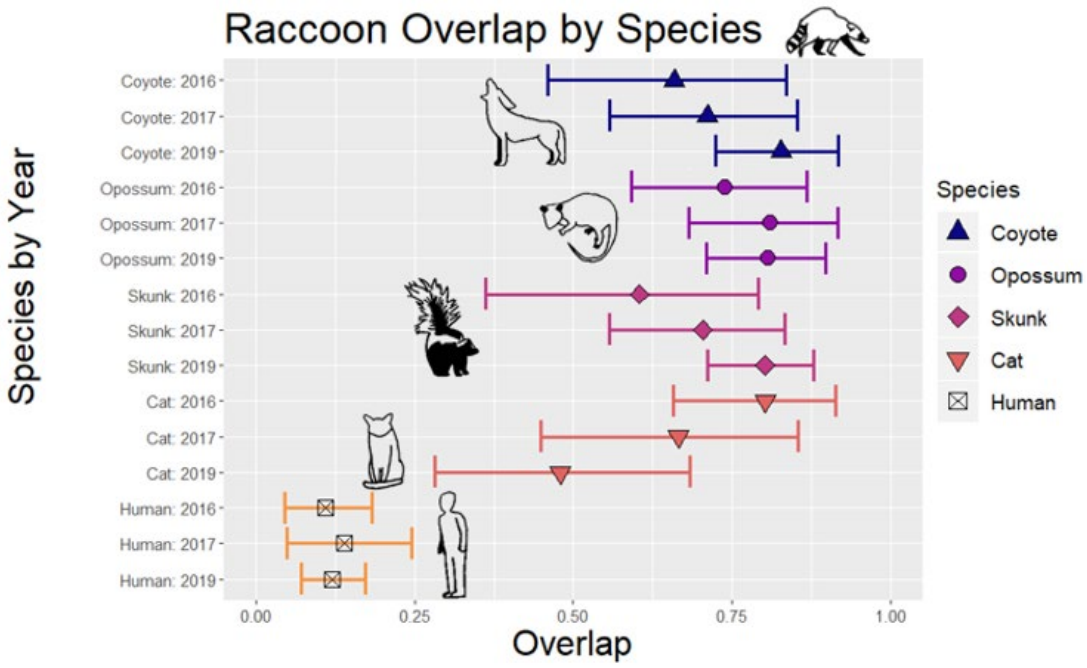

Figure 21. Temporal overlap between raccoons and all other species across all survey years (2016, 2017, and 2019).

Opossums

Opossums were mainly nocturnal but did show some activity during diurnal hours in 2016 and 2017. Opossums were the only mesopredator to have a significant change in activity patterns between 2016 and 2019 (AD = 4.446, T.AD = 4.598, p = 0.005032, α = 0.05), being more active from midnight to sunrise in 2019 than 2016 (Appendix D). Because of this shift in activity, opossums had the lowest range of overlap between 2016 and 2019, yet overlap was still within similar ranges to overlap between 2016 and 2017 and 2017 and 2019 (Figure 19). Opossums generally had high overlap with all mesopredator species across all years. Opossum and human temporal overlap were consistently across all survey years (Figure 22).

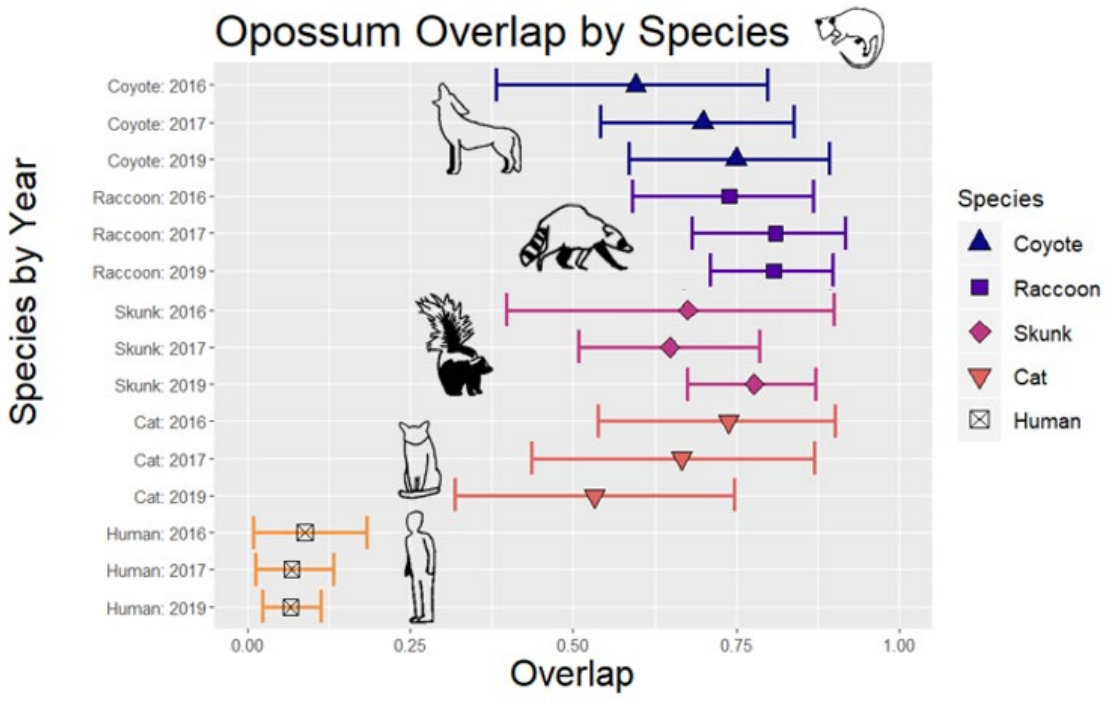

Figure 22. Temporal overlap between opossums and all other species across all survey years (2016, 2017, and 2019).

Striped skunks

Skunks were mainly nocturnal in 2016 and 2017 with some expansion into crepuscular hours in 2019; however, activity patterns did not change significantly across years (Appendix D). Skunks had the greatest and most confined overlap range from 2017 to 2019, but intraspecies temporal overlap was still similar between all three years (Figure 19). Skunks generally had high overlap with all mesopredators, increasing and narrowing in 2019 compared to 2016 and 2017 for wild mesopredators. Skunks displayed a significant increase in temporal overlap over coyotes from 2016 ($\Delta\text{-hat}_1 = 0.38616$, 95% CI = [0.133, 0.638]) to 2019 ($\Delta\text{-hat}_4 = 0.853$, 95% CI = [0.769, 0.925]). Skunks had

a consistently decline in temporal overlap from 2016 to 2019, yet overlap change was not significant across years. Skunks and humans had consistent low overlap for all three years (Figure 23).

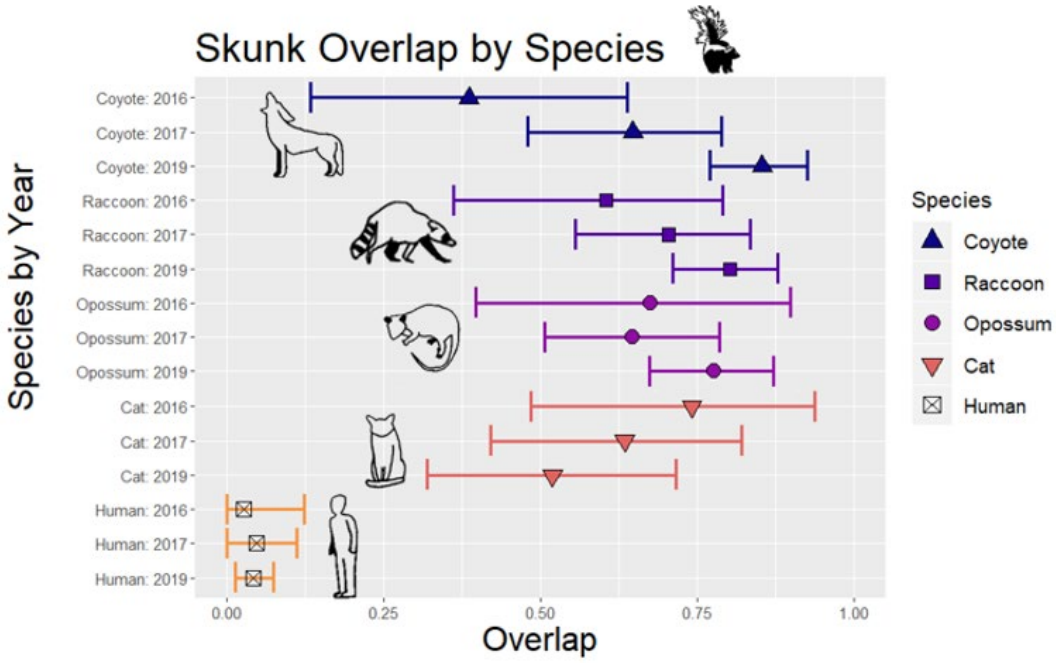

Figure 23. Temporal overlap between skunks and all other species across all survey years (2016, 2017, and 2019).

Domestic cats

Domestic cats had variable daily activity across all three years with a shift towards diurnal activity in 2019 that was not considered significant compared to 2016 or 2017 (Appendix D). Domestic cats had similar ranges for intraspecies temporal overlap, however the lowest overlap occurred in 2017 versus 2019 and the highest in 2016 versus 2017, although not significant (Figure 19). Temporal overlap with raccoons, opossums, and skunks seemed to gradually decrease from 2016 through 2017 and into 2019;

however, confidence intervals also overlap for all three years. In contrast, coyote temporal overlap seemed to decrease with cats more in 2017 than 2019; however, confidence intervals also overlap for all three years as well. Domestic cats only significantly increased overlap with humans from 2017 ((Δ-hat$_1$ = 0.072, 95% CI = [0, 0.171]) to 2019 (Δ-hat$_1$ = 0.445, 95% CI = [0.214, 0.677]), as a result of the increase in diurnal activity of cats in 2019 (Figure 24).

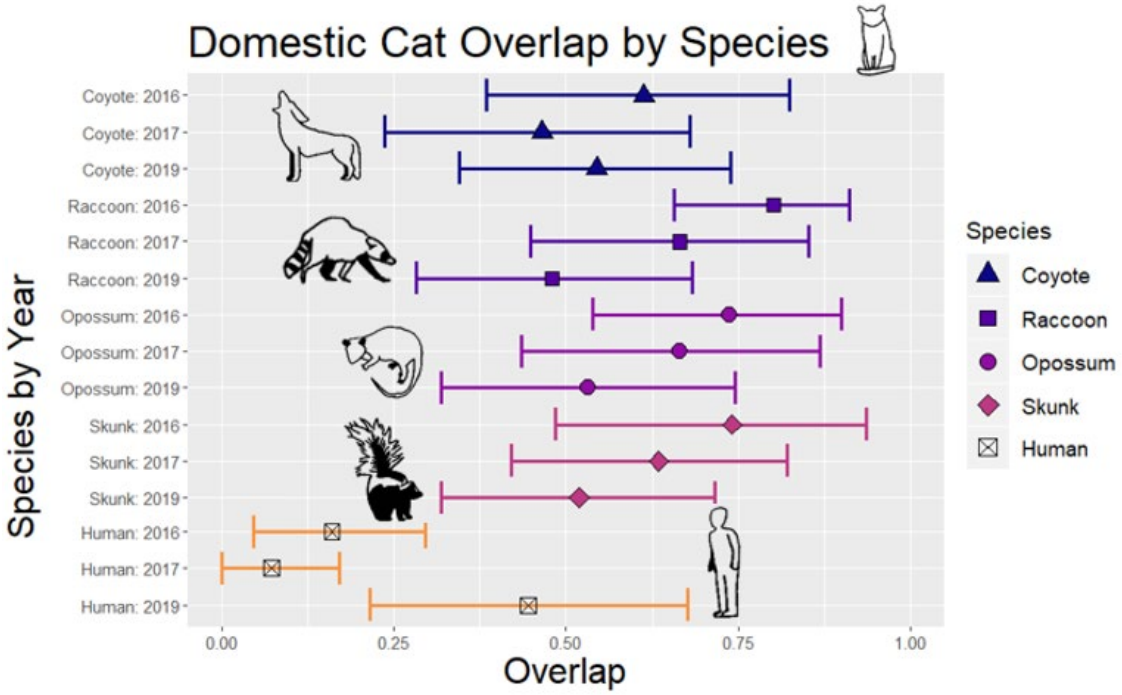

Figure 24. Temporal overlap between domestic cats and all other species across all survey years (2016, 2017, and 2019).

Discussion

I found that mammalian mesopredators changed their spatiotemporal activity in response to California's historic drought of 2012–2016. I had hypothesized that mammalian mesopredator spatiotemporal activity would overlap the most during the drought, especially in areas where coyotes and humans were present. Mammalian mesopredators did have high spatiotemporal overlap, but this occurred both during and after the drought. Additionally, mesopredators did not avoid coyotes during or following drought. Although I did not find evidence that mesopredators avoided coyotes, coyotes may have had greater overlap with mesopredators following the drought due to shifts in their spatial activity to be more around water sites and increased nocturnal activity. Additionally, I found that coyote and skunk spatiotemporal overlap with humans was greater during the drought compared to after, supporting the hypothesis that they may have taken more risks during times of resource scarcity.

Mesopredators responded to the drought in multiple ways, either by contracting activity around areas with available and historic water resources or by widening spatial and temporal activity as a means of increasing their search for limited resources. For instance, small mesopredator species (raccoons and opossums) were associated with wetland environments more during the drought, while domestic cats were associated with dryland agricultural sites during the drought, which suggests these species contracted around preferred resources (Gehring and Swihart 2003). On the other hand, coyotes were found more at water sites during drought recovery and post-drought; suggesting that

during the drought coyotes increases their spatial range to access more resources and only contracting around water resources when they were more available (McKinney and Smith 2007, Kluever et al. 2017). While Brawata and Neeman (2011) found that in Australia, dingoes (*Canis lupus dingo*) reduced red fox and feral cat detection at water sites, it may be unlikely that coyotes may be playing a similar role in shaping other mesopredators spatiotemporal activity at water sites during the drought. My results also suggest that coyotes and skunks may be avoiding humans during drought recovery, but not during the drought, which may indicate a shift in species risk taking behavior when resources are limited (Parren 2019). Mesopredator response to drought and drought recovery were most likely a mixture of both behavioral and demographic changes (Prugh et al. 2018).

The Role of Water

Wetland habitats shaped how mesopredators responded to drought. Raccoons were the only species found to spatially contract by using wetlands more during the drought (2016) compared to expanding habitat usage during drought recovery (2017) and beyond (2019). This may be a result of wetlands being a refugia for raccoons during drought conditions, as sticking to these wetland and riparian areas allows raccoons to buffer against limited water resources in other habitat types even during drier months (Lloyd 1947, Gehring and Swihart 2003, Abernethy et al. 2017). Wetlands also substantially increased opossum detection in drought sites, while having no impact at drought recovery sites. Opossums may benefit from wetland areas for foraging opportunities, especially when scavenging opportunities for herpetofauna and other invertebrates increases compared to dryland areas (Abernethy et al. 2017). Additionally,

domestic cat detection was found to be negatively associated with wetland habitats in 2016 sites, as cats were only found in agricultural areas in 2016 compared to 2017 and 2019. Cats may be benefiting from their associations with humans during the drought while avoiding wetland areas where mesopredators are more active. Finally, while striped skunk detection was seen to increase with wetlands during 2016, overall low detections across habitat types during the drought made this relationship unsubstantiated.

Interestingly, available surface water did not seem to have the same impact on mesopredator relationships as wetland habitat types. For instance, raccoons were found to have higher detection where surface water was available and present across all three drought conditions. This is unsurprising as raccoons often forage in and around open water sources and marshes as they provide both food and cover from predators (Craig and Golightly 2012). Thus, the inclusion of the surface water covariate across the climatic gradient of all three study years for raccoons suggests that aquatic environments play an important role regardless of drought.

Coyotes were the only other mesopredator to increase detection when surface water was available; however, this trend only appears in 2017-2019 sites following drought recovery. This may be a result of niche switching behavior following years of negatively being influenced by the drought. Following the drought, coyote populations may have recovered as a result of these ephemeral water sources increasing in drier areas, providing vegetation and habitat for a recovering small mammals prey base (McKinney and Smith 2007, Atwood et al. 2011, Dickman et al. 2011, Prugh et al. 2018). When taking the whole Central Valley into account, coyote detection at water was more likely,

even during the drought (Parren 2019). It is likely that the northern end of the Central Valley was less impacted by surface water loss compared to the southern end due to a milder climate and access to Northern Sierra run-off into the Sacramento River Delta (Durand et al. 2020).

Drought Limits the Impacts of Coyotes on Mesopredators

Compared to other mesopredators, coyotes may have responded differently to drought conditions by taking advantage of more varied habitat types and resources during the drought. This shift in activity could be a result of both demographic and behavioral changes. First, coyote detection, while constrained to certain sites, increased more during the drought (2016) compared to post-drought years (2019). This may be a result of coyotes being more rare visitors to a higher proportion of sites in 2016 compared to coyotes being more ubiquitous in 2019. In 2019, a much greater number of coyotes were detected compared to 2016, likely due to an increase in coyote pups during sample season following drought recovery (Sacks 2005). These juvenile coyotes may have influenced coyote detection both demographically – increasing the number of coyotes to be detected –as well as behaviorally. For instance, several juvenile coyotes were seen returning to camera sites to sniff and lick bait even after a majority of bait material had been consumed or dissipated. Coyote during the drought did not respond to bait in the same way, as there were likely fewer coyotes on the landscape to come across bait, and coyotes may have been traveling greater distances through a variety of habitats in order to meet energy needs. Additionally, coyotes were more active in the beginning of the season of 2016, possibly capturing a seasonal shift in activity where coyotes in earlier spring

months are more wide ranging and dispersing as they look for mates, while later deployment dates in 2019 captured a period of spatially constrained activity around pup-rearing (Bekoff and Wells 1982).

Even as coyote populations recovered during 2017 and into 2019, my results indicated that coyote presence did not influence mesopredator detection, at least within a 3-day detection period. It is likely that coyotes play a more fine-scale role in shifting mesopredator detection; contrary to my hypothesis, the drought may have reduced coyote overlap with mesopredator species due to a widening of coyote diurnal and spatial activity. Two-species occupancy modeling of coyote presence and detection on raccoons in the Central Valley suggested that raccoon detection around water increased when coyotes were absent during drought recovery in 2017 (Parren 2019). The increased coyote presence at surface water during drought recovery and into post drought supports that coyotes are more present at these water sites compared to during the drought, potentially negatively influencing raccoon detection following the drought. Additionally, coyote temporal activity and behavior shifted to being more nocturnal following drought recovery. For instance, coyotes exhibited a dramatic increase in temporal overlap with striped skunks in post-drought 2019 compared to during the drought in 2016. This suggests that, following the drought, coyotes increased their potential to run into a subordinate mesopredator species, potentially due to switching to exploit similar prey species like rodents (McKinney and Smith 2007, Robinson et al. 2014).

Human as Shields

As with coyotes, humans seemed to only influence certain mesopredators following the drought. Both coyotes and striped skunks had decreased detections following humans in 2017 and 2019. This may indicate that both species may have taken more risks during the drought, being more active in areas humans were present during the drought. This increase in boldness may be a response to obtain limited resources despite the risk of running into a human (Fox 2006). As both of these species are seen as pests or undesirable to humans, with conflict calls and killings of these species often being very high compared to other mesopredators (Rodewald and Gehrt 2014), it is no surprise that these species would unfavorably react to human presence, especially within more open grassland and agricultural lands that these species and humans prefer (Bergstrom et al. 2014). Coyote risk-taking may have been greater than skunks, as coyote diurnal activity created more potential temporal overlap for coyotes and humans during the drought, which may have contributed to coyotes becoming more nocturnal as drought conditions lessened in 2017 and 2019 and began temporally avoiding humans again (Nickel et al. 2020). Additionally, as coyote and skunk populations rebounded, more species may be spatially overlapping with humans than while detections and populations were low during the drought.

The only mesopredator that favorably responded to humans was domestic cats. While cats did not have a direct relationship with human presence, cats may have benefitted from human dominated agricultural lands during the drought as suggested by increases in their detections and presence. Additionally, cats were the only species to also

increase temporal overlap with humans post drought, switching from more nocturnal activity during the drought to being more diurnal. This may have been a result of coyotes becoming more nocturnal; thus, cats switching to being more diurnal may give them more chance to be around humans and be shielded from intraguild predation (Grubbs and Krausman 2009).

Management Implications

I found that drought may cause smaller mesopredators to restrict their spatiotemporal activity, while coyotes may be expanding their activity. For mesopredators that restrict to wetland areas (raccoons and opossums), there may be increased predation and scavenging of prey species such as waterbirds, rodents, and herpetofauna (Abernethy et al. 2017, Barbaree et al. 2020). Increasing and enhancing wetland habitat and surface water availability during the drought may benefit species populations that managers hope to increase, however, at the risk of greater predation from mesopredator populations.

In agricultural areas, drought may increase human-wildlife conflict as mesopredators may seek out anthropogenic food sources and coyotes may turn to preying on domestic animals (McKinney and Smith 2007, Schuette et al. 2013). Coyotes may also be drawn to agriculture areas during the drought to access water, as farmers had observed coyotes biting and destroying irrigation tubing and sprinklers (Baldwin et al. 2013, Ricardo Garcia, personal communication, 25 May, 2019). Farmers may attempt to eliminate mesopredators that feed on crops during times of drought; however, mesopredators might benefit farmers after drought as they feed on the abundance of

rodents that increase after winter rains (Roemer et al. 2009, Eagan II et al. 2011, Olson et al. 2012). Additionally, coyotes may be important for controlling populations of mesopredators, which can be nest predators of bird species and disease carriers (Soulé et al. 1988, Weinstein et al. 2018). Thus, facilitating population of coyotes may benefit ecosystems once drought recovery happens. More research is needed to understand how mammalian mesopredators are responding to drought, especially in human dominated lands. Increased drive for resources might drive human-wildlife conflict in urban areas, as species use urban water sources such as pools, lawns, and gardens to cool down and forage (B. Furnas, CDFW, unpublished data, Gehrt et al. 2010).

Conclusions

Droughts can have negative effects on mesopredator populations; however, quick recovery can follow. While drought can impact species, the onset might be slow, and populations and spatiotemporal activity may not change right away. As drought worsens, more species may become impacted and may exhibit riskier behavior in order to survive. Protection and management of wetland and riparian habitat is crucial to maintaining healthy and functioning ecosystems that impact the agricultural and working lands that surround them (Garone 2011). Enhancing riparian corridors throughout interconnected working lands may allow for mesopredator scavengers and predators of small mammals to provide services into the future and buffer against population crashes and booms during and following droughts.

Literature Cited

Abernethy, E. F., K. L. Turner, J. C. Beasley, and O. E. Rhodes. 2017. Scavenging along an ecological interface: utilization of amphibian and reptile carcasses around isolated wetlands. Ecosphere 8:e01989.

Adams, H. D., M. Guardiola-Claramonte, G. A. Barron-Gafford, J. C. Villegas, D. D. Breshears, C. B. Zou, P. A. Troch, and T. E. Huxman. 2009. Temperature sensitivity of drought-induced tree mortality portends increased regional die-off under global-change-type drought. Proceedings of the National Academy of Sciences 106:7063–7066.

Ancillotto, L., L. Santini, N. Ranc, L. Maiorano, and D. Russo. 2016. Extraordinary range expansion in a common bat: the potential roles of climate change and urbanisation. The Science of Nature 103:15.

Anderson, D. R., and K. P. Burnham. 2002. Avoiding Pitfalls When Using Information-Theoretic Methods. The Journal of Wildlife Management 66:912–918.

Arnold, T. W. 2010. Uninformative Parameters and Model Selection Using Akaike's Information Criterion. The Journal of Wildlife Management 74:1175–1178.

Asner, G. P., P. G. Brodrick, C. B. Anderson, N. Vaughn, D. E. Knapp, and R. E. Martin. 2016. Progressive forest canopy water loss during the 2012–2015 California drought. Proceedings of the National Academy of Sciences 113:E249–E255.

Atwood, T. C., T. L. Fry, and B. R. Leland. 2011. Partitioning of anthropogenic watering sites by desert carnivores. The Journal of Wildlife Management 75:1609–1615.

Bailey, R. G. 1980. Description of the Ecoregions of the United States. U.S. Department of Agriculture, Forest Service.

Baldwin, R. A., T. P. Salmon, R. H. Schmidt, and R. M. Timm. 2013. Wildlife pests of California agriculture: Regional variability and subsequent impacts on management. Crop Protection 46:29–37.

Barbaree, B. A., M. E. Reiter, C. M. Hickey, K. M. Strum, J. E. Isola, S. Jennings, L. M. Tarjan, C. M. Strong, L. E. Stenzel, and W. D. Shuford. 2020. Effects of drought on the abundance and distribution of non-breeding shorebirds in central California, USA. PLOS ONE 15:e0240931. Public Library of Science.

Beatty, W. S., J. C. Beasley, and O. E. Rhodes. 2013. Habitat selection by a generalist mesopredator near its historical range boundary. Canadian Journal of Zoology 92:41–48.

Bechtold, W. A., and P. L. Patterson, editors. 2005. The Enhanced Forest Inventory and Analysis Program--national Sampling Design and Estimation Procedures. USDA Forest Service, Southern Research Station.

Bekoff, M., and M. C. Wells. 1982. Behavioral Ecology of Coyotes: Social Organization, Rearing Patterns, Space Use, and Resource Defense. Zeitschrift für Tierpsychologie 60:281–305.

Bergstrom, B. J., L. C. Arias, A. D. Davidson, A. W. Ferguson, L. A. Randa, and S. R. Sheffield. 2014. License to Kill: Reforming Federal Wildlife Control to Restore Biodiversity and Ecosystem Function. Conservation Letters 7:131–142.

Brawata, R. L., and T. Neeman. 2011. Is water the key? Dingo management, intraguild interactions and predator distribution around water points in arid Australia. Wildlife Research 38:426–436.

Brown, J. H., T. J. Valone, and C. G. Curtin. 1997. Reorganization of an arid ecosystem in response to recent climate change. Proceedings of the National Academy of Sciences 94:9729–9733.

Carroll, C. 2007. Interacting Effects of Climate Change, Landscape Conversion, and Harvest on Carnivore Populations at the Range Margin: Marten and Lynx in the Northern Appalachians. Conservation Biology 21:1092–1104.

Catling, P. C. 1988. Similarities and contrasts in the diets of foxes, Vulpes vulpes, and cats, Felis catus, relative to fluctuating prey populations and drought. Wildlife Research 15:307–317.

Clavel, J., R. Julliard, and V. Devictor. 2011. Worldwide decline of specialist species: toward a global functional homogenization? Frontiers in Ecology and the Environment 9:222–228.

Cook, B. I., T. R. Ault, and J. E. Smerdon. 2015. Unprecedented 21st century drought risk in the American Southwest and Central Plains. Science Advances 1:e1400082–e1400082.

Craig, E. N., and R. T. Golightly. 2012. Coyotes and Mesopredators in the Coastal Wetland at Naval Base Ventura County, Point Mugu. <http://dspace.calstate.edu/handle/2148/938>. Accessed 17 Nov 2020.

Dai, A. 2013. Increasing drought under global warming in observations and models. Nature Climate Change 3:52–58.

DeVault, T. L., Z. H. Olson, J. C. Beasley, and O. E. Rhodes. 2011. Mesopredators dominate competition for carrion in an agricultural landscape. Basic and Applied Ecology 12:268–274.

Dickman, C. R., A. C. Greenville, B. Tamayo, and G. M. Wardle. 2011. Spatial dynamics of small mammals in central Australian desert habitats: the role of drought refugia. Journal of Mammalogy 92:1193–1209.

Durand, J. R., F. Bombardelli, W. E. Fleenor, Y. Henneberry, J. Herman, C. Jeffres, M. Leinfelder–Miles, J. R. Lund, R. Lusardi, A. D. Manfree, J. Medellín-Azuara, B. Milligan, and P. B. Moyle. 2020. Drought and the Sacramento-San Joaquin Delta, 2012–2016: Environmental Review and Lessons. San Francisco Estuary and Watershed Science 18. <https://escholarship.org/uc/item/6hq949t6>. Accessed 24 Nov 2020.

Durant, S. M. 1998. Competition refuges and coexistence: an example from Serengeti carnivores. Journal of Animal Ecology 67:370–386.

Eagan II, T. S., J. C. Beasley, Z. H. Olson, and O. E. Rhodes. 2011. Impacts of generalist mesopredators on the demography of small-mammal populations in fragmented landscapes. Canadian Journal of Zoology. NRC Research Press. <https://cdnsciencepub.com/doi/abs/10.1139/z11-045>. Accessed 24 Nov 2020.

Fedriani, J. M., T. K. Fuller, R. M. Sauvajot, and E. C. York. 2000. Competition and intraguild predation among three sympatric carnivores. Oecologia 125:258–270.

Fiske, I., and R. Chandler. 2011. unmarked: An R Package for Fitting Hierarchical Models of Wildlife Occurrence and Abundance. Journal of Statistical Software 43:1–23.

Fox, C. H. 2006. Coyotes and Humans: Can We Coexist? Proceedings of the Vertebrate Pest Conference 22. <https://escholarship.org/uc/item/6mx0f9pf>. Accessed 24 Nov 2020.

Garone, P. 2011. The Fall and Rise of the Wetlands of California's Great Central Valley. University of California Press.

Gehring, T. M., and R. K. Swihart. 2003. Body size, niche breadth, and ecologically scaled responses to habitat fragmentation: mammalian predators in an agricultural landscape. Biological Conservation 109:283–295.

Gehrt, S. D., and W. R. Clark. 2003. Raccoons, Coyotes, and Reflections on the Mesopredator Release Hypothesis. Wildlife Society Bulletin (1973-2006) 31:836–842.

Gehrt, S. D., and S. Prange. 2007. Interference competition between coyotes and raccoons: a test of the mesopredator release hypothesis. Behavioral Ecology 18:204–214.

Gehrt, S. D., S. P. D. Riley, and B. L. Cypher. 2010. Urban Carnivores: Ecology, Conflict, and Conservation. JHU Press.

Gompper, M. E. 2002. Top Carnivores in the Suburbs? Ecological and Conservation Issues Raised by Colonization of North-eastern North America by Coyotes: The expansion of the coyote's geographical range may broadly influence community structure, and rising coyote densities in the suburbs may alter how the general public views wildlife. BioScience 52:185–190.

Griffin, D., and K. J. Anchukaitis. 2014. How unusual is the 2012–2014 California drought? Geophysical Research Letters 9017–9023.

Grubbs, S. E., and P. R. Krausman. 2009. Observations of Coyote-Cat Interactions. The Journal of Wildlife Management 73:683–685.

Holt, R. D., and G. R. Huxel. 2007. Alternative Prey and the Dynamics of Intraguild Predation: Theoretical Perspectives. Ecology 88:2706–2712.

Howitt, R., J. Medellín-Azuara, D. MacEwan, J. R. Lund, and D. Sumner. 2014. Economic analysis of the 2014 drought for California agriculture. Center for Watershed Sciences University of California, Davis, CA.

Iknayan, K. J., and S. R. Beissinger. 2018. Collapse of a desert bird community over the past century driven by climate change. Proceedings of the National Academy of Sciences of the United States of America 115:8597–8602.

Jannett, F. J., M. R. Broschart, L. H. Grim, and J. P. Schaberl. 2007. Northerly Range Extensions of Mammalian Species in Minnesota. The American Midland Naturalist 158:168–176.

Johnson, W. E., and W. L. Franklin. 1994. Spatial resource partitioning by sympatric grey fox (Dusicyon griseus) and culpeo fox (Dusicyon culpaeus) in southern Chile. Canadian Journal of Zoology 72:1788–1793.

Kitchen, A. M., E. M. Gese, and E. R. Schauster. 1999. Resource partitioning between coyotes and swift foxes: space, time, and diet. Canadian Journal of Zoology 77:1645–1656.

Kluever, B. M., E. M. Gese, and S. J. Dempsey. 2017. Influence of free water availability on a desert carnivore and herbivore. Current Zoology 63:121–129. Oxford Academic.

Kowarik, I., and M. von der Lippe. 2018. Plant population success across urban ecosystems: A framework to inform biodiversity conservation in cities. Journal of Applied Ecology 55:2354–2361.

Kozlowski, A. J., E. M. Gese, and W. M. Arjo. 2008. Niche Overlap and Resource Partitioning Between Sympatric Kit Foxes and Coyotes in the Great Basin Desert of Western Utah. The American Midland Naturalist 160:191–208.

Larivière, S. 2004. Range expansion of raccoons in the Canadian prairies: review of hypotheses. Wildlife Society Bulletin 32:955–963.

Lesmeister, D. B., C. K. Nielsen, E. M. Schauber, and E. C. Hellgren. 2015. Spatial and temporal structure of a mesocarnivore guild in midwestern north America. Wildlife Monographs 191:1–61.

Lewis, J. C., K. L. Sallee, and R. T. Golightly. 1999. Introduction and Range Expansion of Nonnative Red Foxes (Vulpes vulpes) in California. The American Midland Naturalist 142:372–381.

Lund, J., J. Medellin-Azuara, J. Durand, and K. Stone. 2018. Lessons from California's 2012–2016 Drought. Journal of Water Resources Planning and Management 144:04018067. American Society of Civil Engineers.

MacKenzie, D. I., and L. L. Bailey. 2004. Assessing the fit of site-occupancy models. Journal of Agricultural, Biological, and Environmental Statistics 9:300–318.

MacKenzie, D. I., J. D. Nichols, J. A. Royle, K. H. Pollock, L. Bailey, and J. E. Hines. 2017. Occupancy Estimation and Modeling: Inferring Patterns and Dynamics of Species Occurrence. Elsevier.

MacLean, S. A., A. F. Rios Dominguez, P. de Valpine, and S. R. Beissinger. 2018. A century of climate and land-use change cause species turnover without loss of beta diversity in California's Central Valley. Global Change Biology.

Magle, S. B., S. A. Poessel, K. R. Crooks, and S. W. Breck. 2014. More dogs less bite: The relationship between human–coyote conflict and prairie dog colonies in an urban landscape. Landscape and Urban Planning 127:146–153.

Mawdsley, J. R., R. O'malley, and D. S. Ojima. 2009. A Review of Climate-Change Adaptation Strategies for Wildlife Management and Biodiversity Conservation. Conservation Biology 23:1080–1089.

Mazerolle MJ (2020). AICcmodavg: Model selection and multimodel inference based on (Q)AIC(c). R package version 2.3-1, <https://cran.r-project.org/package=AICcmodavg>.

McCain, C. M., and S. R. B. King. 2014. Body size and activity times mediate mammalian responses to climate change. Global Change Biology 20:1760–1769.

McKinney, T., and T. W. Smith. 2007. Diets of sympatric bobcats and coyotes during years of varying rainfall in central Arizona. Western North American Naturalist 67:8–15. Monte L. Bean Life Science Museum, Brigham Young University.

McNab, W. H., D. T. Cleland, J. A. Freeouf, J. E. Keys, G. J. Nowacki, and C. A. Carpenter. 2007. Description of ecological subregions: sections of the conterminous United States. General Technical Report WO-76B 76B:1–82.

Meredith, M., and M. Ridout. 2014. Overview of the overlap package. R. Proj. 1–9.

Moritz, C., J. L. Patton, C. J. Conroy, J. L. Parra, G. C. White, and S. R. Beissinger. 2008. Impact of a Century of Climate Change on Small-Mammal Communities in Yosemite National Park, USA. Science 322:261–264.

Mueller, M. A., D. Drake, and M. L. Allen. 2018. Coexistence of coyotes (Canis latrans) and red foxes (Vulpes vulpes) in an urban landscape. PLOS ONE 13:e0190971.

Nickel, B. A., J. P. Suraci, M. L. Allen, and C. C. Wilmers. 2020. Human presence and human footprint have non-equivalent effects on wildlife spatiotemporal habitat use. Biological Conservation 241:108383.

Niedballa, J., R. Sollmann, A. Courtiol, and A. Wilting. 2016. camtrapR: an R package for efficient camera trap data management. Methods in Ecology and Evolution 7:1457–1462.

Nouvellet, P., G. S. A. Rasmussen, D. W. Macdonald, and F. Courchamp. 2012. Noisy clocks and silent sunrises: measurement methods of daily activity pattern. Journal of Zoology 286:179–184.

Olson, Z. H., J. C. Beasley, T. L. DeVault, and O. E. Rhodes. 2012. Scavenger community response to the removal of a dominant scavenger. Oikos 121:77–84.

Parren, M. 2019. Drought and coyotes mediate the relationship between mesopredators and human disturbance in California. HSU theses and projects. <https://digitalcommons.humboldt.edu/etd/349>.

Pereira, H. M., G. C. Daily, and J. Roughgarden. 2004. A Framework for Assessing the Relative Vulnerability of Species to Land-Use Change. Ecological Applications 14:730–742.

Prugh, L. R., N. Deguines, J. B. Grinath, K. N. Suding, W. T. Bean, R. Stafford, and J. S. Brashares. 2018. Ecological winners and losers of extreme drought in California. Nature Climate Change 8:819–824.

Prugh, L. R., C. J. Stoner, C. W. Epps, W. T. Bean, W. J. Ripple, A. S. Laliberte, and J. S. Brashares. 2009. The Rise of the Mesopredator. BioScience 59:779–791.

R Core Team (2014). R: A language and environment for statistical computing. R Foundation for Statistical Computing, Vienna, Austria. <http://www.R-project.org/>.

Rich, L. N., B. J. Furnas, J. S. Brashares, S. R. Beissinger, and C. A. Cordova. 2018. Evaluating mammalian diversity in the Mojave Desert and Great Valley ecoregions of California using camera trap surveys.

Ridout, M. S., and M. Linkie. 2009. Estimating overlap of daily activity patterns from camera trap data. Journal of Agricultural, Biological, and Environmental Statistics 14:322–337.

Ritchie, E. G., and C. N. Johnson. 2009. Predator interactions, mesopredator release and biodiversity conservation. Ecology Letters 12:982–998.

Robinson, Q. H., D. Bustos, and G. W. Roemer. 2014. The application of occupancy modeling to evaluate intraguild predation in a model carnivore system. Ecology 95:3112–3123.

Rodewald, A. D., and S. D. Gehrt. 2014. Wildlife Population Dynamics in Urban Landscapes. Pages 117–147 *in* R. A. McCleery, C. E. Moorman, and M. N. Peterson, editors. Urban Wildlife. Springer US, Boston, MA.

<http://link.springer.com/10.1007/978-1-4899-7500-3_8>. Accessed 25 Nov 2020.

Roemer, G. W., M. E. Gompper, and B. Van Valkenburgh. 2009. The Ecological Role of the Mammalian Mesocarnivore. BioScience 59:165–173. Oxford Academic.

Rosenzweig, M. L. 1966. Community Structure in Sympatric Carnivora. Journal of Mammalogy 47:602–612.

RStudio Team (2020). RStudio: Integrated Development for R. RStudio. PBC. Boston, MA <http://www.rstudio.com/>.

Roussere, G. P., W. J. Murray, C. B. Raudenbush, M. J. Kutilek, D. J. Levee, and K. R. Kazacos. 2003. Raccoon Roundworm Eggs near Homes and Risk for Larva Migrans Disease, California Communities. Emerging Infectious Diseases 9:1516–1522.

Sacks, B. N. 2005. Reproduction and Body Condition of California Coyotes (Canis latrans). Journal of Mammalogy 86:1036–1041.

Sala, O. E., F. S. Chapin, Iii, J. J. Armesto, E. Berlow, J. Bloomfield, R. Dirzo, E. Huber-Sanwald, L. F. Huenneke, R. B. Jackson, A. Kinzig, R. Leemans, D. M. Lodge, H. A. Mooney, M. Oesterheld, N. L. Poff, M. T. Sykes, B. H. Walker, M. Walker, and D. H. Wall. 2000. Global Biodiversity Scenarios for the Year 2100. Science 287:1770–1774.

Scanlon, B. R., C. C. Faunt, L. Longuevergne, R. C. Reedy, W. M. Alley, V. L. McGuire, and P. B. McMahon. 2012. Groundwater depletion and sustainability of irrigation in the US High Plains and Central Valley. Proceedings of the National Academy of Sciences 109:9320–9325.

Schloss, C. A., T. A. Nuñez, and J. J. Lawler. 2012. Dispersal will limit ability of mammals to track climate change in the Western Hemisphere. Proceedings of the National Academy of Sciences 109:8606–8611.

Schneider, S. H., T. L. Root, and T. Root. 2002. Wildlife Responses to Climate Change: North American Case Studies. Island Press.

Scholz, F. and A. Zhu (2019). kSamples: K-Sample Rank Tests and their Combinations. R package version 1.2-9. <https://CRAN.R-project.org/package=kSamples>.

Schuette, P., A. P. Wagner, M. E. Wagner, and S. Creel. 2013. Occupancy patterns and niche partitioning within a diverse carnivore community exposed to anthropogenic pressures. Biological Conservation 158:301–312.

Shamoon, H., D. Saltz, and T. Dayan. 2017. Fine-scale temporal and spatial population fluctuations of medium sized carnivores in a Mediterranean agricultural matrix. Landscape Ecology 32:1243–1256.

Smith, J. A., A. C. Thomas, T. Levi, Y. Wang, and C. C. Wilmers. 2018. Human activity reduces niche partitioning among three widespread mesocarnivores. Oikos 127:890–901.

Smith, W. P., and P. A. Zollner. 2005. Sustainable management of wildlife habitat and risk of extinction. Biological Conservation 125:287–295.

Soulard, C. E., and T. S. Wilson. 2015. Recent land-use/land-cover change in the Central California Valley. <https://pubag.nal.usda.gov/catalog/1229956>. Accessed 11 Nov 2020.

Soulé, M. E., D. T. Bolger, A. C. Alberts, J. Wrights, M. Sorice, and S. Hill. 1988. Reconstructed Dynamics of Rapid Extinctions of Chaparral-Requiring Birds in Urban Habitat Islands. Conservation Biology 2:75–92.

Swain, D. L. 2015. A tale of two California droughts: Lessons amidst record warmth and dryness in a region of complex physical and human geography. Geophysical Research Letters 42:9999–10,003.

Terborgh, J., and J. A. Estes. 2013. Trophic Cascades: Predators, Prey, and the Changing Dynamics of Nature. Island Press.

Tevis, L. 1947. Summer Activities of California Raccoons. Journal of Mammalogy 28:323–332. [American Society of Mammalogists, Oxford University Press].

Theimer, T. C., A. C. Clayton, A. Martinez, D. L. Peterson, and D. L. Bergman. 2015. Visitation rate and behavior of urban mesocarnivores differs in the presence of two common anthropogenic food sources. Urban Ecosystems 18:895–906.

Thorne, K. M., J. Y. Takekawa, and D. L. Elliott-Fisk. 2012. Ecological Effects of Climate Change on Salt Marsh Wildlife: A Case Study from a Highly Urbanized Estuary. Journal of Coastal Research 28:1477–1487. Allen Press.

Traill, L. W., M. L. M. Lim, N. S. Sodhi, and C. J. A. Bradshaw. 2010. Mechanisms driving change: altered species interactions and ecosystem function through global warming. Journal of Animal Ecology 79:937–947.

Travis, J. M. J. 2003. Climate change and habitat destruction: a deadly anthropogenic cocktail. Proceedings of the Royal Society of London B: Biological Sciences 270:467–473.

Tylianakis, J. M., R. K. Didham, J. Bascompte, and D. A. Wardle. 2008. Global change and species interactions in terrestrial ecosystems. Ecology Letters 11:1351–1363.

Walther, G.-R., E. Post, P. Convey, A. Menzel, C. Parmesan, T. J. C. Beebee, J.-M. Fromentin, O. Hoegh-Guldberg, and F. Bairlein. 2002. Ecological responses to recent climate change. Nature 416:389–395.

Wang, Y., M. L. Allen, and C. C. Wilmers. 2015. Mesopredator spatial and temporal responses to large predators and human development in the Santa Cruz Mountains of California. Biological Conservation 190:23–33.

Weinstein, S. B., C. W. Moura, J. F. Mendez, and K. D. Lafferty. 2018. Fear of feces? Tradeoffs between disease risk and foraging drive animal activity around raccoon latrines. Oikos 127:927–934.

Williams, A. P., R. Seager, J. T. Abatzoglou, B. I. Cook, J. E. Smerdon, and E. R. Cook. 2015. Contribution of anthropogenic warming to California drought during 2012–2014. Geophysical Research Letters 42:6819–6828.

Appendix A

Appendix A. Camera deployment, placement, and settings for Terrestrial Species Stressor Monitoring sites in California's Central Valley used during 2016, 2017, and 2019.

Recoynx PC900 camera settings to collect digital photos of mammalian mesopredators in California's Central Valley in 2016, 2017, and 2019. Adapted from Parren, Molly K., "Drought and coyotes mediate the relationship between mesopredators and human disturbance in California" (2019). HSU theses and projects. 349. https://digitalcommons.humboldt.edu/etd/349. CC BY-NC.

Tab	Sub-category	Selection
Trigger	Motion Sensor	ON
	Sensitivity	High
	Pictures per trigger	3
	Picture Interval	1 second
	Quiet Period	No Delay
Time Lapse	AM Period	OFF
	PM Period	OFF
Resolution		1080p
Night Mode	Balanced	
	Illuminator	ON
Date/Time/Temp	Temp	Celsius
Codeloc		None
User Label	Change	HexID (12345A)

Recoynx PC900 set-up at Central Valley sites. Cameras were attached to the top (~1 m) of a T-post and stabilized using a board, bungee cords, and cable locks (left). T-posts were angled down to have cameras face the ground where bait was placed. A can of fishy cat food was emptied in the middle of the camera frame and spread around over covered with vegetation to prolong animals near camera sites. Black arrow points to bait location during camera set-up (top-right) and during a coyote detection 5 days later (bottom right).

Appendix B

Appendix B. Covariates by survey year and Pearson correlation values for single-season single species occupancy modeling.

Covariates across survey years. Wetland is classified by whether a camera was within either a wetland, riparian, or rice cultivated area. Water is classified by whether surface water was readily available to mesopredators at the beginning of the survey period. Human and coyote presence are classified by whether humans or coyotes were detected at a site. Date is classified as the Julian date range cameras were set up in. Bait is classified by which baits were present at the start of the survey; either cat food (CF), peanut butter and oats (PBO), or salt lick (SL).

Camera Survey	Year	Wetland	Water	Human Presence	Coyote Presence	Date	Bait
Drought (n = 22)	2016	13	5	22	5	Mar-Jul	CF, PBO, SL
Recovery (n = 23)	2017	13	5	23	8	Apr-Jun	CF, PBO, SL
Resurvey 2016 (n = 22)	2019	13	15	22	11	May-Aug	CF
Resurvey 2017 (n = 23)	2019	13	12	23	8	May-Aug	CF

Pearson correlation coefficients for wetland, available surface water, and Julian date detection covariates for 2016-2019 survey season. Wetland habitat types did not change between survey years, while available surface water and date of camera placement did. Pearson coefficient (r) values ≥ |0.70| are considered moderately correlated.

	Wetland	Water (2016)	Water (2019)	Date (2016)	Date (2019)
Wetland		0.45	0.62	-0.16	-0.33
Water (2016)			0.14	-0.49	-0.2
Water (2019)				0.13	-0.58
Date (2016)					0.01
Date (2019)					

Pearson correlation coefficients for wetland, available surface water, and Julian date detection covariates for 2017-2019 survey season. Wetland habitat types did not change between survey years, while available surface water and date of camera placement did. Pearson coefficient (r) values ≥ |0.70| are considered moderately correlated.

	Wetland	Water (2017)	Water (2019)	Date (2017)	Date (2019)
Wetland		0.04	0.39	0.35	0.05
Water (2017)			0.08	-0.22	0.14
Water (2019)				-0.14	-0.07
Date (2017)					-0.08
Date (2019)					

Appendix C

Appendix C. Single species multi-season occupancy candidate model sets for coyotes, raccoons, opossums, striped skunks, and domestic cats for 2016-2019 and 2017-2019 survey seasons.

Single species multi-season occupancy candidate model sets for coyotes, raccoons, opossums, striped skunks, and domestic cats. Two tables exist for each species, one representing the 2016-2019 sites, the other representing 2017-2019 sites. Variables include initial occupancy (psi, ψ), colonization (gamma, γ), extinction (epsilon, ε) and detection (p). Covariates included are wetland (wet), available surface water (water), year, human presence (hum), coyote presence (coy), Julian date (date), and bait decay (bait). When interaction terms between year and wet, water, hum, and coy were included in the model, both covariates and the interaction term were included as a variable (ex. p(year:hum) includes year + hum +year*hum for detection). Only variables with an included covariate were included in model names, all other variables were still included in the model but did not have a covariate (ex. when ψ(.) or initial occupancy had no covariates). The null model is the model with no included covariates (ψ(.) γ(.) ε(.) p(.)), and the global model is the model that includes all appropriate covariates for each variable. Interaction terms were left out of the global model due to problems with goodness of fit.

Included for each model is the number of parameters (K), Akaike's Information Criterion for small sample size (AICc), change in AICc (Delta_AICc), model weight (AICcWt), cumulative weight (Cum.Wt), and -2*log likelihood (LL). Global models were used to determine the goodness of fit for each candidate model set using c-hat values estimated from using bootstrapping (n = 99). If c-hat was greater than 1, quasi-Akaike's Information Criterion for small sample sizes were used to calculate model ranking (QAICc). If c-hat was below 1, c-hat was set to 1 and AICc was used instead. Top models for each year are highlighted in gray and were selected following the same protocol, selecting for models 1) within top 2 Delta_AICc, 2) with the most general model (greatest K), and 3) with the most informative covariates (β confidence intervals did not cross zero).

Coyotes:

Candidate model set for coyote occupancy models for 2016 and 2019. C-hat is 0.82. Top model is highlighted in gray. Global model is ψ(wet + water), γ(wet +water), ε(wet + water), p(wet + water + year + hum + date + bait).

Model Name	K	AICc	Delta_AICc	AICcWt	Cum.Wt	LL
ψ(water) p(date)	7	221.24	0	0.24	0.24	-99.62
ψ(water)	6	221.29	0.05	0.24	0.48	-101.84
ψ(water) p(year+date)	8	221.46	0.22	0.22	0.7	-97.19
p(year:water)	7	223.49	2.25	0.08	0.78	-100.74
ψ(water) γ(wet) p(date)	8	224.09	2.85	0.06	0.84	-98.51
ψ(wet+water)	7	225.69	4.45	0.03	0.86	-101.84
ψ(water) p(date+bait)	8	225.77	4.53	0.03	0.89	-99.35
ψ(wet+water) p(date)	8	226.32	5.08	0.02	0.91	-99.62
ψ(water) p(year+water+date)	9	226.45	5.21	0.02	0.92	-96.72
p(date)	5	227.2	5.96	0.01	0.94	-106.72
Null	4	227.35	6.11	0.01	0.95	-108.5
γ(wet)	5	227.7	6.46	0.01	0.96	-106.97
ψ(water) γ(wet) ε(wet) p(date)	9	228.99	7.75	0.01	0.96	-98
γ(water)	5	229.23	7.99	0	0.97	-107.74
ψ(wet)	5	229.53	8.29	0	0.97	-107.89
ε(wet)	5	229.62	8.38	0	0.98	-107.93
ε(water)	5	229.78	8.54	0	0.98	-108.01
ψ(wet) p(date)	6	229.79	8.55	0	0.98	-106.1
p(wet)	5	230.01	8.77	0	0.99	-108.13
p(year)	5	230.07	8.83	0	0.99	-108.16
p(bait)	5	230.22	8.98	0	0.99	-108.24
p(water)	5	230.52	9.28	0	0.99	-108.38
p(hum)	5	230.66	9.42	0	1	-108.46
γ(wet+water)	6	230.73	9.5	0	1	-106.57
ψ(water)p(year:water)	9	233.06	11.82	0	1	-100.03

Model Name	K	AICc	Delta_AICc	AICcWt	Cum.Wt	LL
ε(wet+water)	6	233.29	12.05	0	1	-107.84
p(year:wet)	7	233.35	12.11	0	1	-105.67
ψ(water) p(year:water+date)	10	233.37	12.13	0	1	-96.69
p(year:hum)	7	238.29	17.05	0	1	-108.15
p(wet+water+year+date+bait)	9	239.05	17.81	0	1	-103.02
Global	20	1068.93	847.69	0	1	-94.47

Candidate model set for coyote occupancy models for 2017 and 2019. C-hat is 0.72. Top model is highlighted in gray. Global model is ψ(wet + water), γ(wet + water), ε(wet + water), p(wet + water + year + hum + date + bait).

Model Name	K	AICc	Delta_AICc	AICcWt	Cum.Wt	LL
p(water+hum+bait)	7	219.18	0	0.36	0.36	-98.86
ε(water) p(water+hum+bait)	8	220.61	1.44	0.18	0.54	-97.16
ε(wet) p(water+hum+bait)	8	221.22	2.04	0.13	0.67	-97.47
p(year:water+hum+bait)	9	221.65	2.47	0.11	0.78	-94.9
ε(water+wet) p(water+hum+bait)	9	221.73	2.56	0.1	0.88	-94.94
p(water+year+hum+bait)	8	222.67	3.49	0.06	0.94	-98.19
ε(water) p(year:water+hum+bait)	10	224.67	5.49	0.02	0.97	-93.17
γ(water) ε(water) p(water+hum+bait)	9	226.09	6.92	0.01	0.98	-97.12
p(year:water)	7	226.4	7.22	0.01	0.99	-102.46
p(water+bait)	6	228.36	9.18	0	0.99	-105.56
ψ(water) p(water+hum+bait)	9	229.11	9.93	0	0.99	-98.63
p(water)	5	230.09	10.91	0	1	-108.28
p(bait)	5	231.02	11.84	0	1	-108.75
ε(wet+water)	6	232.61	13.43	0	1	-107.68
Null	4	232.79	13.61	0	1	-111.28
ε(water)	5	232.86	13.68	0	1	-109.66

Model Name	K	AICc	Delta_AICc	AICcWt	Cum.Wt	LL
γ(wet)	5	233.37	14.19	0	1	-109.92
ε(wet)	5	233.77	14.59	0	1	-110.12
p(hum)	5	234.07	14.89	0	1	-110.27
p(wet)	5	235.11	15.93	0	1	-110.79
ψ(water) p(year:water+hum+bait)	11	235.35	16.17	0	1	-94.67
p(year)	5	235.53	16.35	0	1	-111
p(date)	5	235.68	16.5	0	1	-111.07
ψ(wet)	5	235.84	16.66	0	1	-111.15
γ(water)	5	236.02	16.84	0	1	-111.25
γ(wet+water)	6	236.89	17.71	0	1	-109.82
p(wet+water+year+date+bait)	9	238.65	19.48	0	1	-103.4
ψ(water)	6	239.23	20.05	0	1	-110.99
ψ(water) γ(water) ε(water) p(water+hum+bait)	11	239.77	20.59	0	1	-96.89
p(year:hum)	7	240.83	21.66	0	1	-109.68
p(year:wet)	7	240.87	21.7	0	1	-109.7
ψ(wet+water)	7	242.59	23.42	0	1	-110.56
Global	20	625.62	406.44	0	1	-82.81

Raccoons:

Candidate model set for raccoon occupancy models for 2016 and 2019. C-hat is 0.94. Top model is highlighted in gray. Global model is ψ(wet + water), γ(wet + water), ε(wet + water), p(wet + water + year + hum + coy + date + bait).

Model Name	K	AICc	Delta_AICc	AICcWt	Cum.Wt	LL
ψ(wet) p(water+bait)	7	326.39	0	0.36	0.36	-152.19
p(water+bait)	6	326.77	0.38	0.3	0.66	-154.58
ψ(water) p(water+bait)	8	328.88	2.49	0.1	0.77	-150.9
p(wet+water+year+bait)	9	329.25	2.86	0.09	0.85	-148.12
p(water+date+bait)	7	329.52	3.13	0.08	0.93	-153.76
p(water+hum+bait)	7	330.81	4.42	0.04	0.97	-154.41
ψ(wet) p(bait)	6	332.97	6.58	0.01	0.98	-157.69
p(bait)	5	334.04	7.65	0.01	0.99	-160.14
ψ(wet) p(wet+water+date+bait)	9	335.33	8.94	0	0.99	-151.16
ψ(wet) p(year:water+bait)	9	336.74	10.35	0	1	-151.87
p(water)	5	337.89	11.5	0	1	-162.07
ψ(wet+water) p(bait)	8	339.53	13.14	0	1	-156.23
ψ(water) p(wet+water+date+bait)	10	339.62	13.23	0	1	-149.81
ψ(wet) ε(wet) p(wet+water+date+bait)	10	340.35	13.96	0	1	-150.17
ψ(wet) p(year:hum+water+bait)	10	343.13	16.74	0	1	-151.57
ψ(wet)	5	343.53	17.14	0	1	-164.89
ψ(wet) p(year:coy+water+bait)	10	343.61	17.22	0	1	-151.81
p(wet)	5	344.11	17.72	0	1	-165.18
p(hum)	5	344.37	17.98	0	1	-165.31
ψ(water)	6	344.67	18.28	0	1	-163.54
Null	4	345.05	18.66	0	1	-167.35
p(year)	5	345.47	19.08	0	1	-165.86
p(year:wet)	7	345.53	19.14	0	1	-161.77
p(year:water)	7	345.55	19.16	0	1	-161.78
p(water+hum+coy+date+bait)	10	345.62	19.23	0	1	-152.81

Model Name	K	AICc	Delta_AICc	AICcWt	Cum.Wt	LL
p(date)	5	345.76	19.37	0	1	-166.01
ε(wet)	5	346.48	20.09	0	1	-166.36
γ(water)	5	347.18	20.79	0	1	-166.72
ψ(wet) γ(water) ε(wet) p(wet+water+date+bait)	11	347.55	21.16	0	1	-149.57
ε(water)	5	347.94	21.55	0	1	-167.09
p(coy)	5	348.31	21.92	0	1	-167.28
γ(wet)	5	348.39	22	0	1	-167.32
ψ(wet+water)	7	348.87	22.48	0	1	-163.44
p(year:hum)	7	349.02	22.64	0	1	-163.51
ε(wet+water)	6	350.23	23.84	0	1	-166.32
γ(wet+water)	6	350.55	24.17	0	1	-166.48
p(year:coy)	7	353.57	27.18	0	1	-165.79
Global	18	548.16	221.77	0	1	-142.08

Candidate model set for raccoon occupancy models for 2017 and 2019. C-hat is 1.22. Top model is highlighted in gray. Global model is ψ(wet + water), γ(wet + water), ε(wet + water), p(wet + water + year + hum + coy + date + bait).

Model Name	K	QAICc	Delta_QAICc	QAICcWt	Cum.Wt	Quasi.LL
p(water)	6	269.72	0	0.21	0.21	-126.24
p(year)	6	270.86	1.14	0.12	0.33	-126.81
Null	5	271.53	1.81	0.09	0.42	-129
γ(wet) p(water)	7	271.73	2.01	0.08	0.5	-125.13
p(water+hum)	7	272.2	2.48	0.06	0.56	-125.37
p(hum)	6	272.48	2.75	0.05	0.62	-127.61
γ(wet)	6	272.79	3.06	0.05	0.66	-127.77
p(water+year)	7	273.09	3.37	0.04	0.7	-125.81
p(bait)	6	273.23	3.51	0.04	0.74	-127.99

Model Name	K	QAICc	Delta_QAICc	QAICcWt	Cum.Wt	Quasi.LL
ψ(wet) p(water)	7	273.75	4.03	0.03	0.77	-126.14
p(date)	6	274.1	4.37	0.02	0.79	-128.42
ε(water)	6	274.46	4.74	0.02	0.81	-128.6
p(year:hum)	8	274.55	4.83	0.02	0.83	-124.13
ψ(water) p(water)	8	274.68	4.96	0.02	0.85	-124.2
γ(wet) p(water+hum)	8	274.81	5.09	0.02	0.87	-124.26
ψ(wet)	6	275.02	5.29	0.02	0.88	-128.88
ε(wet)	6	275.1	5.38	0.01	0.9	-128.93
p(coy)	6	275.18	5.46	0.01	0.91	-128.96
γ(water)	6	275.19	5.47	0.01	0.92	-128.97
p(wet)	6	275.2	5.48	0.01	0.94	-128.98
γ(wet) ε(water) p(water)	8	275.7	5.98	0.01	0.95	-124.71
γ(wet) p(water+year)	8	275.79	6.06	0.01	0.96	-124.75
p(water+hum+bait)	8	276.02	6.3	0.01	0.97	-124.87
p(water+year+hum)	8	276.27	6.55	0.01	0.98	-124.99
ψ(water)	7	276.75	7.03	0.01	0.98	-127.64
γ(wet+water)	7	276.96	7.23	0.01	0.99	-127.74
p(year:water)	8	277.89	8.17	0	0.99	-125.8
ε(wet+water)	7	278.47	8.75	0	0.99	-128.5
p(year:coy)	8	278.68	8.96	0	1	-126.2
p(year:wet)	8	279.14	9.42	0	1	-126.43
ψ(wet+water)	8	280.13	10.41	0	1	-126.92
ψ(wet) γ(wet) e (water) p(water)	9	281.02	11.3	0	1	-124.59
p(wet+water+year+date+bait)	10	286.7	16.98	0	1	-124.18
Global	19	530.11	260.39	0	1	-119.39

Opossums:

Candidate model set for opossum occupancy models for 2016 and 2019. C-hat is 1.59. Top model is highlighted in gray. Global model is ψ(wet + water), γ(wet + water), ε(wet + water), p(wet + water + year + hum + coy + date + bait).

Model Name	K	QAICc	Delta_QAICc	QAICcWt	Cum.Wt	Quasi.LL
p(bait)	6	132.56	0	0.25	0.25	-57.48
p(wet+bait)	7	133.86	1.3	0.13	0.38	-55.93
ψ(wet)	6	134.17	1.61	0.11	0.5	-58.29
Null	5	134.26	1.7	0.11	0.6	-60.25
p(wet)	6	135.03	2.47	0.07	0.68	-58.72
p(date)	6	135.86	3.3	0.05	0.72	-59.13
p(year)	6	136.3	3.74	0.04	0.76	-59.35
ψ(wet) p(wet+bait)	8	136.63	4.07	0.03	0.8	-54.78
ε(water)	6	136.75	4.19	0.03	0.83	-59.57
p(wet+date+bait)	8	136.94	4.38	0.03	0.86	-54.93
p(hum)	6	136.95	4.39	0.03	0.88	-59.68
p(coy)	6	137.71	5.15	0.02	0.9	-60.06
γ(wet)	6	137.75	5.19	0.02	0.92	-60.08
γ(water)	6	137.77	5.21	0.02	0.94	-60.08
p(water)	6	138.08	5.52	0.02	0.96	-60.24
ε(wet)	6	138.1	5.54	0.02	0.97	-60.25
ψ(water)	7	139.25	6.69	0.01	0.98	-58.63
p(year:wet)	8	140.28	7.72	0.01	0.99	-56.6
ε(wet+water)	7	141.15	8.59	0	0.99	-59.57
ψ(wet) ε(water) p(wet+bait)	9	141.17	8.61	0	0.99	-54.09
γ(wet+water)	7	142.04	9.48	0	1	-60.02
ψ(wet+water)	8	142.89	10.33	0	1	-57.91
p(year:water)	8	143.05	10.49	0	1	-57.99
p(year:coy)	8	144.23	11.67	0	1	-58.58
p(year:hum)	8	144.84	12.28	0	1	-58.88

Model Name	K	QAICc	Delta_QAICc	QAICcWt	Cum.Wt	Quasi.LL
p(wet+water+year+date+bait)	10	146.51	13.95	0	1	-53.26
ψ(wet) γ(wet) ε(water) p(wet+bait)	10	147.96	15.4	0	1	-53.98
Global	19	517.44	384.88	0	1	-49.72

Candidate model set for opossum occupancy models 2017 and 2019. C-hat is 0.23. Top model is highlighted in gray. Global model is ψ(wet + water), γ(wet + water), ε(wet + water), p(wet + water + year + hum + coy + date + bait).

Model Name	K	AICc	Delta_AICc	AICcWt	Cum.Wt	LL
γ(wet) p(date)	6	248.28	0.02	0.33	0.67	-115.52
p(date)	5	250.57	2.31	0.11	0.77	-118.52
γ(wet+water) ε(water) p(date)	8	251.45	3.19	0.07	0.84	-112.58
ψ(wet) γ(wet+water) p(date)	8	251.63	3.37	0.06	0.9	-112.67
γ(wet+water) p(date+year)	8	252.65	4.39	0.04	0.94	-113.18
γ(wet+water) p(wet+water+date+bait)	10	254.3	6.03	0.02	0.95	-107.98
p(year)	5	254.82	6.56	0.01	0.97	-120.64
p(wet+water+year+date+bait)	9	255.89	7.63	0.01	0.97	-112.02
p(bait)	5	256.24	7.97	0.01	0.98	-121.35
γ(wet+water)	6	256.79	8.52	0	0.98	-119.77
p(year:water)	7	256.98	8.71	0	0.99	-117.75
γ(wet)	5	257.43	9.17	0	0.99	-121.95
p(year:coy)	7	259.23	10.96	0	0.99	-118.88
Null	4	259.67	11.41	0	1	-124.73
γ(water)	5	260.33	12.06	0	1	-123.4
p(year:wet)	7	260.69	12.42	0	1	-119.61
p(water)	5	260.73	12.47	0	1	-123.6
ε(water)	5	261.25	12.99	0	1	-123.86
ψ(wet)	5	261.55	13.29	0	1	-124.01
ψ(water)	6	262.14	13.87	0	1	-122.44

Model Name	K	AICc	Delta_AICc	AICcWt	Cum.Wt	LL
p(hum)	5	262.26	14	0	1	-124.36
p(year:hum)	7	262.3	14.04	0	1	-120.42
p(wet)	5	262.78	14.51	0	1	-124.62
ε(wet)	5	262.85	14.58	0	1	-124.66
p(coy)	5	262.97	14.71	0	1	-124.72
ε(wet+water)	6	264.97	16.71	0	1	-123.86
ψ(wet+water)	7	265.85	17.58	0	1	-122.19
p(wet+water+date+bait)	8	333.79	85.53	0	1	-153.36
Global	18	413.61	165.35	0	1	-103.31

Striped skunks:

Candidate model set for striped skunk occupancy models for 2016 and 2019. Top model is highlighted in gray. C-hat is 0.55. Global model is ψ(wet + water), γ(wet + water), ε(wet + water), p(wet + water + year + hum + coy + date + bait).

Model Name	K	AICc	Delta_AICc	AICcWt	Cum.Wt	LL
p(year)	5	206.25	0	0.16	0.16	-96.25
p(wet+year)	6	206.77	0.52	0.12	0.28	-94.59
p(year:wet)	7	207.25	1	0.1	0.38	-92.62
p(wet)	5	207.58	1.34	0.08	0.46	-96.92
p(water)	5	207.84	1.6	0.07	0.53	-97.05
p(wet+year+bait)	7	207.98	1.73	0.07	0.6	-92.99
p(wet+bait)	6	208.22	1.98	0.06	0.66	-95.31
ψ(wet) p(wet)	6	208.5	2.25	0.05	0.71	-95.45
p(year:water)	7	208.87	2.63	0.04	0.75	-93.44
p(year:wet+bait)	8	209.05	2.81	0.04	0.79	-90.99
p(water+year)	6	209.4	3.15	0.03	0.82	-95.9
ψ(wet) p(water)	6	210.02	3.77	0.02	0.85	-96.21
p(year:hum)	7	210.05	3.8	0.02	0.87	-94.02
p(wet+water)	6	210.09	3.85	0.02	0.89	-96.25
Null	4	210.69	4.44	0.02	0.91	-100.17
p(bait)	5	211	4.76	0.01	0.93	-98.63
γ(wet) p(wet)	6	211.43	5.18	0.01	0.94	-96.91
ψ(water) p(wet)	7	211.68	5.43	0.01	0.95	-94.84
p(date)	5	212.32	6.08	0.01	0.96	-99.29
p(hum)	5	212.72	6.48	0.01	0.96	-99.49
ψ(water) p(year)	7	213.07	6.82	0.01	0.97	-95.53
ψ(wet)	5	213.3	7.06	0	0.97	-99.78
γ(wet)	5	213.37	7.13	0	0.98	-99.81
γ(water)	5	213.61	7.36	0	0.98	-99.93
p(coy)	5	213.62	7.38	0	0.99	-99.94

Model Name	K	AICc	Delta_AICc	AICcWt	Cum.Wt	LL
ε(wet)	5	213.72	7.47	0	0.99	-99.98
p(year:coy)	7	213.82	7.57	0	0.99	-95.91
ε(water)	5	214.08	7.84	0	1	-100.17
ψ(water)	6	215.14	8.89	0	1	-98.77
γ(wet+water)	6	217.11	10.86	0	1	-99.76
ε(wet+water)	6	217.57	11.32	0	1	-99.98
ψ(wet) γ(wet) ε(wet) p(wet)	8	217.94	11.7	0	1	-95.43
p(wet+water+year+date+bait)	9	218.5	12.26	0	1	-92.75
ψ(wet+water)	7	219.46	13.22	0	1	-98.73
Global	18	438.57	232.32	0	1	-87.28

Candidate model set for striped skunk occupancy models for 2017 and 2019. C-hat is 1.18. Top model is highlighted in gray. Global model is ψ(wet + water), γ(wet + water), ε(wet + water), p(wet + water + year + hum + coy + date + bait).

Model Name	K	QAICc	Delta_QAICc	QAICcWt	Cum.Wt	Quasi.LL
p(hum+date)	7	245.66	0	0.26	0.26	-112.1
ε(water) p(hum+date)	8	247.42	1.76	0.11	0.37	-110.57
p(date)	6	247.52	1.86	0.1	0.47	-115.13
p(hum)	6	247.63	1.97	0.1	0.56	-115.19
Null	5	248.08	2.42	0.08	0.64	-117.28
p(hum+coy+date)	8	248.46	2.8	0.06	0.71	-111.09
ε(water)	6	248.62	2.96	0.06	0.76	-115.68
p(coy)	6	249.82	4.16	0.03	0.8	-116.28
p(wet)	6	249.84	4.19	0.03	0.83	-116.3
ψ(wet) p(hum+date)	8	250.33	4.67	0.03	0.85	-112.02
γ(water)	6	250.98	5.32	0.02	0.87	-116.87
p(bait)	6	251.08	5.42	0.02	0.89	-116.92
γ(wet)	6	251.13	5.47	0.02	0.91	-116.94

Model Name	K	QAICc	Delta_QAICc	QAICcWt	Cum.Wt	Quasi.LL
ε(wet)	6	251.23	5.57	0.02	0.92	-116.99
ε(wet+water)	7	251.4	5.74	0.01	0.94	-114.97
p(water)	6	251.68	6.02	0.01	0.95	-117.21
ψ(wet)	6	251.68	6.02	0.01	0.96	-117.22
p(year)	6	251.74	6.08	0.01	0.97	-117.24
γ(water) ε(water) p(hum+date)	9	252.12	6.46	0.01	0.98	-110.14
p(year:water)	8	253.03	7.37	0.01	0.99	-113.37
γ(wet+water)	7	254.6	8.94	0	0.99	-116.57
p(year:hum)	8	254.98	9.32	0	1	-114.35
ψ(water)	7	255.47	9.81	0	1	-117
p(year:coy)	8	257.6	11.94	0	1	-115.66
ψ(wet) γ(water) ε(water) p(hum+date)	10	258.49	12.83	0	1	-110.08
p(year:wet)	8	258.76	13.1	0	1	-116.24
ψ(wet+water)	8	260.18	14.52	0	1	-116.95
p(wet+water+year+date+bait)	10	262.88	17.22	0	1	-112.27
Global	19	497.26	251.6	0	1	-102.96

Domestic cats:

Candidate model set for domestic cat occupancy models for 2016 and 2019. C-hat is 1.21. Top model is highlighted in gray. Global model is ψ(wet + water), γ(wet + water), ε(wet + water), p(wet + water + year + hum + coy + date + bait).

Model Name	K	QAICc	Delta_QAICc	QAICcWt	Cum.Wt	Quasi.LL
p(wet+bait)	7	82.05	0	0.29	0.29	-30.03
p(wet)	6	82.92	0.87	0.19	0.47	-32.66
p(water)	6	84.68	2.63	0.08	0.55	-33.54
p(year)	6	85.02	2.97	0.07	0.62	-33.71
ψ(wet)	6	85.93	3.88	0.04	0.66	-34.17
p(bait)	6	86.06	4	0.04	0.7	-34.23
p(wet+year+bait)	8	86.08	4.03	0.04	0.74	-29.5
p(wet+water+bait)	8	86.09	4.03	0.04	0.77	-29.5
p(wet+year)	7	86.38	4.33	0.03	0.81	-32.19
ψ(wet) p(wet+bait)	8	86.39	4.34	0.03	0.84	-29.66
p(wet+hum+bait)	8	86.54	4.49	0.03	0.87	-29.73
ψ(wet) p(wet)	7	86.62	4.57	0.03	0.9	-32.31
Null	5	87.06	5.01	0.02	0.92	-36.66
p(wet+water)	7	87.6	5.55	0.02	0.94	-32.8
p(year:wet)	8	88.19	6.14	0.01	0.95	-30.56
p(hum)	6	88.92	6.87	0.01	0.96	-35.66
γ(wet)	6	90.29	8.23	0	0.97	-36.34
γ(water)	6	90.4	8.35	0	0.97	-36.4
p(date)	6	90.62	8.57	0	0.98	-36.51
ψ(wet) γ(wet) p(wet+bait)	9	90.76	8.71	0	0.98	-28.88
p(coy)	6	90.82	8.77	0	0.98	-36.61
ε(wet)	6	90.9	8.85	0	0.99	-36.65
ε(water)	6	90.91	8.86	0	0.99	-36.65
p(year:water)	8	91.73	9.68	0	0.99	-32.33
p(wet+water+year+bait)	9	91.77	9.72	0	1	-29.39

Model Name	K	QAICc	Delta_QAICc	QAICcWt	Cum.Wt	Quasi.LL
p(year:hum)	8	92.94	10.89	0	1	-32.93
ψ(wet+water)	8	93.57	11.51	0	1	-33.24
γ(wet+water)	7	93.85	11.8	0	1	-35.93
ψ(water)	7	93.92	11.87	0	1	-35.96
p(year:coy)	8	94.12	12.07	0	1	-33.52
ε(wet+water)	7	95.28	13.23	0	1	-36.64
p(wet+water+year+date+bait)	10	97.58	15.53	0	1	-28.79
Global	19	466.37	384.31	0	1	-24.18

Candidate model set for domestic cat occupancy models for 2017 and 2019. C-hat is 1.49. Top model is highlighted in gray. Global model is ψ(wet + water), γ(wet + water), ε(wet + water), p(wet + water + year + hum + coy + date + bait).

Model Name	K	QAICc	Delta_QAICc	QAICcWt	Cum.Wt	Quasi.LL
ψ(wet) p(date)	7	73.83	0	0.28	0.28	-26.18
p(date)	6	75.06	1.23	0.15	0.43	-28.91
Null	5	75.45	1.63	0.12	0.55	-30.96
ψ(water) p(date)	8	77.28	3.46	0.05	0.6	-25.5
p(hum)	6	77.29	3.46	0.05	0.65	-30.02
ψ(water)	7	77.32	3.5	0.05	0.7	-27.93
ψ(wet)	6	77.8	3.97	0.04	0.74	-30.27
γ(wet)	6	77.9	4.07	0.04	0.77	-30.33
γ(water)	6	78.26	4.43	0.03	0.8	-30.51
ψ(wet) γ(wet) p(date)	8	78.65	4.82	0.02	0.83	-26.18
p(coy)	6	78.88	5.05	0.02	0.85	-30.81
p(year)	6	79	5.17	0.02	0.87	-30.88
p(bait)	6	79	5.17	0.02	0.89	-30.88
p(water)	6	79.04	5.21	0.02	0.91	-30.89
p(wet)	6	79.13	5.3	0.02	0.93	-30.94

Model Name	K	QAICc	Delta_QAICc	QAICcWt	Cum.Wt	Quasi.LL
ε(wet)	6	79.17	5.35	0.02	0.95	-30.96
ε(water)	6	79.17	5.35	0.02	0.97	-30.96
γ(wet+water)	7	81.24	7.41	0.01	0.98	-29.89
ψ(wet+water) p(date)	9	81.74	7.92	0.01	0.98	-24.95
ψ(water) γ(wet) p(date)	9	81.94	8.12	0	0.99	-25.05
ψ(wet+water)	8	82.01	8.18	0	0.99	-27.86
ψ(water) p(hum+date)	9	82.68	8.85	0	1	-25.42
ε(wet+water)	7	83.39	9.56	0	1	-30.96
p(year:water)	8	85.16	11.33	0	1	-29.44
p(year:hum)	8	86.23	12.4	0	1	-29.97
p(year:wet)	8	86.43	12.6	0	1	-30.07
p(year:coy)	8	87.42	13.59	0	1	-30.57
ψ(water) γ(wet) ε(wet) p(date)	10	88.43	14.6	0	1	-25.05
p(wet+water+year+date+bait)	10	95.74	21.92	0	1	-28.7
Global	19	336.17	262.34	0	1	-22.42

Appendix D

Appendix D. Temporal activity patterns for species across the three survey years (2016, 2017, and 2019). Plots are scaled from a 24-hour clock to sun-time to account for daylight from sunrise to sunset. Rug at the bottom of the plots indicate when species were detected.

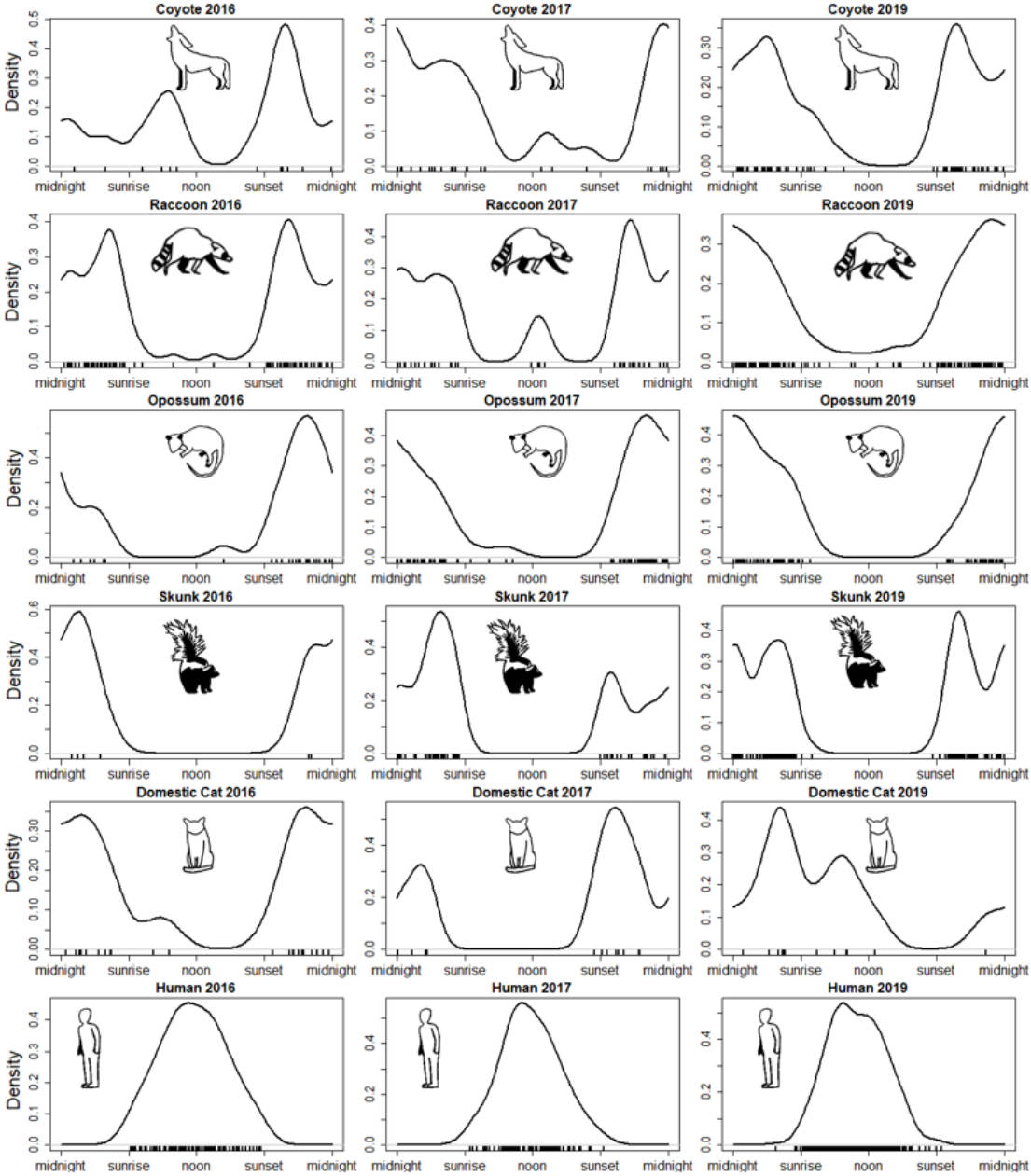

PREFACE TO CHAPTER 2

While it is uncertain when mammalian mesopredators in the Central Valley will be faced another drought, mesopredators are currently facing the challenges of an ever-increasing human presence on the landscape. This high level of human presence leads to a highly fragmented and heterogeneous patchwork of functioning, available, and novel habitat configurations that mesopredators must navigate in their search for food and water resources. While the original study design of the TSM project includes this patchwork of risk and reward to some degree, it largely avoided areas of dense human populations—exurban, towns, suburbs, and cities—as available habitat. Thus, the analysis and conclusions provided in Chapter 1 are limited to the spatiotemporal activity of mesopredator populations in these areas of relatively low human presence in the Central Valley. Additionally, while previous work by Parren (2019) speculated on how mesopredators are responding to increasing human footprint in the area, the conclusions that can be drawn are limited in scale as TSM dataset alone was not designed to address how urbanization may have altered species spatiotemporal patterns during and following the drought.

In the following chapter, I addressed the role that urban environments have on spatiotemporal relationships between mesopredators, coyotes, and humans following drought. While I was unable to address the role of drought along with urbanization simultaneously, as my study was designed following drought data collection in 2016 and 2017, I was able to capture a baseline for mesopredator spatiotemporal activity and

relationships throughout a highly human dominated landscape at multiple spatial and temporal scales. The conclusions on relationships mesopredators have to each other and urban environments can help inform future studies connecting mesopredator response to drought throughout the spectrum of urban intensities.

CHAPTER 2: SPATIOTEMPORAL RESPONSES OF MAMMALIAN MESOPREDATORS TO URBANIZATION IN CALIFORNIA'S CENTRAL VALLEY

Abstract

In the Central Valley of California, mammalian mesopredator activity patterns and species overlap may differ as a result of resource availability and tolerance of humans between different levels of urban intensity. To evaluate the effects urbanization may have on mesopredator spatiotemporal behavior and species interactions, I deployed camera traps across a gradient of urban intensities in the Sacramento Metropolitan Area. I hypothesized that as urban intensity increased, species spatial and temporal overlap would increase, especially with potentially risky neighbors: coyotes (*Canis latrans*) and humans. I used single-season single species and two-species conditional occupancy models and temporal overlap analyzes to evaluate 1 domestic (cat, *Felis catus*) and 4 wild (including coyote) mesopredator spatiotemporal activity patterns. My results indicate that urban intensity impacts mesopredators at different spatial and temporal scales. Raccoons (*Procyon lotor*), opossums (*Didelphis virginiana*), and cats had increased detection near buildings while skunks (*Mephitis mephitis*) had increased detection with imperviousness. Coyotes were the least tolerant to urban areas and human presence. Thus, high intensity urban areas may provide refuge for raccoons and cats that are negatively impacted by coyote presence. Opossums and cats may also avoid humans while benefiting from human dominated landscapes. As mesopredator temporal overlap was high across urban

intensities, fine-scale spatial and temporal movements and microhabitat and resource use may allow for species coexistence at intermediate to high urban intensity, especially in urban greenspaces that facilitate mesopredator movement. These urban greenspaces may allow for increased connectivity between non-urban and urban areas, benefiting human health and ecosystem function.

Introduction

Urban areas are often extreme forms of anthropogenic land-use and generally represent disturbance to surrounding natural ecosystems and wildlife communities (Foley et al. 2005, Ditchkoff et al. 2006, Gehrt et al. 2010). As human development expands further into natural habitat, the rapid conversion of large areas of wildland creates a heterogeneous patchwork of anthropogenic disturbance and biodiversity loss (Leu et al. 2008, Venter et al. 2016). While this conversion of land often results in the loss of species, a surprising number of mesopredator species worldwide are able to thrive across a variety of urban areas and take advantage of the resources present regardless of the numerous risks associated with these human-dense habitats (Bateman and Fleming 2012). The behaviors and interactions of mesopredators in urban environments are subject to large amounts of anthropogenic influence, altering the behavior of urban species substantially compared to non-urban individuals (Ditchkoff et al. 2006). Shifts in mesopredator behaviors and interactions within highly populated urban areas can exacerbate human-wildlife conflict, increase transmission of zoonotic diseases, and decrease overall biodiversity (McKinney 2002, Stieger et al. 2002). Therefore,

understanding the interplay between mesopredator interactions and the "risk and reward" structure of urban areas may allow us to investigate which mesopredators may be able to thrive as urbanization increases at accelerating rates (Elmqvist et al. 2013).

While ecologists are often interested in how species respond to urbanization, they often omit the effects of scale and magnitude of urbanization when quantifying and defining urban areas (McKinney 2002, McIntyre et al. 2008). By relying on dichotomous descriptions of urbanized study areas as "urban" versus "not urban" or "disturbed" versus "undisturbed", this leaves out analysis of the mechanisms for how species may react and respond to the unique stressors of urban environments (McDonnell and Pickett 1990, Ramalho and Hobbs 2012). However, in order to choose which features define an urban area, one must surmise the impacts each feature may have on their species of interest (Moll et al. 2019). For mesopredators, urban features can elicit a variety of behaviors and responses. For instance, human presence in an urban areas is important to consider given that mesopredators may see humans as a "super-predators" that can negatively impact foraging and distribution through fear (Clinchy et al. 2016). Urban areas are also known to support anthropogenic food sources in the forms of refuse, bird seed, fruit trees, and pets, all of which can increase population numbers and decrease home range size (Larivière 2004, Bateman and Fleming 2012, Magle et al. 2014). Small mammalian prey availability and predation success of mesopredators may increase with increased availability of debris and materials associated with construction and development (Price and Banks 2017), as well as increased light pollution (Longcore and Rich 2004). Size and distribution of land-use type within urban areas may also determine the distribution and

activity of mesopredators, as fragmented vegetation, areas of recreation, and road use may increase the amount of risk associated with moving between habitat patches (Tigas et al. 2002, Baker et al. 2007, Markovchick-Nicholls et al. 2008, Wang et al. 2015). Combining these features of urbanization and ranking their importance to mesopredator viability can allow us to establish a gradient of urbanization in which the stressor intensity and risk can change across a landscape. Understanding how these urban features and stressors impact species may allow us to determine the magnitude and direction of spatiotemporal risk avoidance strategies of mesopredators.

Spatial and temporal occupancy and activity are often used to evaluate mesopredator community interactions in urban areas. For instance, mesopredators occupying urban areas have been seen to decrease their home range sizes, spatially constraining themselves as they forage for more aggregated food sources, potentially causing impacts on dispersal, competition, and disease transmission compared to non-urban areas (Prange et al. 2003, Prange et al. 2004, Šálek et al. 2014, Murray et al. 2015). Because of this trend of decreasing home ranges, mesopredator populations are often more densely packed, increasing the potential for competition and intraguild predation. Thus, species that are more tolerant of urban stressors may rely on more intensive forms of urbanization as spatial refugia from their competitors/intraguild predators (Gosselink et al. 2003, Kowalski et al. 2015, Mueller et al. 2018). While some mesopredators may be able to spatially partition themselves away from humans and competitors when there is sufficient diversity in habitat use and area (Schuette et al. 2013, Baker 2016, Shamoon et al. 2017), when space becomes limited in the presence of anthropogenic stressors, there

can be a shift to relying on temporal partitioning (Wang et al. 2015). Yet, there is evidence that mammalian mesopredator temporal activity is becoming increasingly nocturnal in response to human presence and activity (Gaynor et al. 2018). This restriction of fine-scale activity patterns due to increased levels of human disturbance and development can increase mesopredator temporal overlap, further impacting subordinate species which are then more likely to encounter dominant intraguild predators and competitors (Wang et al. 2015, Baker 2016, Smith et al. 2018). Thus, while mesopredator species may be able to adapt to the effects of urbanization and competitors/ intraguild predators independently, the synergistic effects of both negative stressors may suppress certain mesopredator populations substantially (Mueller et al. 2018).

While many studies in urban areas focus on spatiotemporal partitioning as an important feature of mesopredator interactions, the limitations of capturing the fine-scale data on both urbanization stressors and spatiotemporal data are apparent. Until recently, urbanization studies have focused on relatively low levels of human development surrounded by more intact habitat features such as in urban parks and nature preserves (Riley 2006, Prange and Gehrt 2004, Riley 2006, Ordeñana et al. 2010). While important in analyzing how species may react to low levels of intensity, these studies do not capture the full range of urbanization intensities. Thus, to fully assess mesopredator spatiotemporal responses to urbanization intensity and species interactions, fine-scale detail across a diverse gradient of urban features is needed.

I evaluated whether coyote (*Canis latrans*) and human presence influence the spatial and temporal activity of four mammalian mesopredator species—raccoon (*Procyon*

lotor), opossum (*Didelphis virginiana*), striped skunk (*Mephitis mephitis*), and domestic cat (*Felis catus*)—across a gradient of urban intensity created using varying spatial scales. I hypothesized that mesopredator species would increase their risk-taking behavior in areas of higher urban intensity compared to lower urban intensity. Thus, I predicted increasing spatiotemporal overlap for all mesopredators and humans as urban intensity increases, while mesopredators would spatiotemporally avoid coyotes and humans more in non-urban areas. Additionally, I hypothesized that coyotes would have the most negative response to urbanization at the highest intensities, thus allowing mesopredators to use high intensity urban areas as refuges from intraguild predators.

Methods

Study Area

My study was conducted in the Central Valley in California, focusing on the Sacramento Metropolitan Area (SMA) and surrounding urban areas (Figure 25). Survey sites were in part based on previously surveyed Terrestrial Species Stressor Monitoring project (TSM) sites as well as new sites in highly populated cities and suburbs (Sacramento, Stockton, Elk Grove, Roseville) to smaller townships (Davis, Woodland, Rancho Cordova, Lodi) and exurban areas (Winters, Galt) of the Central Valley (Figure 26). More than 2 million people live in this area, with a majority (around 1.5 million) residing in Sacramento County (USCB 2019). Populations are expected to grow substantially in this region, with increasing demand for housing, development, and economic growth (Soulard and Wilson 2015). Interspersed between these urban centers

are areas of varying levels of rural, exurban, suburban, and urban development, as well as highly productive agricultural land and several natural parks, refuges, and preserves (Wassmer 2000).

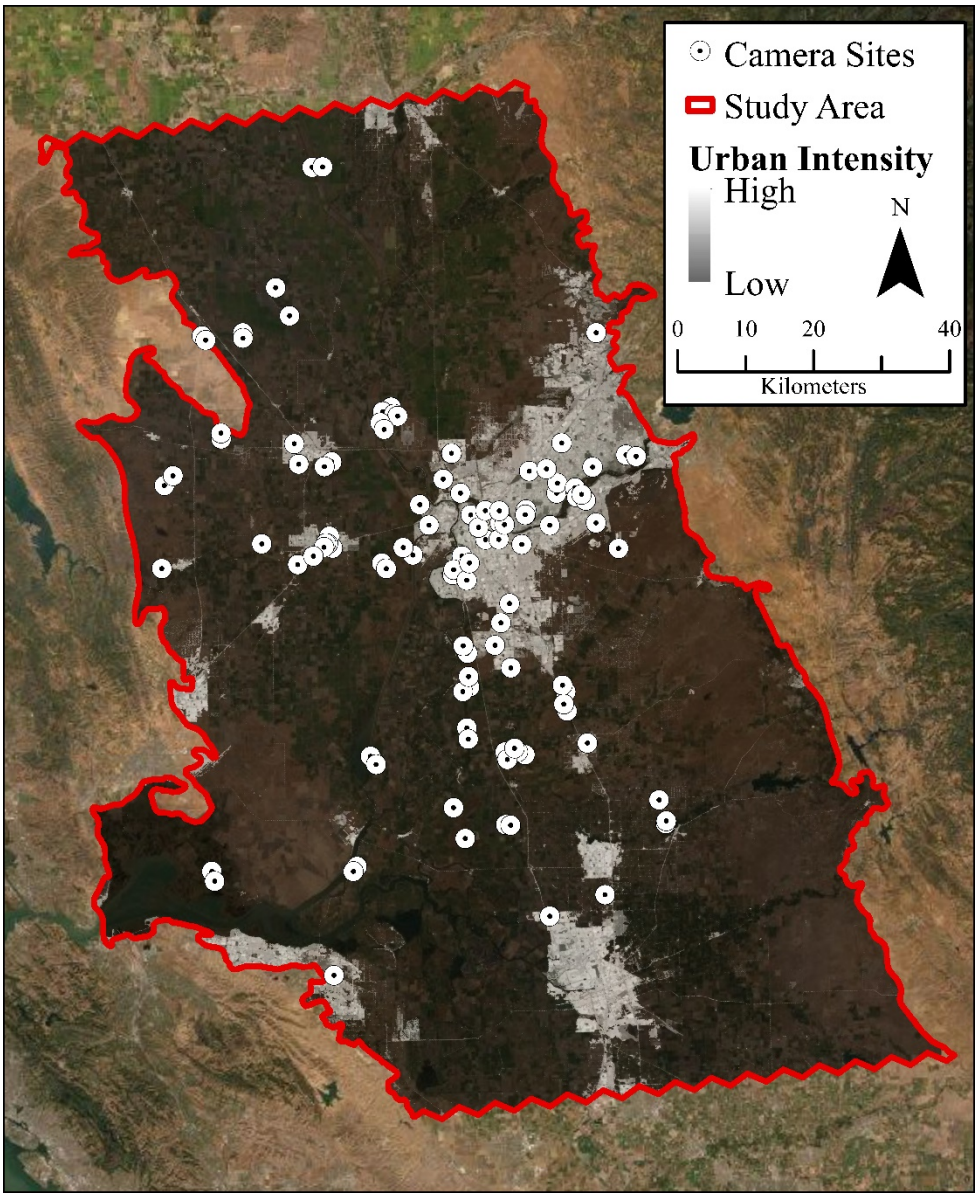

Figure 25. Sacramento Metropolitan Area camera sites (n = 110; white circles) in reference to urban intensity. Urban intensity is based on a combination of imperviousness

coefficients within every 60 m^2 pixel and building density within a 500 m kernel density search radius at a 60 m^2 pixel. Study area (black outline) is based on a 20 x 20 USDA Forest Inventory and Analysis Program Hexagon grid for the Central Valley based around the Sacramento Metropolitan Area.

The Sacramento Metropolitan Area generally exhibits a Mediterranean climate, with winter rainfall from the Sierras feeding into the Sacramento Delta, which is heavily diverted to agriculture and urban areas along the way (Durand et al. 2020). The Sacramento and American Rivers come to a confluence in the study area, acting as major ecological corridors for a variety of species, while also facilitating a highly biodiverse and productive landscape for hydrological function and socio-economic importance. This mosaic of ecological resources, urban development, and anthropogenic land-use provides a great model system for quantifying mesopredator response across a gradient in which urbanization intensity varies across a landscape.

Study Design

In order to fully sample the urbanization gradient, I developed a mixture of stratified and opportunistic camera site selection. Camera sites resurveyed for the TSM were selected as sites that would most likely represent the lowest level of urbanization (Figure 25). To sample for sites within urban areas that might represent low to intermediate urbanization intensities, I selected city and county parks and natural corridors along the Sacramento and American rivers for camera placement. Finally, I used an opportunistic site selection process recruiting volunteers that would allow cameras to be placed around their residences or properties to sample for mesopredators appearing in high density city

centers and residential areas. A variety of households and properties within smaller rural communities (e.g. Winters, Knights Landing), exurban suburbs (e.g. Galt), small towns (e.g. Woodland, Davis), and contiguous developed cities (e.g. Sacramento, Elk Grove) were used for camera placement sites. Due to the ease of access and landowner permissions, a majority of these urban areas represented single-family households, rather than apartments or business/commercial buildings.

Thirty cameras were rotated through a total of 110 camera sites during the survey period from May to August 2019. Camera sites were at least 1km apart to reduce spatial correlation. To avoid temporal correlation, I deployed cameras sites using a stratified design to reduce the chance of individual animals being detected on nearby cameras deployed within the same sample period.

Due to the unique challenges and risks associated with human presence and development, camera trap surveys within urban areas used a modified TSM camera survey protocols described in Chapter 1 (Rich et al. 2018). I used a 14-day survey period instead of a 28-day period for each camera site to maximize camera detection while also reducing the risk of theft or damage to cameras in urban areas. Cameras were attached to T-posts only in areas that were open, secure, and had explicit landowner permission; otherwise, cameras were attached to any available attachment point (buildings, fence-posts, trees, poles). Cameras at residential houses were placed either within backyards or front yards depending on landowner preference, to decrease the potential for pet dog disturbance, or where wildlife were most likely to be found. I preferentially positioned cameras to face north in areas where direct sunlight could cause false triggers and glare

on the camera lens; however, microsite characteristics such as attachment structure, landowner permission, and movement corridors also determined camera direction. Cameras were secured with lockboxes, cable locks, and padlocks as well as placed in inconspicuous locations to avoid human interference when necessary. Each site was baited with a can of fishy cat food at the beginning of the sample period and certain cameras were checked one to two times in areas of high human activity for camera functionality, battery, and condition. Three cameras experienced failure upon first deployment and needed to be redeployed, meaning cameras experienced two rounds of bait; however, this did not seem to alter expected camera detection rates compared to similar camera site detections. Camera set-up between urban and non-urban sites can be viewed in Appendix E.

Data Processing

I imported the camera trap photo files and extracted metadata using MapView Professional (MapView Professional Version 3.7.2.2, https://www.reconyx.com/software/mapview, accessed 11 Nov 2020). Trained technicians and I visually inspected all photos and all wildlife observations were identified to species when possible. Photos were inspected up to three times, with a first round of inspection happening after SD card collection in the field, the second happening as a preliminary analysis of all species detections, and the third being a final quality assurance/quality check. All species were recorded for every photo they appear in, including detections of humans and any field technicians. Species records were considered independent following 30 minutes of a previous detection. From all

consolidated species records, I created independent records using the assessTemporalIdenepdence function in the package "camptrapR" using R (Niedballa et al. 2016). Species were included in the analysis if they appeared within all three types of camera sites (residential, park, and TSM resurveyed sites) with enough detections (n = 10) for comparison. All statistical analysis was done in R and RStudio (R Core Team 2014, RStudio Team 2020).

Data Analysis

Single-season, single species occupancy modeling

I used single-season, singlespecies occupancy models to evaluate whether mammalian mesopredators spatiotemporally responded to changes in urbanization, human presence, and coyote presence. Occupancy models represent the probability of species occurrence at sampled sites through the occupancy variable (psi or ψ) and the probability of detecting a species is represented by the detection variable (p; MacKenzie et al. 2017). Since the mesopredator species I am studying are expected to have large home ranges and the ability to potentially move between camera sites sampled, occupancy can be viewed as species "use" of sampled areas. Additionally, both occupancy and detection variables can be expected to change as a result of covariates. I used environmental covariates representing urbanization to evaluate changes in occupancy probability of mesopredators, while also accounting for imperfect detection and changes in detection probability by evaluated covariates representing urbanization, anthropogenic influences, and intraguild predation/intimidation. The sample period for single species occupancy models run for 14 days across all camera sites, with each

occasion being 1 day. Days where cameras were not functioning were coded as "NA" in detection histories and did not contribute to occupancy or detection estimates. Detection histories were created for all mesopredator species as well as humans using the package "camtrapR" in R (Niedballa et al. 2016).

Occupancy covariates

I expected mesopredator occupancy probability to change across the urban gradient that moves from public and private greenspaces and agricultural areas into increasing levels of exurban, suburban, and urban development. I used two covariates – building density and imperviousness—to define this urbanization gradient. Building density is a measure of development localized to the number of built structures within a given area. Likewise, imperviousness is a measure of how much of an area is covered by impervious surfaces – often areas of concrete or other built surfaces associated with roads, buildings, and urban sprawl. These two covariates represent urban areas at different intensities that mesopredators may experience. For instance, building density may differ going from a suburban neighborhood to a concentrated city center; however, imperviousness may be more similar across those neighborhoods given that both have concrete infrastructure as the main land cover type.

Building density was derived from the Microsoft Building Footprint dataset (https://github.com/Microsoft/USBuildingFootprints, accessed 11 Nov 2020) which defines building polygons for the whole conterminous United States. I converted building footprint polygons in my study area into centroid point data, which I then used as an input into the Kernel Density function in ArcMap (version 10.1). I ran the Kernel Density

function using four different search radii (100, 200, 500, and 1,000 m) to create four 30 by 30 m raster layers representing the influence of buildings on mesopredators dropping off at each increasing distances. I then calculated the mean value of each kernel density raster at four increasing buffer sizes around each camera site (500, 1,000, 2,000, and 5,000 m) using the "raster" and "rgdal" packages in R (Bivand et al. 2020, Hijmans 2020). This created 16 permutations for the building density covariate at multiple search radii and buffer size scales that mesopredators may be responding to.

Imperviousness was derived from US Geological Survey's mapping of impervious surfaces across the conterminous United States at a 60 m resolution (Falcone 2017). Imperviousness is calculated as the ratio of land cover within each 60 m^2 pixel that is covered in impervious surfaces, where a completely concrete landscape is classified as a 1, and a natural area with some water seepage would be classified as a 0. In order to measure the scale of effect for imperviousness around each camera site, I calculated the mean value of the imperviousness raster at the same four increasing buffer sizes (500, 1,000, 2,000, and 5,000 ms) used for building density. This created 4 permutations for the imperviousness covariate at each buffer size.

Detection covariates

The covariates I used to determine detection probability were selected for two primary purposes. First, detection covariates were included to address whether variation in camera placement and deployment across camera sites lead to imperfect detection of mesopredator species. Second, detection covariates dealing with coyote presence, human

presence, and urbanization were included to elucidate whether mesopredators were spatiotemporally avoiding camera sites at higher intensities of each covariate.

Variation in sample periods across the survey period and site level variation in camera locations were included as well to test for imperfect detection. Camera placement was included to test whether placing the camera in an open greenspace (i.e. agricultural area, city park, area with minimal fencing), or in a resident's front yard (fencing, open to a street) or backyard (highest level of fencing) would change detection of mesopredator species. I also recorded if anthropogenic food resource such as residential fruit and vegetables, open trash, dog or cat food left outside, or bird feeders were present in the immediate camera area. This "food" covariate was coded as binary covariate (two levels, 1 = food present, 0 = food absent) and was only noted at the beginning of the sample period and for the immediate area surrounding the camera, potentially being subject to change throughout the sample period if another food resource became available (e.g., trash cans). Camera sites were also baited with cat food to increase detection of mesopredators. To quantify the potential drop-off in detection, I included a bait age covariate representing decay of bait over the 14-day study period. Finally, Julian date was included to test whether species detection changed as a result of sample period.

Mesopredators of smaller body size (raccoons, opossums, skunks, and cats) may avoid camera sites as a result of larger intraguild intimidators—coyotes—being present. To account for this potential negative species interaction, I included coyote presence to account for changing detection probability by using the coyote detection history gathered from cameras as a covariate. Smaller mesopredators may respond to an area with coyotes

disproportionally; thus, coyote "presence" may have a lingering effect as a result of scent marking or other sign or behavior not captured on camera. To test whether coyote presence at a site had longer lasting effects in smaller mesopredator detection, coyote presence was tested at three temporal scales—either being present for one, two, or three days. Covariates for coyote presence after two and three days were created by adding an extra "detection" to the coyote detection history for one day and two days, respectively. A maximum of three days was used as variation in covariate levels beyond three days decreased.

Mesopredators may also avoid camera sites as a result of humans being present. Thus, I included a covariate representing the daily detection history of humans at each camera site across each sample period of two weeks. Human presence was treated with the same sequential temporal scale as coyote presence where a covariate was created for 1, 2, and 3-day lingering effects of human presence.

Urbanization covariates used for occupancy—building density and imperviousness—were also included to determine variation in mesopredator detection probability as well. Urbanization may influence detection of a species for a number of reasons, one of which being increased human presence in urban areas. To test whether changing human presence across the urbanization gradient influenced mesopredator detection probability, an interaction term between the two covariates was included in detection models. All continuous occupancy and detection covariates (building density, imperviousness, and Julian date) were standardized to make sure differences in variation

and ranges of covariate units were all comparable. Covariates by urban intensity and Pearson correlation coefficients can be viewed in Appendix F.

Candidate model sets and model selection

I created candidate model sets for each of the five mesopredator species using step-wise selection using the package "unmarked" in R (Fiske and Chandler 2011). First, a null model of occupancy and detection without influence of covariates was created. Next, I built models to compare occupancy at each spatial scale for both buildings and imperviousness covariates. The top building or imperviousness scale was then included when testing detection models. Study site variation models included detection covariates for camera placement, anthropogenic food, bait age, Julian date and combinations of these covariates; the top covariates were then included for all remaining models. I then examined models for both coyote and human presence to determine which temporal scale (one, two or three days) best explain mesopredator detection. Finally, models including building density and imperviousness as detection covariates (at the same scale as occupancy) along with interaction terms between both urbanization covariates and the best human presence temporal scale were created.

I determined goodness of fit for each model set by creating a partial global model representing a combination of both detection and occupancy models at the best scale. This global model was then used for a goodness of fit test using the package "AICmodgavg" in R to determine the median c-hat value with 2,000 bootstraps (Mazerolle 2020). The global model for opossums was the only model that failed the goodness of fit test due to overdispersion (c-hat > 2). The addition of a detection

covariate representing a lag effect was included to correct this goodness of fit test, where including the detection history of opossums plus a lag of three days helped bring the c-hat value down to appropriate levels. This lag effect, opo3, was then included in all of the previous models as a detection covariate to correct for overdispersion. I compared models using Akaike's Information Criterion for small sample sizes (AICc; Anderson and Burnham 2002). If the c-hat value of the global model was over 1, a quasi-AICc (QAICc) methodology was used to select for top models by correcting for overdispersion, otherwise, if the c-hat value was 1 or below, c-hat was set to 1 and AICc was used (Mackenzie and Bailey 2004). The top model used for interpretation of results in each candidate model set was determined by being 1) within the top 2 Δ AICc 2) being the most conservative (highest number of parameters, K) and 3) having the least amount of uninformative beta estimates for all covariates. I then inspected the beta estimates for each covariate response by calculating beta estimate 95% confidence intervals. If covariate beta estimate 95% confidence intervals overlapped with zero, the covariate's response and interpretation were considered uninformative (Arnold 2010). Thus, covariates within the top model are only considered competitive and interpretable if their beta estimates result in a significant 95% confidence interval.

Conditional two-species occupancy modeling

While single species occupancy models were used in part to determine whether mesopredator species responded to coyote presence at the 1, 2 or 3-day temporal scale; coyotes may change the spatiotemporal activity of subordinate mesopredators at much finer scales. Thus, I used single season, two species occupancy modeling to capture how

subordinate mesopredators responded to coyotes and whether mesopredators land use and detection were conditional on coyotes' presence and detection. I used conditional two-species occupancy models to estimate several variables associated with occupancy and detection of coyotes and a subordinate mesopredator (raccoons, opossums, striped skunks, and domestic cats). These occupancy and detection variables can either be conditional (estimated separately) or unconditional (estimated together, no difference between variables) in order to predict the relationship between a dominant species (coyotes) and a subordinate species (all other mesopredators; (Richmond et al. 2010)). A summary of all parameters using in conditional two-species occupancy modeling are displayed in Table 2 (Parren 2019; pg 33).

Table 2. All possible parameters using conditional two-species occupancy modeling. SIF is a derived parameter only able to be estimated if ψBA and ψBa are estimated separately.

Parameter	Description
φ	Species Interaction Factor (SIF)
ψA	Probability of occupancy for species A
ψBA	Probability of occupancy for species B, given species A is present
ψBa	Probability of occupancy for species B, given species A is absent
pA	Probability of detection for species A, given species B is absent
rA	Probability of detection for species A, given both species are present
pB	Probability of detection for species B, given species A is absent
rBA	Probability of detection for species B, given both species are present and species A is detected
rBa	Probability of detection for species B, given both species are present and species A is not detected

Note: From Parren, Molly K., "Drought and coyotes mediate the relationship between mesopredators and human disturbance in California" (2019). HSU theses and projects. 349. https://digitalcommons.humboldt.edu/etd/349. CC BY-NC.

Coyote occupancy/area use can be estimated directly as in a single species model (ψA), while coyote detection can be determined by the presence (pA) or absence (rA) of another species. Since I was interested only in whether subordinate species (species B) responded to coyotes as a dominant intraguild predator/intimidator (species A), I made coyote detection unconditional, setting pA = rA. For subordinate species, occupancy/use probability can be either conditional, depending on coyote presence (ψBA) and absence (ψBa); or unconditional, or unchanging depending on whether coyotes are present at a site or not (ψBA = ψBa). Subordinate species detection probabilities depend on whether coyotes are absent (ψB), whether both species are present and detected (rBA) and whether both species are present, but coyotes are not detected (rBa). If coyote detection does not influence subordinate mesopredator detection, then subordinate mesopredator detection is unconditional on coyote detection (rBA = rBa) but conditional on presence; while if coyote presence does not influence subordinate species detection at all, then subordinate mesopredator detection is fully unconditional on coyotes (pB = rBA = rBa).

Covariates

Like single species occupancy models, two-species occupancy models can have covariates for each occupancy and detection variable; however, this time there can be covariates for each species. To reduce the amount of potential candidate models, I used top single species occupancy models to inform two-species models. Top occupancy

covariates for coyotes were used for ψA, and top detection covariates were used for pA and rA (as pA =rA). For subordinate species, top occupancy covariates were used for ψBa and top detection covariates were used for pB. Continuous covariates were standardized in the same way as they were for single species occupancy modeling.

Candidate model sets and model selection

I used two rounds of model selection and candidate model sets, the first for detection probability and the second for occupancy probability, to determine top two-species models. First, null models, (every variable set to be conditional) were created for each coyote-subordinate species pair (coyote-raccoon, coyote-opossum, coyote-skunk, and coyote-cat). Next, full conditional models using top single species detection covariates for both coyote (pA = rA) and subordinate species (pB) were created, where occupancy variables were left without covariates and conditional (ψA, ψBA, ψBa). Detection covariates for subordinate mesopredators (pB) were checked using a backwards selection process, eliminating detection covariates until models had the least number of problematic covariates. Detection covariates for coyotes were inspected and remained untouched for each species pairing to keep coyote detection similar across all four candidate model sets. Once I selected top detection covariates for pB, I checked detection of subordinate species versus coyote detection for unconditionality (rBA = rBa), as well as subordinate species detection versus coyote presence (pB = rBA = rBa). The top detection model was selected using the same protocol as single species model selection (within the top 2 Δ AICc, the most general/most parameters, the least amount of

uninformative beta estimates), as well as selecting for the top configuration of conditional/unconditional detection variables.

I then used the top detection model to decide the top occupancy model. Top detection covariates in the top configuration were included in the full conditional occupancy model which included top occupancy covariates from single species models for coyotes (ψA) and the subordinate mesopredator (ψBa). Occupancy models were then tested to see if subordinate species occupancy was unconditional on coyote presence (ψBA = ψBa). Top occupancy covariates were tested for ψBA and ψBa in both conditional and unconditional configurations. Top occupancy models were then selected using the same protocol as before. If subordinate mesopredator occupancy was considered conditional, a Species Interaction Factor (SIF) could be calculated (Richmond et al 2010). The SIF is centered around 1 and tells us if subordinate species were more likely to be around the coyotes (SIF >1) or if they avoided coyotes (SIF < 1). If there was a discrepancy between whether a model was conditional or unconditional within the top 2 AICc ranking for both detection and occupancy models, I would choose the conditional model to see if the beta estimate 95% confidence intervals crossed zero. If the confidence intervals did cross zero, the beta estimate for the conditional variable would be considered uninformative and uninterpretable I chose this method as supposed to inspecting model-averaged results to avoid misinterpretation of model interpretation that may come from model averaging (Richmond et al. 2010, Cade 2015).

All models were built using program PRESENCE (PRESENCE Version 2.12.43, https://www.mbr-pwrc.usgs.gov/software/presence.html, accessed 11 Nov 2020) using

condensed detection history formatting. As there are currently no goodness of fit tests for two species occupancy global models, goodness of fit for each model is assumed based from single species occupancy models for each species pairing.

Temporal overlap

I extracted times and dates from photo metadata to interpret the temporal activity patterns of species detected on cameras. I used k-means clustering to group my sites into 3 groups based on two main variables—building density from the Microsoft Buildings Layer and imperviousness from the USGS. These variables were selected based on previous spatial analysis of species responses to urbanization at a 500 m buffer scale. Species detections were combined for the three clusters: Non-urban (n = 60), Low Intensity Urban (n = 16), and High Intensity Urban (n = 34). If the same species was detected at a site within 30 minutes of a previous detection, it was removed from the analysis.

I used the "overlap" package in R, which relies on a non-parametric kernel density analysis of species temporal data to estimate activity patterns and temporal overlap of each species (Meredith and Ridout 2014). Temporal overlap is calculated as the coefficient of overlap ($\hat{\Delta}$ or D-hat) between two species' activity patterns. D-hat ranges from 0 to 1, where a value of 0 indicates no temporal overlap and a value of 1 indicates complete temporal overlap. As suggested by Ridout and Linkie (2009), I used two methods to estimate D-hat as provided by the *overlap* package; D-hat$_1$ ($\hat{\Delta}_1$) for when at least one species had a small sample size (n < 50), and D-hat$_4$ ($\hat{\Delta}_4$) for when both species had large sample sizes (n > 50). To account for changing daylight hours between

surveys influencing species activity, I used the sunTime command in the "overlap" package to scale temporal activity to be between sunrise and sunset across survey periods (Nouvellet et al. 2012).

I first compared within species overlap from urban intensity to urban intensity (intraspecies) and then compared overlap of species pairs for each urban intensity (interspecies). I used 95% confidence intervals for each D-hat estimate determined from 10,000 bootstrap samples to compare overlap estimates of species pairs between years. Thus, if a species pairs' confidence intervals from one urban intensity overlapped the same species pairs' confidence intervals for another urban intensity, the change of temporal overlap of that species pairing from one urban intensity to another is considered non-significant. Four mesopredator species had adequate data ($n > 5$) to compare between all three urban intensities including four wild mesopredator species (raccoon, opossum, and striped skunk) and one domestic mesopredator (domestic cat). Coyotes had enough detections for comparisons between two of the urbanization intensity categories (non-urban and low urban intensity) which are included for analysis. While predictions could not be made for intraspecies or interspecies comparisons of coyotes at the highest urban intensity, as there was only one coyote detection at high intensity urban camera sites, coyotes are still included in temporal overlap analyzes due to interest in their role as potential intraguild predators even at lowest levels of urban intensity. I also used human detections to compare mesopredator overlap to changes in human presence across urbanization intensities.

Results

Single-Season Single Species Occupancy Models

Urbanization covariates had varying effects on occupancy (use) and detection probability for all mesopredator species. For standardized continuous covariates, odds ratios are in reference to the change in one standard deviation for each range of values. For building density, units are reported as the number of buildings within a given kernel density search radius and buffer size/km^2, and one standard deviation change depends on the scale of building density (ex. one standard deviation for a kernel density radius of 500 m at the 500 m buffer size is 19.6 buildings/km^2. Imperviousness is measured by the average increase in the sum of imperviousness coefficients within either a select radius buffer, and one standard deviation at the 500 m buffer scale is equal to 27.5/km^2. Odds ratios for Julian date are represented as the change in the odds of detecting a species if cameras were placed with one standard deviation for the range of Julian dates from the beginning of the season onward, or ever 25 and a half days.

The covariate for coyote presence within a 1, 2 or 3-day period did not explain or influence mesopredator detection, as it was not included in any top models for any smaller wild or domestic mesopredators. Additionally, coyote presence and an interaction term with building density and imperviousness were tested for all subordinate mesopredators, with no significant improvement of AICc rankings in models that included the interaction term. All other covariates are represented by the change in odds

from one factor level to another. Candidate model sets for single species models can be viewed in Appendix G.

Coyotes

Coyotes were detected at 29 out of 110 camera sites, mostly within resurveyed TSM sites outside of urban areas as well as at county and city parks within or between densely populated urban areas. Top model for coyotes included building density for estimating occupancy probability and camera placement, Julian date, bait age, and human presence for estimating detection probability. Coyote occupancy included building density at the 200m kernel density and 500m buffer scale, although this relationship was not significant (Figure 26).

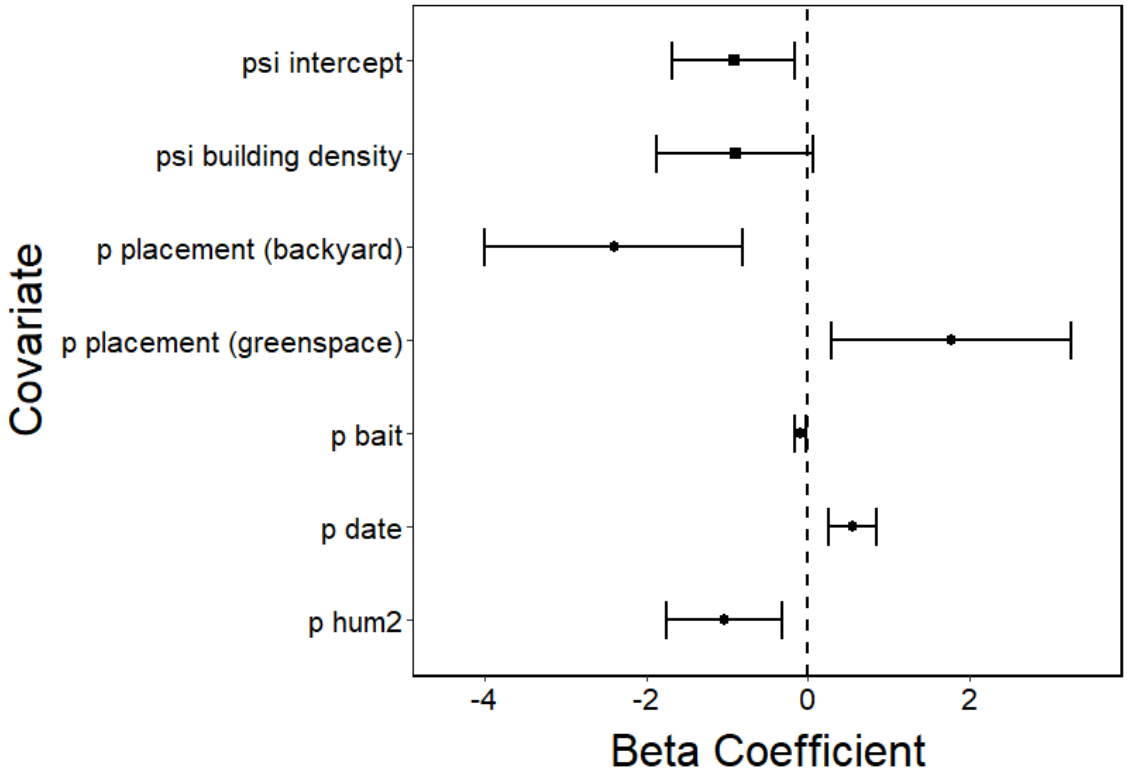

Figure 26. Beta coefficients for occupancy (psi, squares) and detection (p, circles) intercepts and covariates for top coyote model. If error bars, representing 95% confidence intervals, cross the zero dashed line, the beta estimate is considered not statistically significant. Detection beta estimates used for placement (backyard) are the same as beta estimates for the detection intercept. Omitted beta estimates include placement (front yard) as a detection covariate due to uninterpretable beta estimates and large standard errors, as coyotes were not detected in any residential front yards.

Coyote detection was negatively influenced by human presence within a 2-day period, with odds of detection decreasing by 64.5% when humans were present (β = -1.035, OR = 0.355, OR 95% CI = [0.169, 0.702]; Figure 27). Camera placement greatly influenced coyote detection, as backyards decreased the odds of coyote detection by 91%

(β = -2.408, OR = 0.090, OR 95% CI = [0.016, 0.387]), while odds at greenspaces were increased by 494.5% (β =1.783, OR = 5.945, OR 95% CI = [1.596, 31.410];Figure 26). It should be noted that the only coyotes detected in a backyard were in a residential area open to a riparian corridor, allowing for easy access and minimal fencing. In contrast, coyotes were undetected in residences front yards, which had minimal fencing but were often open to the street and close to the front of a house, and thus estimation of coyote presence in front yards could not be determined. Julian date had a positive relationship with coyote detection, with odds of coyote detection increasing by 75.4% every 25 and a half days (β =0.562, OR = 1.754, OR 95% CI = [1.307, 2.373]). Otherwise, odds of coyote detection decreased by 8.7% for every day bait was left out (β = -0.091, OR = 0.913, OR 95% CI = [0.845, 0.983]).

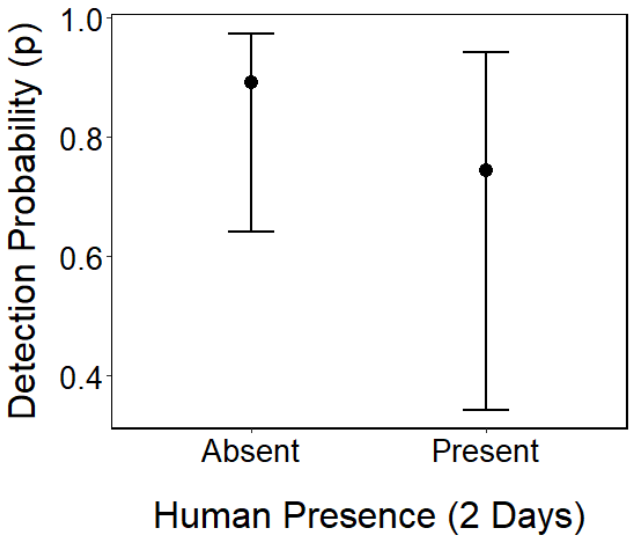

Figure 27. Coyote detection probability (p) estimates based on human presence at a camera site for at least 2 days (hum2). Values for other continuous detection predictors

are set as their average value, and placement is set as a greenspace camera, and bait is set to 0.

Raccoons

Raccoons were detected at 38 out of 110 camera sites, comprised of a variety of open, residential, and highly urban sites. The top model for raccoons included building density for estimating occupancy probability and camera placement, Julian date, bait age, as well as building density and imperviousness for estimating detection probability.

Raccoon occupancy showed no discernable trend towards building density at the 500 m kernel density and 500 m buffer scale. While raccoon site use did not change as a result of urbanization covariates, raccoon detection had a mixed response to building density and imperviousness (Figure 28). The odds of detecting a raccoon increased by 825.3% as building density increased by 19.6 buildings/km^2 ($\beta = 2.225$, OR = 9.253, OR 95% CI = [2.819, 30.387]); however, odds of raccoon detection decreased by 81% as imperviousness increased by 27.5 imperviousness coefficient increase/km^2 ($\beta = -1.662$, OR = 0.190, OR 95% CI = [0.071, 0.506]; Figure 29).

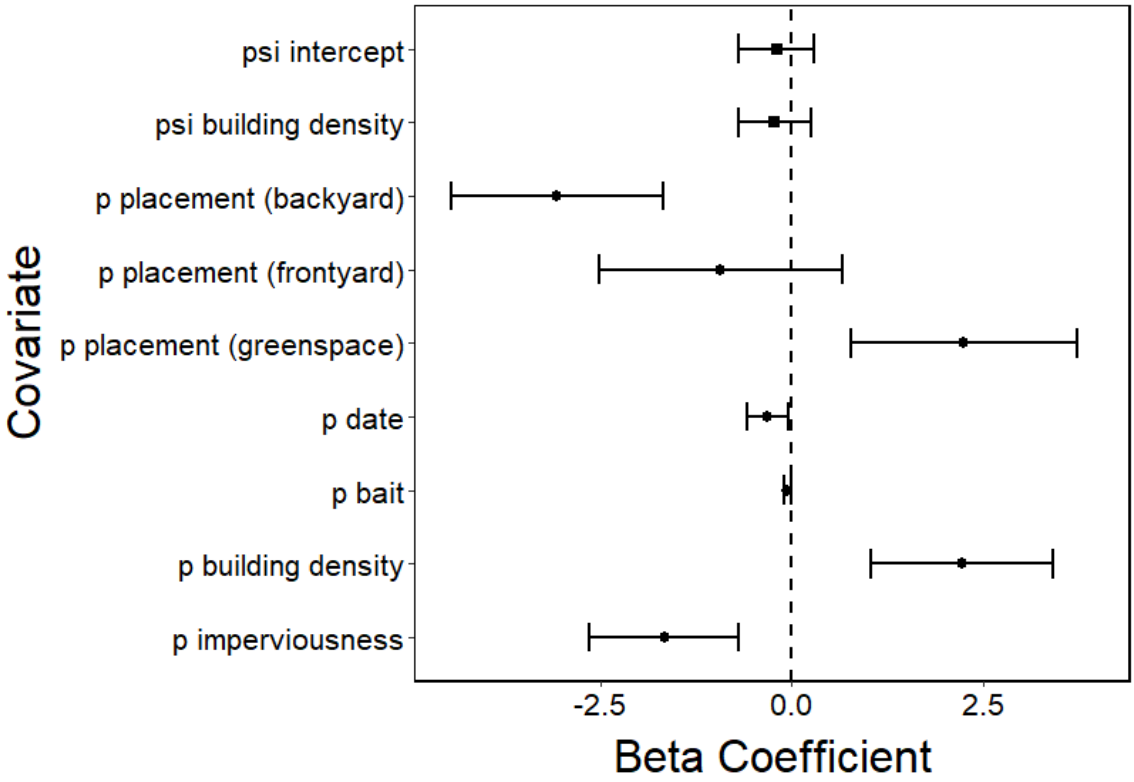

Figure 28. Beta coefficients for occupancy (psi, squares) and detection (p, circles) intercepts and covariates for top raccoon model. If error bars, representing 95% confidence intervals, cross the zero dashed line, the beta estimate is considered not statistically significant. Detection beta estimates used for placement (backyard) are the same as beta estimates for the detection intercept.

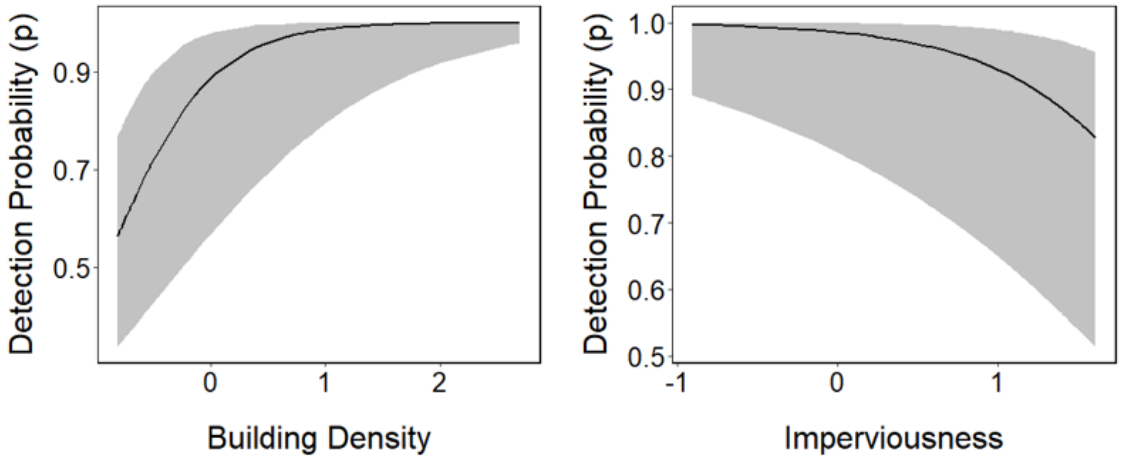

Figure 29. Raccoon detection probability (p) estimates based on building density and imperviousness. Values for other continuous detection predictors are set as their average value, and placement is set as a greenspace camera.

Camera placement influenced raccoon detection in a variety of ways, as odds of raccoon detection decreased by 95.3% in residential backyards (β = -3.063, OR = 0.047, OR 95% CI = [0.012, 0.187]); front yards had no discernable trend in raccoon detection; while cameras in greenspaces increased odds of raccoon detection by 853.5% (β = 2.255, OR = 9.535, OR 95% CI = [2.176, 41.751]). Julian date had a negative impact on raccoon detection, decreasing odds of detection by 26.7% for every 25 and a half days (β = -0.310, OR = 0.733, OR 95% CI = [0.561, 0.960]). Finally, bait decay throughout the survey period trended negatively with raccoon detection; however, this relationship was not significant (β = -0.048, OR = 0.953, OR 95% CI = [0.903, 1.006]; Figure 28).

Opossums

Opossums were detected at 37 out of 110 camera sites, including some of the most densely urban sites along with sites far from urban influence. The top model for opossums did not include any covariates for estimating occupancy probability while detection probability covariates included Julian date, bait age, as well as building density, human presence in a 3-day period, and an interaction term between human presence and building density (Figure 30). For opossum global model to pass goodness of fit testing, a lag effect to account for opossum trap happiness during a 3-day period was included (opo3) for detection probability.

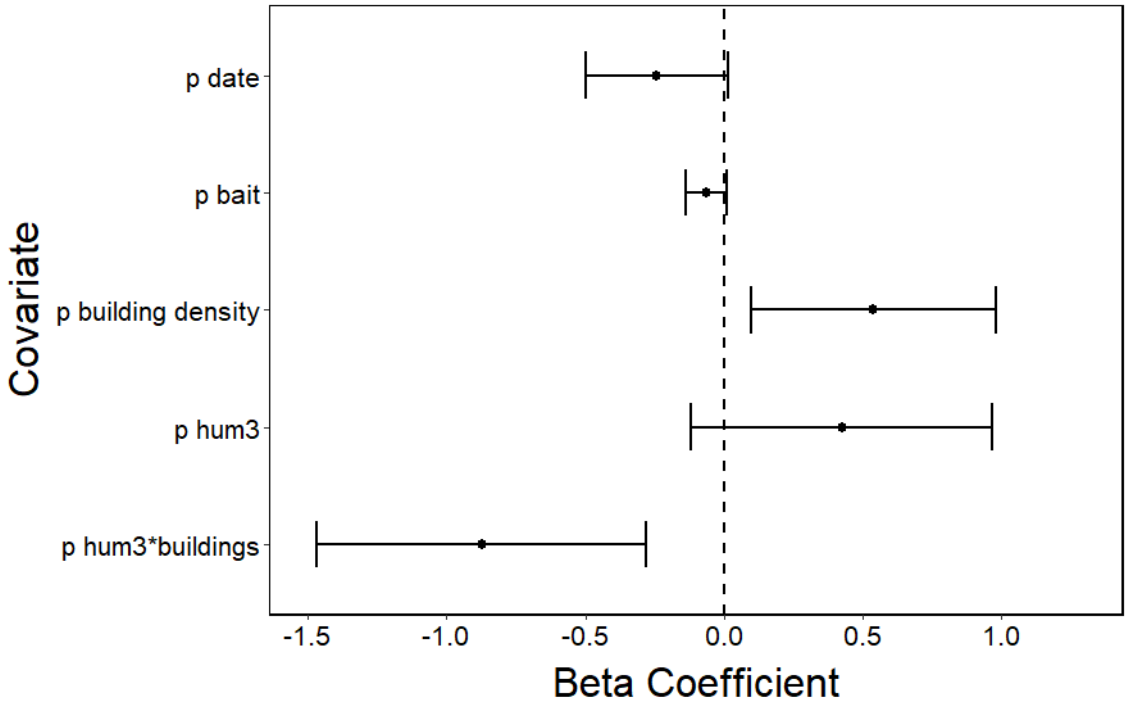

Figure 30. Beta coefficients for occupancy (psi, squares) and detection (p, circles) intercepts and covariates for top opossum model. If error bars, representing 95% confidence intervals, cross the zero dashed line, the beta estimate is considered not

statistically significant. Omitted beta estimates include psi intercept and the lag effect for opossums after 3-days (opo3) as a detection covariate due to uninterpretable beta estimates and large standard errors.

Opossum detection probability had a mixed relationship with building density at the 100 m kernel density and 1000 m buffer scale depending on whether humans were present or not within a 3-day period. For instance, when humans were not present, the odds of opossum detection increased by 71.4% as building density increased by 7.5 buildings/km^2 ($\beta = 0.539$, OR = 1.714, OR 95% CI = [1.101, 2.670]). However, when humans are present in a 3-day period, odds of opossum detection decrease by 58.2% as building density increased by 7.5 buildings/km^2 ($\beta = -0.8719$, OR = 0.418, OR 95% CI = [0.230, 0.757]; Figure 31). While human presence is included in the top model to better inform the interaction term with building density, human presence does not directly influence opossum detection. Both Julian date and bait decay trended towards decreasing opossum detection probability, however, these covariates were not significant (Figure 30).

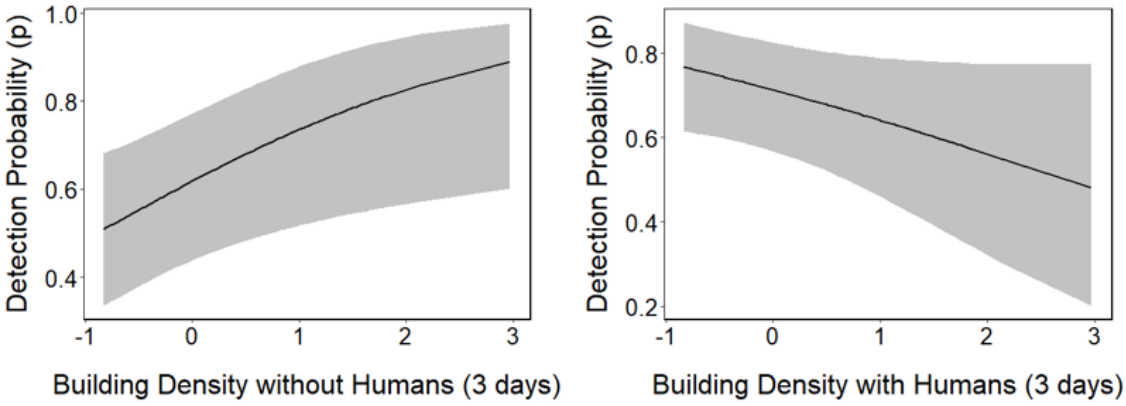

Figure 31. Opossum detection probability (p) estimates based on building density and human presence at a camera site for at least 3 days (hum3). Values for other continuous detection predictors are set as their average value, coy1 is set at 0 (no coyote presence), and opo3 is set at 1 (lag effect of opossums at a camera site for at least 3 days).

Striped skunks

Striped skunks were detected at 33 out of 110 camera sites, in natural, agricultural, exurban, and residential urban camera sites. The top model for skunks included building density as a covariate for estimating occupancy probability while detection probability covariates included camera placement, Julian date, as well as building density and imperviousness as urbanization covariates.

Building density at the 200 m kernel density and 500 m buffer scale was included as an occupancy covariate for skunk occupancy; however, no significant relationship could be interpreted (Figure 32). For skunk detection, building density decreased the odds of detection by 69.6% for every increase in 11.5 buildings/km^2 (β = -1.191, OR = 0.304, OR 95% CI = [0.107, 0.862]), while imperviousness at the 500 m buffer scale increased

the odds of detection by 168.9% for every increase in 27.5 imperviousness coefficient/km^2 (β = 0.989, OR = 2.689, OR 95% CI = [1.428, 5.060]; Figure 33).

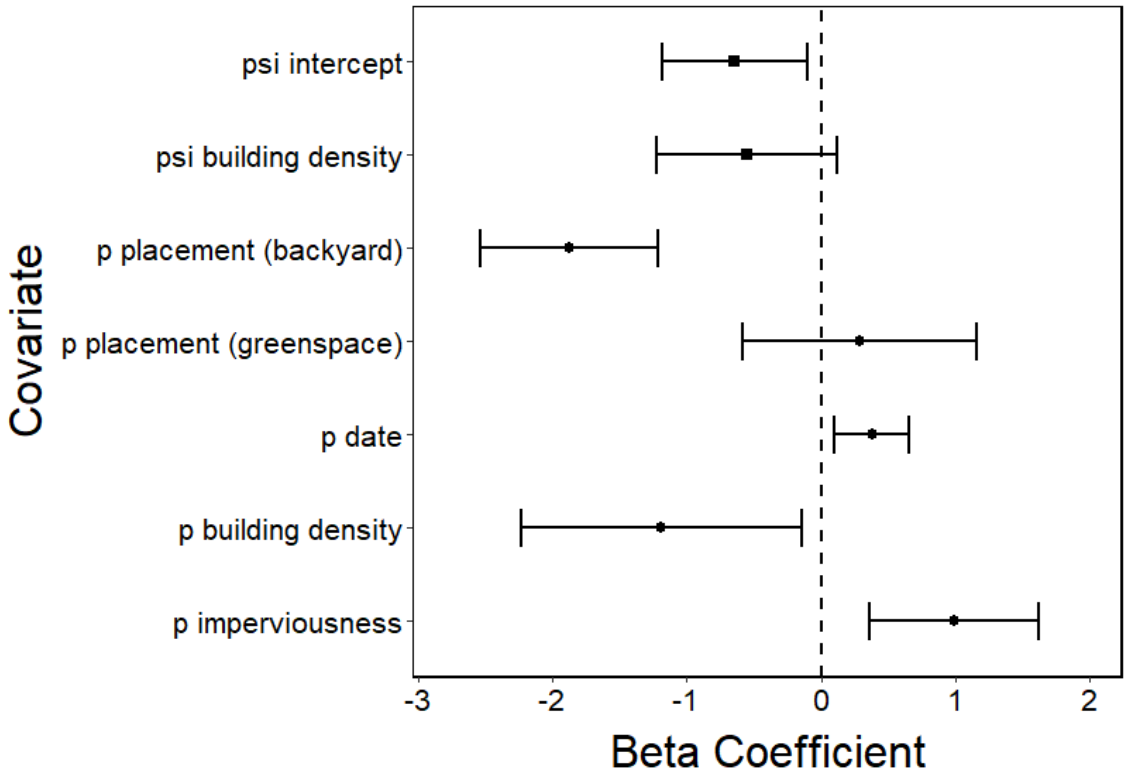

Figure 32. Beta coefficients for occupancy (psi, squares) and detection (p, circles) intercepts and covariates for top skunk model. If error bars, representing 95% confidence intervals, cross the zero dashed line, the beta estimate is considered not statistically significant. Detection beta estimates used for placement (backyard) are the same as beta estimates for the detection intercept. Omitted beta estimates include placement (front yard) as a detection covariate due to uninterpretable beta estimates and large standard errors, as skunks were not detected in any residential front yards.

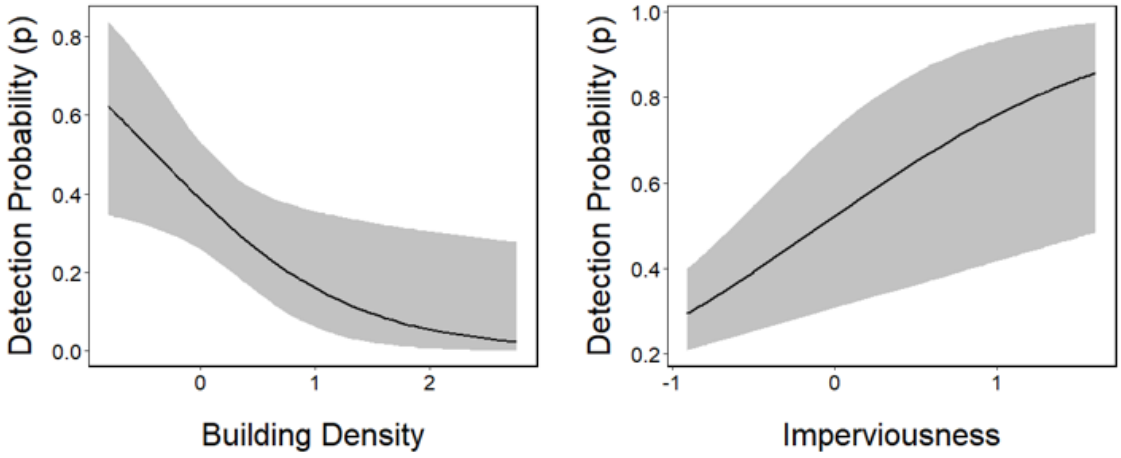

Figure 33. Skunk detection probability (p) estimates based on building density and imperviousness. Values for all continuous detection predictors are set as their average value.

Camera placement was included in top model for skunk detection, with differing effects for each factor level (backyard, front yard, and greenspace). Backyard camera sites decreased the odds of skunk detection by (β = -1.877, OR = 0.153, OR 95% CI = [0.079, 0.298]), while greenspaces trended towards positive odds of skunk detection, this relationship was not significant. Skunks were not detected in any residential front yards, and therefore trends for skunk detection could not be determined. Julian date had a positive relationship with skunk detection, increasing odds by 46.1% for every subsequent 25 and a half days (β = 0.379, OR = 1.461, OR 95% CI = [1.106, 1.930]; Figure 32).

Domestic cats

Domestic cats were detected at 44 out of 110 camera sites, with cats mostly occurring at urban residences and parks. The top model for cats was the only one to

included imperviousness as a covariate for estimating occupancy probability; while detection probability covariates included camera placement, anthropogenic food sources, bait decay as well as human presence within a 1-day period, building density, and an interaction term between human presence and building density.

Imperviousness at the 500 m scale had a large, positive effect on domestic cat occupancy, increasing the odds of cat occupancy by 357.2% as imperviousness increases by 27.5 times per km^2 ($\beta = 1.52$, OR = 4.572, OR 95% CI = [2.660, 7.855]; Figure 34). While building density at the 500 m kernel density and 500 m buffer scale was not included as a covariate for occupancy for cats, it did have a positive effect on cat detection, increasing the odds of cat detection by 58% as building density increased by 19.6 buildings/km^2 ($\beta = 0.4573$, OR = 1.580, OR 95% CI = [1.204, 2.072]; Figure 35). Human presence had a negative impact on cat detection, decreasing odds of detection by 69.9% when humans were present within a 1-day period ($\beta = -1.200$, OR = 0.301, OR 95% CI = [0.157, 0.577]; Figure 36). While an interaction term between human presence and building density was included in the top model for cats, there was no significant difference in cat detection with building density when humans were present (Figure 35).

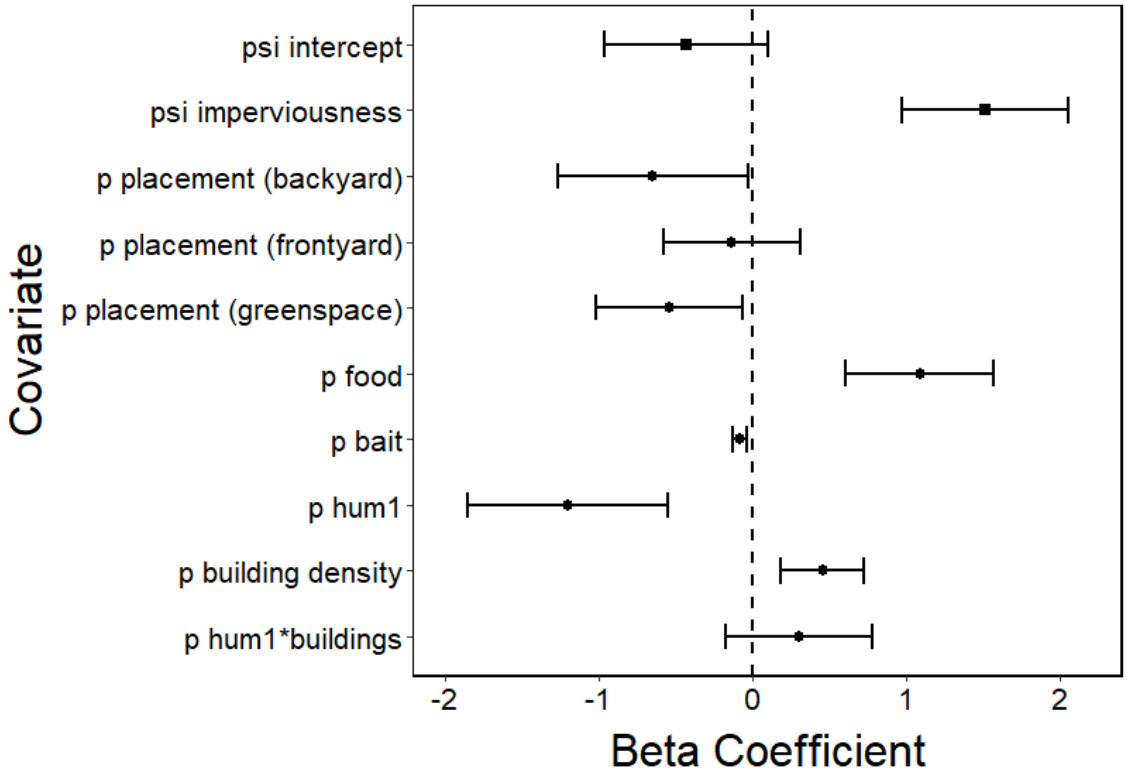

Figure 34. Beta coefficients for occupancy (psi, squares) and detection (p, circles) intercepts and covariates for top domestic cat model. If error bars, representing 95% confidence intervals, cross the zero dashed line, the beta estimate is considered not statistically significant. Detection beta estimates used for placement (backyard) are the same as beta estimates for the detection intercept.

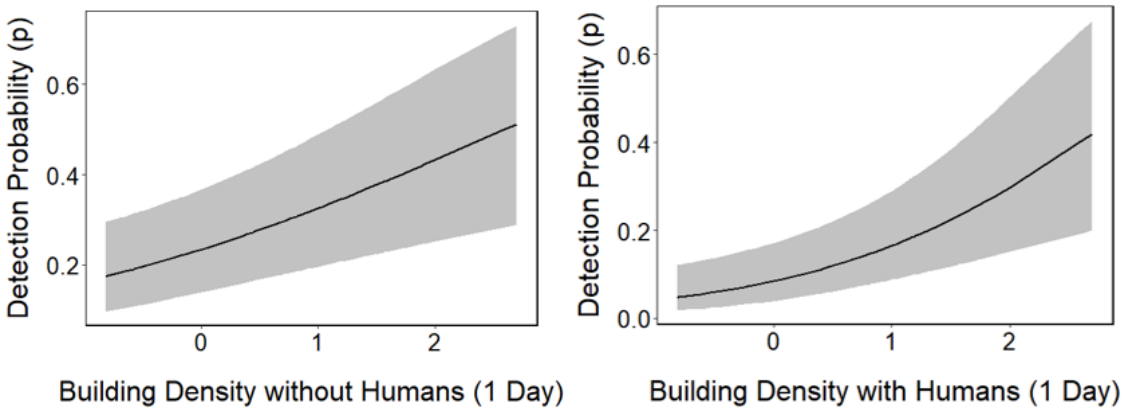

Figure 35. Cat detection probability (p) estimates based on building density at the 500 m kernel density radius and 500 m buffer size in the presence and absence of humans. Values for other continuous detection predictors are set as their average value, placement is set as a greenspace camera, food is set to 0 (no food present), bait is set to 0, and hum1 is set to 0 (humans absent for at least 1 day).

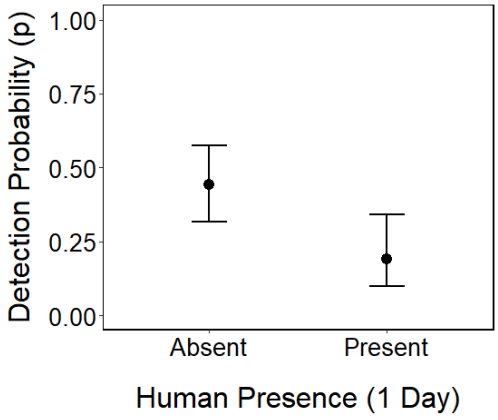

Figure 36. Cat detection (p) estimates based on human presence at a camera site for at least 1 day (hum1). Values for other continuous detection predictors are set as their average value, placement is set as a greenspace camera, food is set to 0 (no food present), and bait is set to 0.

Camera placement had varying effects on cat detection. Backyard camera sites decreased the odds of cat detection by 47.6% (β = -0.646, OR = 0.524, OR 95% CI = [0.281, 0.975]), while cameras in front yards did not significantly influence cat detection (β = -0.133, OR = 0.876, OR 95% CI = [0.562, 1.365]). Greenspaces also decreased the odds of cat detection by 41.6% (β = -0.538, OR = 0.584, OR 95% CI = [0.363, 0.939]). Cats were the only mesopredator to be influenced by anthropogenic food sources, which increased the odds of detection by 197.8% when anthropogenic food sources were present at a camera site (β = 1.091, OR = 2.978, OR 95% CI = [1.837, 4.829]). Bait decay also had a negative impact on cat detection; as bait decayed each day, the odds of cat detection fell by 7.5% (β = -0.078, OR = 0.925, OR 95% CI = [0.885, 0.968]; Figure 34).

Conditional Two-Species Occupancy Models

Coyote presence and detection had varying influence on smaller bodied, or subordinate, mesopredators (Table 3). If there was a discrepancy between occupancy or detection conditionality, as both unconditional and conditional models could be displayed within the top 2 ΔAICc rankings, model selection favored conditional models as they represented a more general model (greater number of parameters). While top models are reported as either conditional or unconditional in regard to the top selected model configuration, the strength and significance of coyote-mesopredator occupancy and detection conditionality must be determined by model parameter estimations and performance of key parameters (ψBA, rBA, and rBa). Additionally, the derived parameter for Species Interaction Factor (SIF) can only be estimated for species pairings

in which occupancy was considered conditional (coyote-raccoon and coyote-skunk pairings).

Table 3. Predicted two species occupancy model conditionality for dominant coyotes versus subordinate mesopredator species based on top detection and occupancy model configurations. Conditional means variable is estimated individually in the top model, while unconditional means variable is estimated as being set equal to other variables. Conditional configuration does not necessitate statistical significance of conditional variables.

Subordinate Species	Occupancy (ψBA)	Detection (Coyote detected - rBA)	Detection (Coyote not detected - rBa)
Raccoon	Conditional	Conditional	Conditional
Opossum	Unconditional	Unconditional	Unconditional
Skunk	Conditional	Unconditional	Unconditional
Cat	Unconditional	Conditional	Conditional

All two-species top models included top covariates for coyote detection from single species occupancy modeling. These covariates included camera placement, Julian date, bait decay, and human presence in a 2-day period for estimating coyote detection with and without subordinate species presence and detection (pA=rA). All coyote detection covariate estimates followed similar trends to single species modeling estimates, with Julian date significantly increasing coyote detection while bait decay and human presence significantly decreased coyote detection. Camera placement also followed similar trends, with backyards negatively influencing coyote detection and greenspaces positively influencing coyote detection, while front yard estimations could not be calculated due to coyote not being detected at all front yard camera sites.

Additionally, top models for all species pairings included building density at the 200 m kernel density and 500 m buffer size as a covariate for coyote occupancy (ψA). While single species models in "unmarked" estimated building density for coyotes to be trending negative, but non-significant; all two-species models built in PRESENCE except for coyote-cat pairings determined building density at this scale to have a strong negative influence on coyote occupancy. Reporting of top models for species pairings below will focus on subordinate species parameters and responses to coyotes; candidate model sets for detection and occupancy models can be found in Appendix H.

Coyotes and raccoons

The top two-species detection model for coyotes and raccoons had Julian date and building density at the 500 m kernel density and 500 m buffer scale as covariates for raccoon detection (pB), and raccoon detection being conditional on coyote presence (rBA) and detection (rBa; Figure 37).

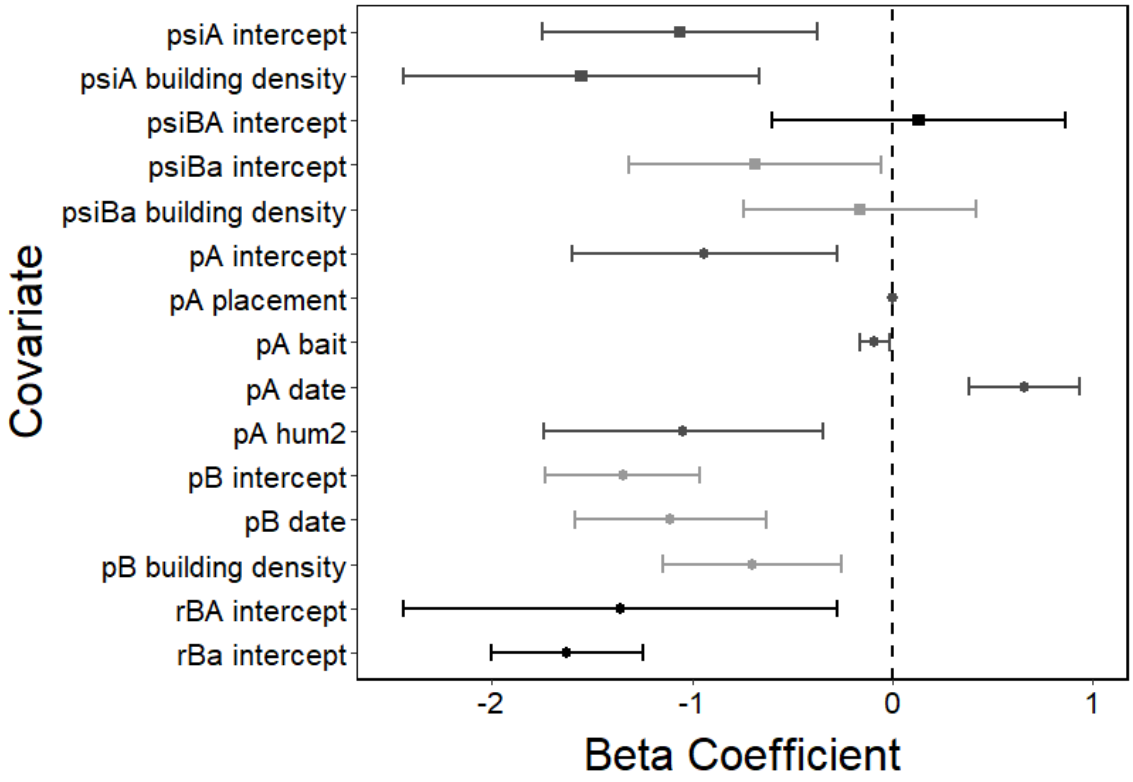

Figure 37. Beta coefficients for occupancy (psi, squares) and detection (p, r, circles) intercepts and covariates for top coyote-raccoon detection and occupancy model. Variables representing coyotes (species A) are dark gray, raccoons (species B) are light gray, and both coyote and raccoon presence (BA) are black. If error bars, representing 95% confidence intervals, cross the zero dashed line, the beta estimate is considered not statistically significant.

Like the raccoon single species top model, Julian date decreased the odds of raccoon detection by 67% (β = -1.109, OR = 0.330, OR 95% CI = [0.205, 0.532]). However, in the absence of imperviousness, building density is seen to decrease the odds of detection of raccoons by 50.4% (β = -0.702, OR = 0.496, OR 95% CI = [0.319, 0.772]). When coyotes were present and detected (rBA), odds of raccoon detection

decreased by 74.3% (β = -1.358, OR = 0.257, OR 95% CI = [0.087, 0.758]); however, when coyotes were present but not detected, odds of raccoon detection had a greater decrease of 80.3% (β = -1.625, OR = 0.197, OR 95% CI = [0.135, 0.287]).

The top occupancy model included building density at the same spatial scale for raccoon occupancy (ψBa), and raccoon occupancy being conditional on coyote presence (ψBA). While building density trended towards negatively effecting raccoon occupancy in the absence of coyotes, the relationship was not significant just as in single species occupancy modeling. Additionally, while raccoon occupancy was determined to be conditional on coyote presence (ψBA estimated separately from ψBa), no relationship could be estimated (β = 0.130, OR = 1.139, OR 95% CI = [0.546, 2.376]). While an SIF estimated an increased attraction of raccoons and coyotes across the urbanization gradient, confidence intervals cross below the SIF threshold of 1, resulting in a non-significant relationship (SIF = 1.449, 95% CI = [0.751, 2.148]; Figure 38).

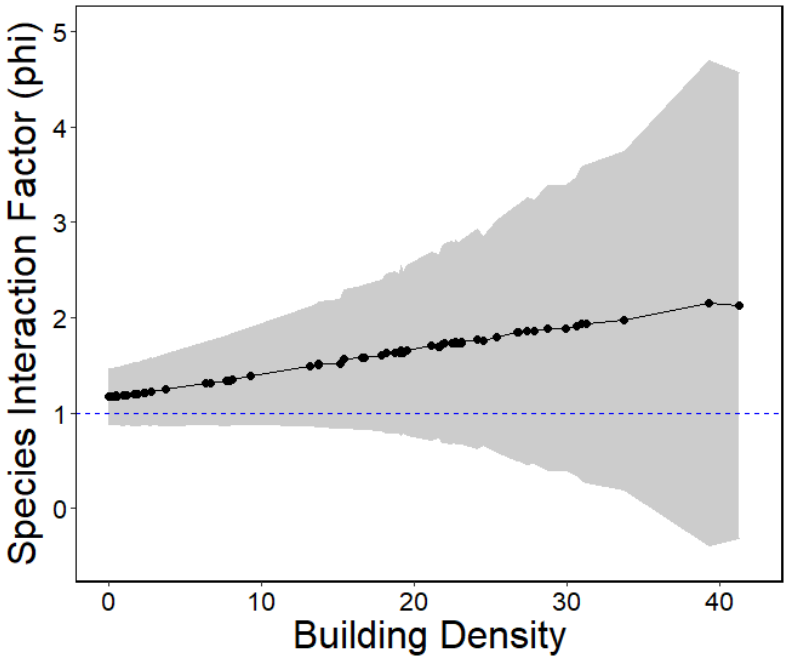

Figure 38. Species Interaction Factor (SIF, phi) for coyotes and raccoons as building density increases. Building density is represented by buildings within a 500 m kernel density radius and 500 m buffer size/km^2. Gray polygon represents 95% confidence interval. Dashed line at 1 represents SIF threshold, where values over 1 represent species attraction and values less than 1 represent species avoidance.

Coyotes and opossums

The top two-species detection model for coyotes and opossums included human presence within a 3-day period, building density at the 100 m kernel density and 1000 m buffer scale, and an interaction term between human presence and building density as covariates for opossum detection (pB), as well as the 3-day lag effect (opo3) to improve model estimation. Opossum detection was considered unconditional on both coyote presence and detection (pB = rBA = rBa; Figure 39).

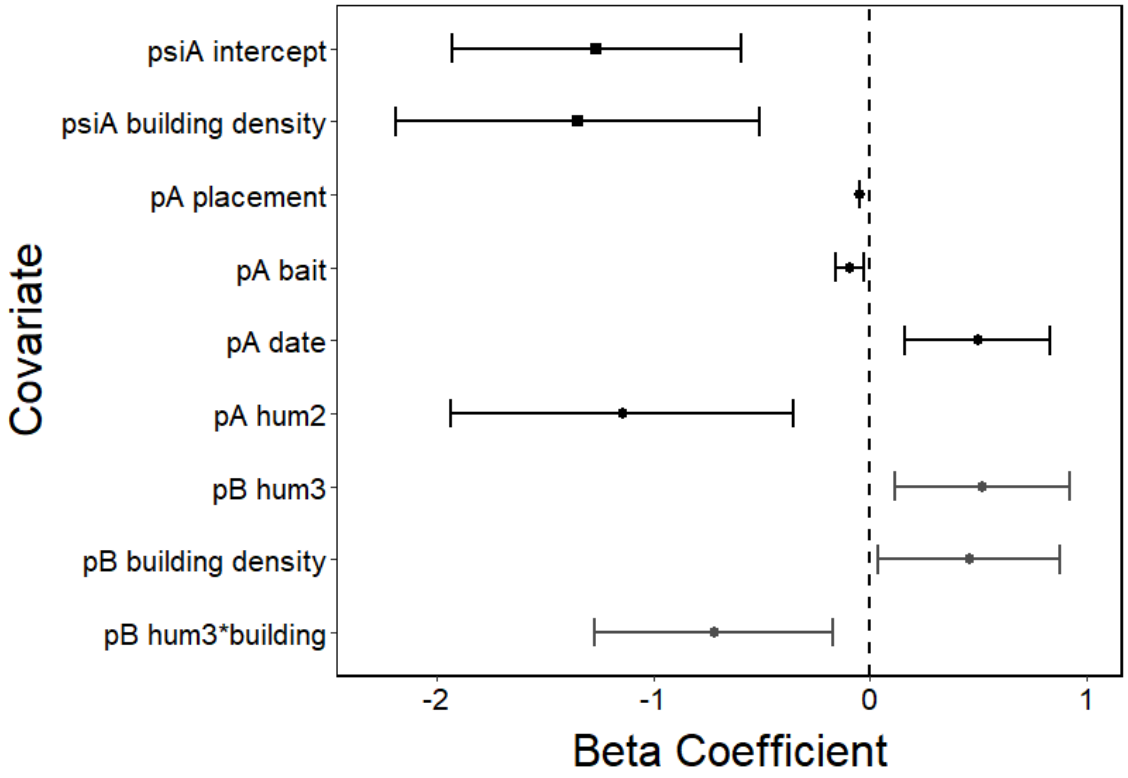

Figure 39. Beta coefficients for occupancy (psi, squares) and detection (p, r, circles) intercepts and covariates for top coyote-opossum detection and occupancy model. Variables representing coyotes (species A) are black and opossums (species B) are dark gray. If error bars, representing 95% confidence intervals, cross the zero dashed line, the beta estimate is considered not statistically significant. Omitted beta estimates include intercepts for opossum detection (pB) and occupancy (psiBA) as well as the lag effect for opossums after 3-days (opo3) due to uninterpretable beta estimates and large standard errors.

As with single-species occupancy modeling, two-species modeling shows opossum detection to positively influenced by building density, increasing the odds of opossum detection by 58.1% as building density increases ($\beta = 0.458$, OR =1.581, OR

95% CI = [1.039, 2.407]) unless humans are present within a 3-day period; as odds of opossum detection then drop by 51.4% as building density increases (β = -0.722, OR = 0.486, OR 95% CI = [0.280, 0.844]). Alternative to single species model estimation, opossums were found to be positively influenced by human presence, increasing the odds of opossum detection when humans were present in a 3-day period by 68%, regardless of building density (β = 0.519, OR = 1.680, OR 95% CI = [1.119, 2.522]).

The top occupancy model did not include any covariates for opossum occupancy (ψBa), and opossum occupancy was considered unconditional on coyote presence (ψBa = ψBA). Opossum occupancy could not be estimated through ψBa or ψBA. As opossum and coyote occupancy was unconditional, no SIF could be estimated as well.

Coyotes and striped skunks

The top two-species detection model for coyotes and striped skunks included Julian date, building density at the 200 m kernel density and 500 m buffer scale, and imperviousness at the 500 m buffer scale as covariates for skunk detection (pB). Skunk detection was considered unconditional on both coyote presence and detection (pB = rBA = rBa; Figure 40).

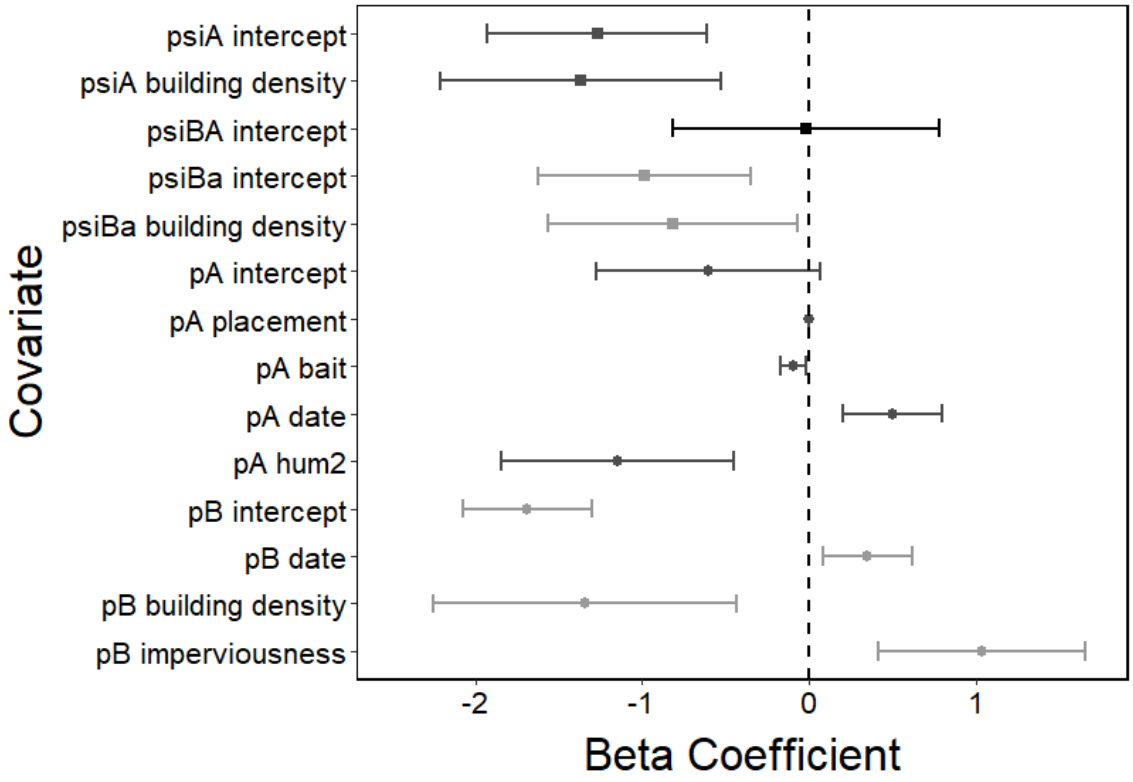

Figure 40. Beta coefficients for occupancy (psi, squares) and detection (p, r, circles) intercepts and covariates for top coyote-skunk detection and occupancy model. Variables representing coyotes (species A) are dark gray, striped skunks (species B) are light gray, and both coyote and skunk presence (BA) are black. If error bars, representing 95% confidence intervals, cross the zero dashed line, the beta estimate is considered not statistically significant.

Two-species modeling provided similar estimation for skunk detection variables compared to single-species top models. Building density decreased the odds of skunk detection by 73.9% as building density increased (β = -1.341, OR = 0.261, OR 95% CI = [0.105, 0.649]), while imperviousness increased the odds of skunk detection by 181.4% as imperviousness increased (β = 1.035, OR = 2.814, OR 95% CI = [1.518, 5.217]).

Julian date also increased the odds of skunk detection (β = 0.350, OR = 1.419, OR 95% CI = [1.086, 1.854]).

The top model for occupancy included building density at the 200 m kernel density and 500 m buffer size for both coyote (ψA) and skunk detection (ψBa). While skunk detection was considered unconditional, skunk occupancy was considered conditional upon coyote detection (ψBA estimated separately). However, while the conditional top model was selected, parameter estimations for ψBA did not provide any meaningful trend in skunk occupancy when coyotes were present (β = -0.020, OR = 0.980, OR 95% CI = [0.441, 2.181]). As with coyotes and raccoons, coyote and skunk SIF suggested an increasing attraction of species across the urbanization gradient, but this trend was not significant (SIF = 2.519, 95% CI = [0.034, 5.005]; Figure 41).

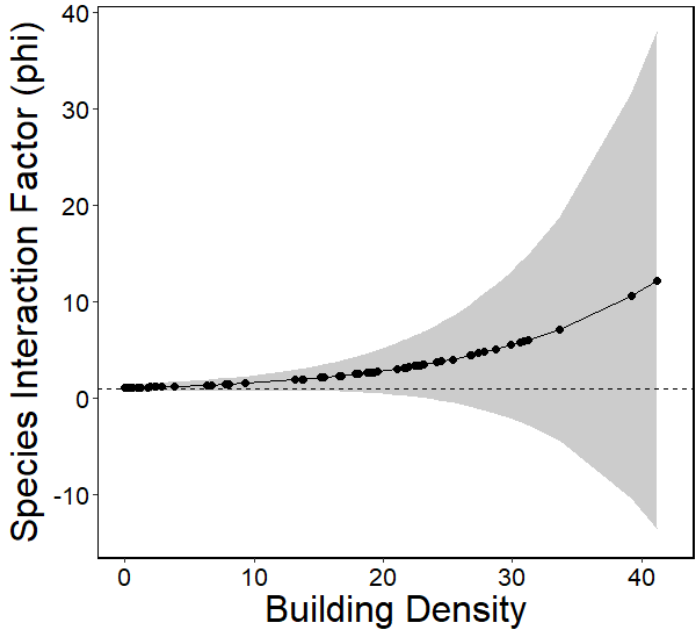

Figure 41. Species Interaction Factor (SIF, phi) for coyotes and skunks as building density increases. Building density is represented by buildings within a 200 m kernel

density radius and 500 m buffer size/km^2. Gray polygon represents 95% confidence interval. Dashed line at 1 represents SIF threshold, where values over 1 represent species attraction and values less than 1 represent species avoidance.

Although single species models did not find significant trends in coyotes and skunk occupancy estimation, two-species models for this species pairing had both species negatively impacted by building density at the same spatial scale. Odds of detection decreased by 74.5% (β = -1.367, OR = 0.255, OR 95% CI = [0.110, 0.590]) for coyotes as building density increased; as odds of skunk detection decrease by 55.8% (β = -0.815, OR = 0.442, OR 95% CI = [0.209, 0.935]) following the same increase in building density.

Coyotes and domestic cats

The top two-species detection model for coyotes and domestic cats included camera placement, anthropogenic food, bait decay, human presence within a 1-day period and building density at the 500 m kernel density and 500 m buffer scale as covariates for cat detection (pB), and cat detection being conditional on coyote presence (rBA) and detection (rBa; Figure 42).

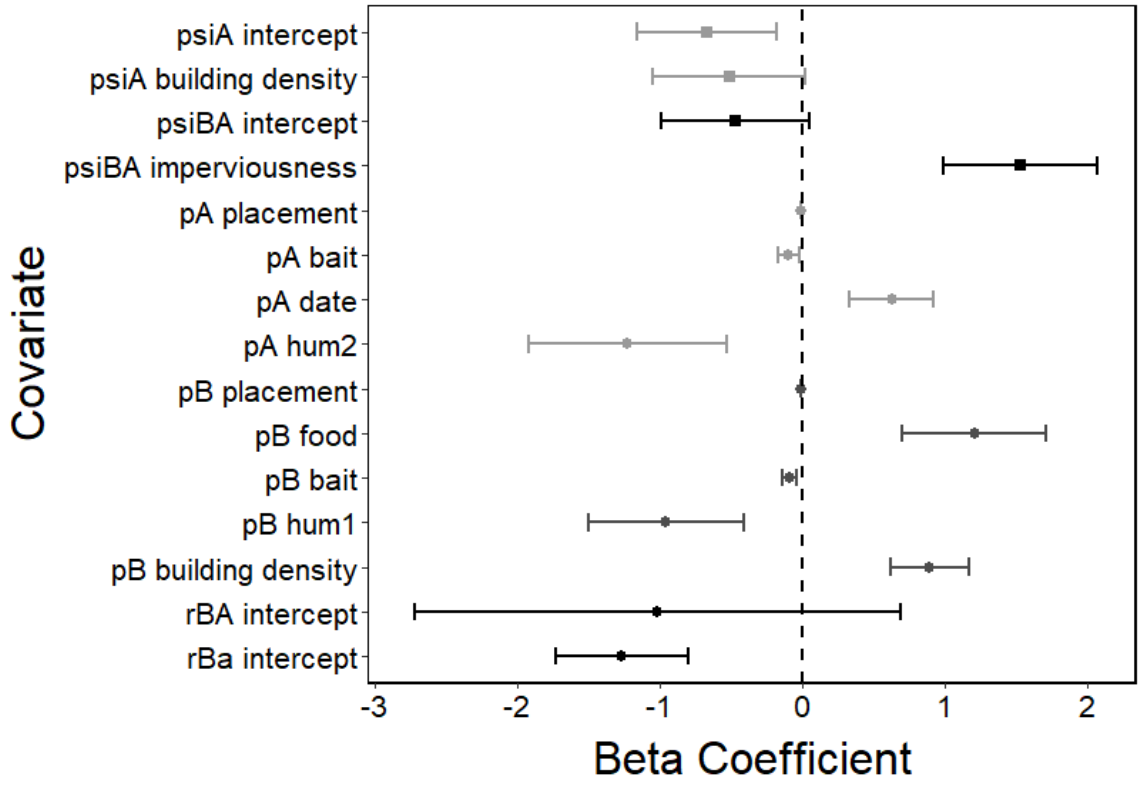

Figure 42. Beta coefficients for occupancy (psi, squares) and detection (p, r, circles) intercepts and covariates for top coyote-cat detection and occupancy model. Variables representing coyotes (species A) are dark gray, domestic cats (species B) are light gray, and both coyote and cat presence (BA) are black. If error bars, representing 95% confidence intervals, cross the zero dashed line, the beta estimate is considered not statistically significant. Omitted beta estimates include intercepts for coyote detection (pA) and cat detection (pB) due to uninterpretable beta estimates and large standard errors.

Estimation of covariates for cat detection in the two-species model were similar to covariates estimates in the single species model. Anthropogenic food sources increased odds of cat detection by 235% ($\beta = 1.209$, OR = 3.350, OR 95% CI = [2.014, 5.572]).

Bait decay decreased odds of cat detection by 8.3% (β = -0.086, OR = 0.917, OR 95% CI = [0.874, 0.963]). Human presence decreased odds of cat detection by 61.5% within a 1-day period (β = -0.954, OR =0.385, OR 95% CI = [0.223, 0.664]). Building density increased the odds of cat detection by 145% as building density increased (β = 0.896, OR = 2.450, OR 95% CI = [1.857, 3.232]). Camera placement decreased odds of cat detection in both backyards and greenspaces while not impacting cat detection in residential front yards.

Although cat detection was considered conditional on coyote presence and detection, the odds of cat detection were only seen to decrease significantly when coyotes were present but not detected (rBa; β = -1.264, OR = 0.282, OR 95% CI = [0.178, 0.449]); yet, when coyotes were present and detected (rBA), cat detection did not show a significant relationship (β = -1.014, OR = 0.363, OR 95% CI = [0.066, 1.992]).

The top two-species occupancy model for coyotes and domestic cats included imperviousness at the 500 m buffer size as a covariate for cat occupancy, while cat occupancy was considered to be unconditional upon coyote presence (ψBA = ψBa). Cat occupancy was estimated to have a positive relationship with imperviousness as was shown in the single species top model, increasing cat occupancy by 363.7% as imperviousness increased (β = 1.534, OR = 4.637, OR 95% CI = [2.707, 7.942]). Although coyote occupancy used the same building density at the 200 m kernel density and 500 m buffer size scale as used in previous two-species pairings, the top model for coyote-cat occupancy did not show a significant relationship between coyote occupancy and building density (β =-0.508, OR = 0.601, OR 95% CI = [0.353, 1.025]). As coyote-

cat occupancy was determined to be unconditional, no SIF could be derived from the top model.

Temporal Overlap

Wild mesopredator species had more detections in non-urban camera sites than low and high intensity urban areas (Table 4). Mesopredators displayed mainly crepuscular and nocturnal activity across the urbanization gradient with slight variability (Appendix I). Domestic cats were the only mesopredator to vary significantly from non-urban to urban camera sites, both in number of detections and activity patterns. Humans remained mostly diurnal across the urbanization gradient; however, shifts in both range and peaks of activity occurred as urbanization intensity increased. Intraspecies temporal overlap was consistently high for wild mesopredators across the urban gradient, with no significant change in overlap between urban gradients (Figure 43).

Table 4. Species detections (# of independent records) across urban intensities (n = 110 sites).

Urban Intensity	Coyote	Raccoon	Opossum	Striped Skunk	Domestic Cat	Human
Non-urban (n = 60)	62	99	99	91	34	208
Low Intensity Urban (n = 16)	25	11	33	28	20	159
High Intensity Urban (n = 34)	1	29	49	18	498	333
Total	88	139	181	137	552	700

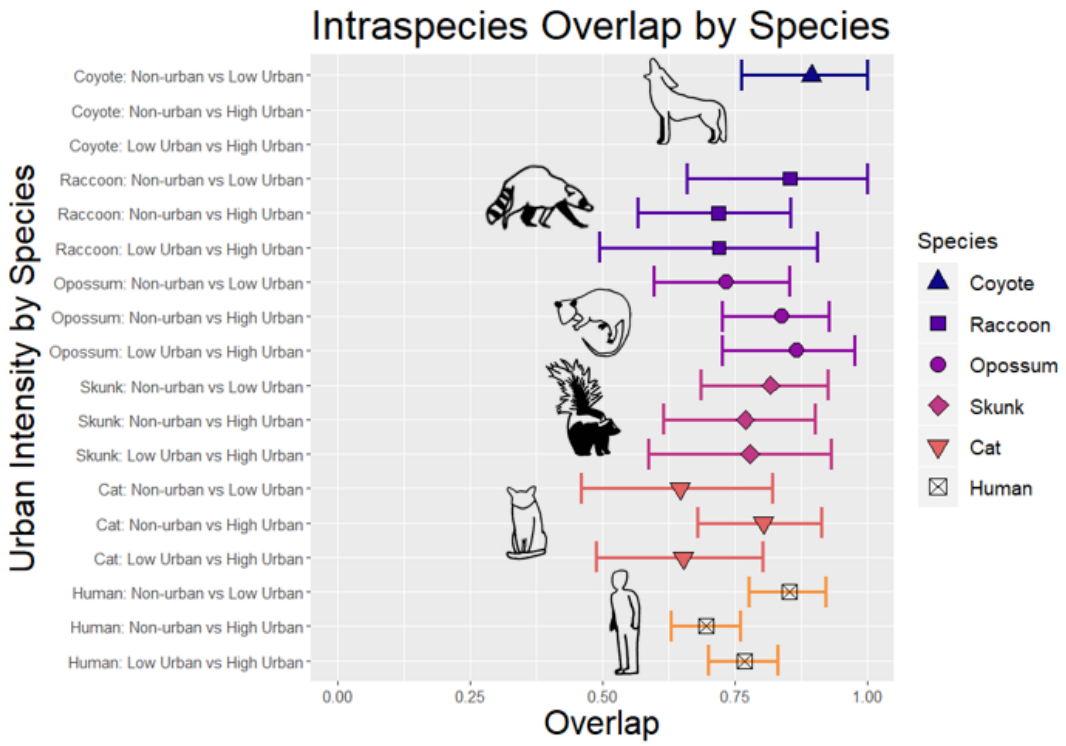

Figure 43. Temporal overlap within species across the three urban intensities (non-urban, low urban, and high urban). Points represent temporal overlap value (D-hat) for the same species between two different survey years. Error bars are 95% confidence intervals are given from calculating D-hat from bootstrapping (n = 10,000).

Humans

Human activity shifted from being mainly diurnal in non-urban areas (falling between sunrise to sunset) to having a wider range of crepuscular and nighttime activities in low and high intensity urban areas. This shift from strictly diurnal activity to include more crepuscular and nocturnal activity was significant between non-urban areas and low intensity urban areas (AD = 11.17, T.AD = 13.42, $p = 2.2e^{-06}$, $\alpha = 0.05$), as well as non-urban and high intensity urban areas (AD = 16.95, T.AD = 21.02, $p = 1.46e^{-09}$, $\alpha = 0.05$;

Appendix I). While human activity in high intensity urban areas starts to have two bimodal peaks of activity around morning and sunset, activity patterns were not statistically significant between low intensity and high intensity urban areas (AD = 2.452, T.AD = 1.914, p = 0.523, $\alpha = 0.05$). This dramatic shift in human activity between non-urban and urban areas is apparent as temporal overlap significantly decreased between non-urban and low intensity sites ($\Delta\text{-hat}_4 = 0.852$, 95% CI = [0.776, 0.922]) and non-urban and high intensity urban sites ($\Delta\text{-hat}_4 = 0.696$, 95% CI = [0.630, 0.760]; Figure 43).

Coyotes

Coyotes were only detected once at a high intensity urban camera (a mother and juvenile pair at 10:33PM in an urban resident's backyard) and thus their temporal activity could not be compared for the high intensity urban areas (Table 4). Coyote activity did not change substantially between non-urban areas and low intensity urban areas, and temporal overlap between coyotes in these two areas remained relatively high (Figure 43). Although coyotes displayed some increased diurnal activity compared to other mesopredators in low intensity urban areas, temporal overlap with all mesopredator species across non-urban and low intensity urban sites remained high (Figure 44).

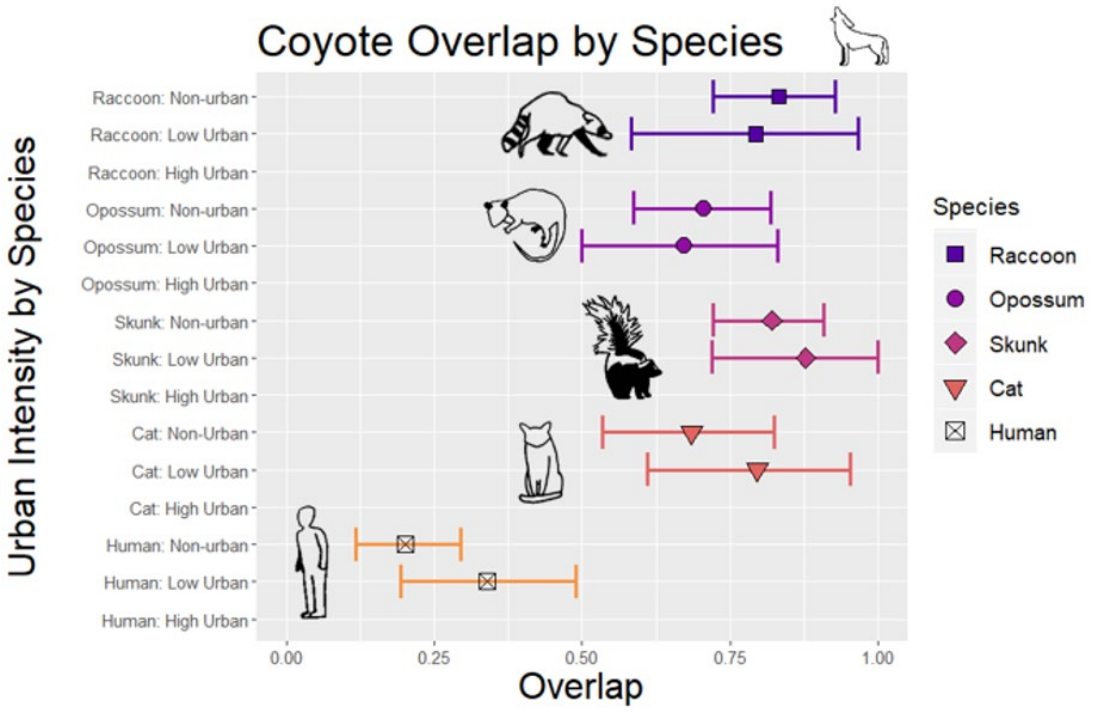

Figure 44. Temporal overlap between coyotes and all other species across the three urban intensities (non-urban, low urban, and high urban).

Raccoons

Raccoons had a majority of their detections in non-urban and high intensity urban areas, while having the fewest detections in low intensity urban areas (Table 4). Raccoon activity, while exhibiting more diurnal detections in non-urban areas, did not change significantly across the urbanization gradient. Raccoons had their greatest intraspecies temporal overlap between non-urban and low intensity urban sites; although, temporal overlap values were consistently high amongst all urban intensity pairings (Figure 43). Raccoon overlap with wild mesopredator species in non-urban areas tended to be greatest and had the most confined range, while overlap in high intensity urban areas tending to

be wider and lower; however, this variability proved to not be significant as confidence intervals for all species across the urbanization gradient overlapped as well. Raccoons had consistently low overlap values with humans that tended to slowly increase as urbanization intensity increased; however, confidence intervals for overlap values also overlapped for all three urban intensities (Figure 45).

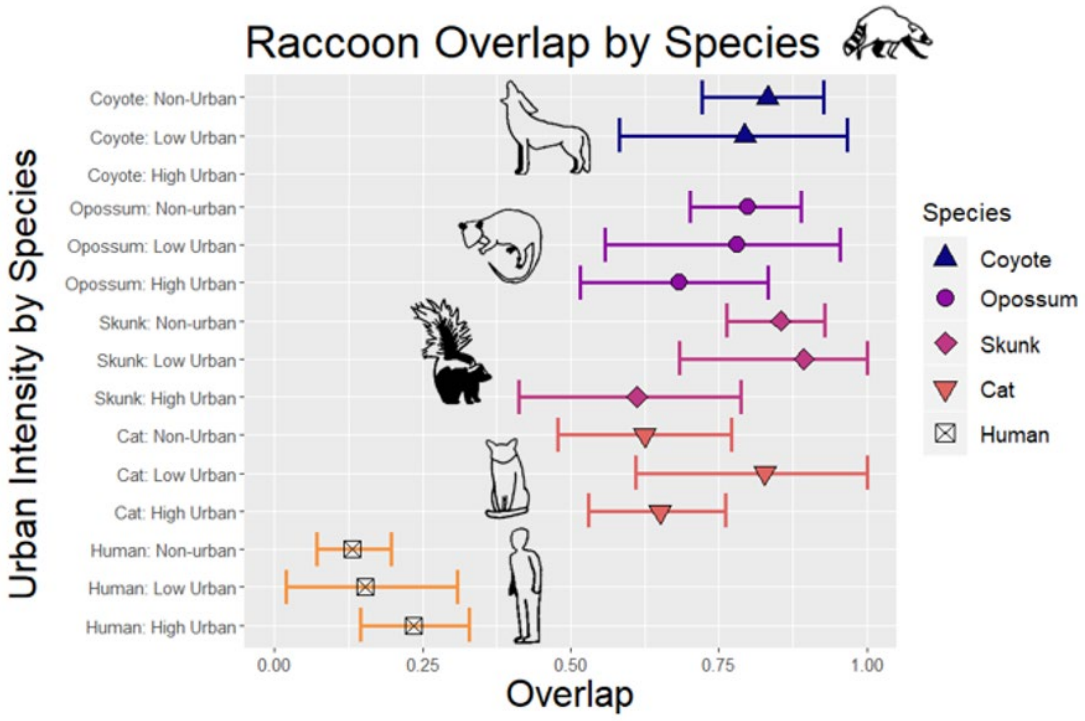

Figure 45. Temporal overlap between raccoons and all other species across the three urban intensities (non-urban, low urban, and high urban).

Opossums

Like raccoons, opossums had the highest detections in non-urban and high intensity urban areas compared to low intensity urban areas (Table 4). Opossum were the only wild mesopredator to have their activity patterns differ between non-urban and high

intensity urban areas (AD = 2.786, T.AD = 2.376, p = 0.034, α = 0.05), likely due to a drop in crepuscular activity in high intensity urban areas (Appendix I). While opossum activity did shift, intraspecies temporal overlap remained high between all three pairings of urban intensities (Figure 43). Opossum temporal activity was consistently high for all wild mesopredator species across the urbanization gradient. Opossum temporal overlap drops slightly with domestic cats in non-urban and high intensity urban areas compared to other mesopredators; yet temporal overlap between opossums and cats remains within predicted confidence intervals for all three urban intensities. Opossum overlap with humans, while low, follows a trend of slightly increasing as urbanization increases; however, this trend is not statistically significant (Figure 46).

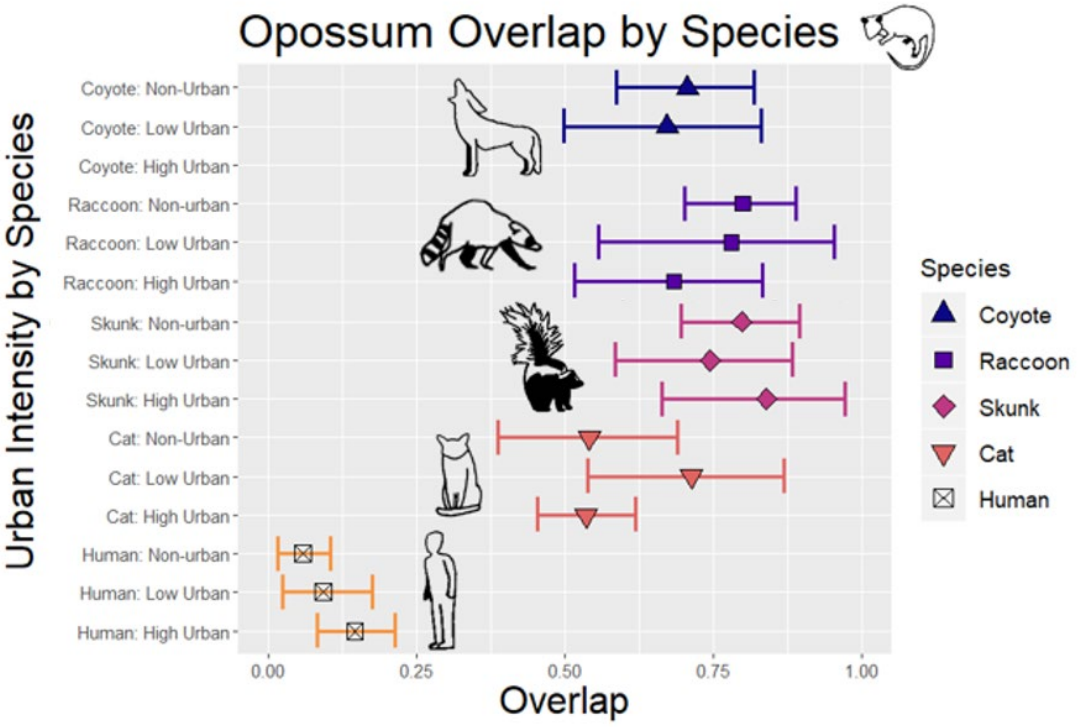

Figure 46. Temporal overlap between opossums and all other species across the three urban intensities (non-urban, low urban, and high urban).

Striped skunks

Striped skunks had the most detections in non-urban, followed by low intensity urban areas, and the least detection in high intensity urban areas (Table 4). Skunk activity was consistently crepuscular and nocturnal across the urbanization gradient (Appendix I). Because of this, skunk intraspecies temporal overlap was consistently high across the urbanization gradient (Figure 43). Skunks displayed high to moderate overlap with mesopredator species across the urbanization gradient with lower initial temporal overlap with raccoons in high intensity urban sites and lower temporal overlap with cats in non-urban and high intensity urban areas, although temporal overlap values do not change

significantly. Skunks did significantly increase temporal overlap with humans between non-urban (D-hat$_4$ = 0.060, 95% CI = [0.018, 0.108]) and low intensity urban areas (D-hat$_1$ = 0.227, 95% CI = [0.117, 0.338]; Figure 47).

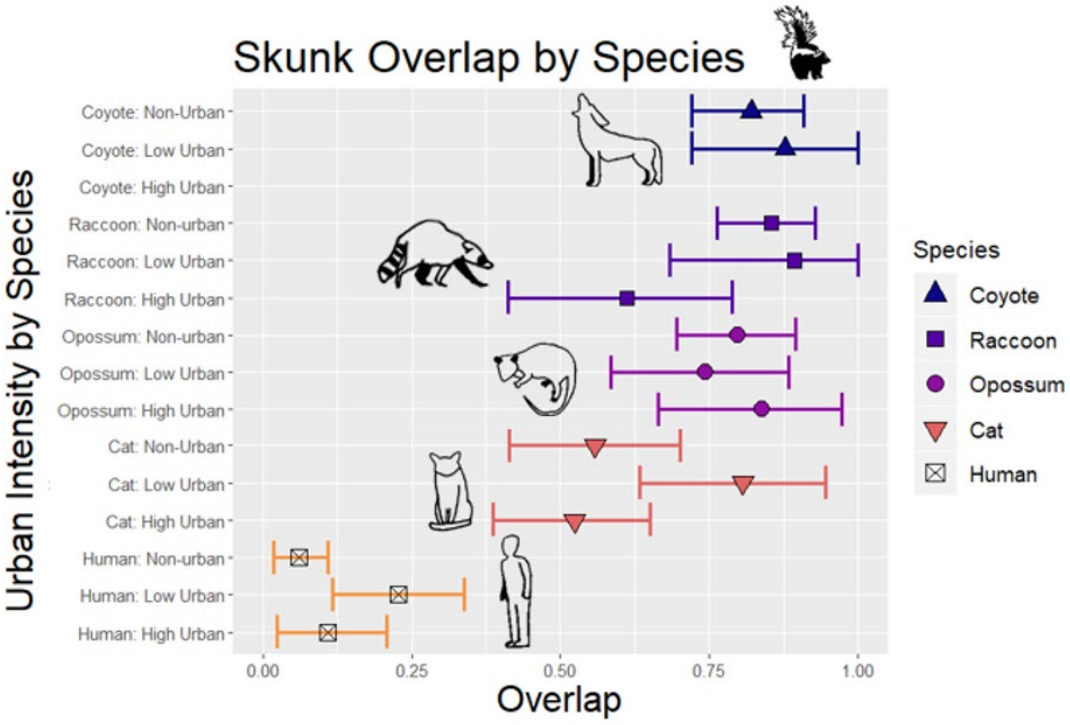

Figure 47. Temporal overlap between skunks and all other species across the three urban intensities (non-urban, low urban, and high urban).

Domestic cats

Domestic cat detections increased substantially in the high intensity urban areas compared to non-urban and low intensity urban sites. Domestic cats had highly variable activity patterns across each of the three urban intensities; having peaks of nocturnal, diurnal, and crepuscular activity in non-urban areas, mainly nocturnal activity in low intensity urban areas, and a strong shift from early morning to afternoon activity followed

by a nocturnal peak following sunset in high intensity urban areas (Appendix I). Because of this, cat activity in non-urban areas was considered significantly different from activity in both low intensity (AD = 5.313, T.AD = 5.737, p = 0.002, $\alpha = 0.05$) and high intensity urban areas (AD = 2.772, T.AD = 2.332, p = 0.036, $\alpha = 0.05$). While activity patterns differed between non-urban and urban areas, intraspecies temporal overlap for cats remained relatively high, with non-urban and high intensity urban areas seeming to have the highest overlap, although not statistically significant Figure 43).

Domestic cats seemed to have the highest temporal overlap with all mesopredator species at low intensity urban sites, although confidence intervals between all three urban intensities overlap greatly (Figure 48). Additionally, cat temporal overlap with humans was significantly lower at low intensity urban sites ($\hat{D}_1 = 0.266$, 95% CI = [0.112, 0.426]) versus high intensity urban sites ($\hat{D}_4 = 0.533$, 95% CI = [0.485, 0.583]).

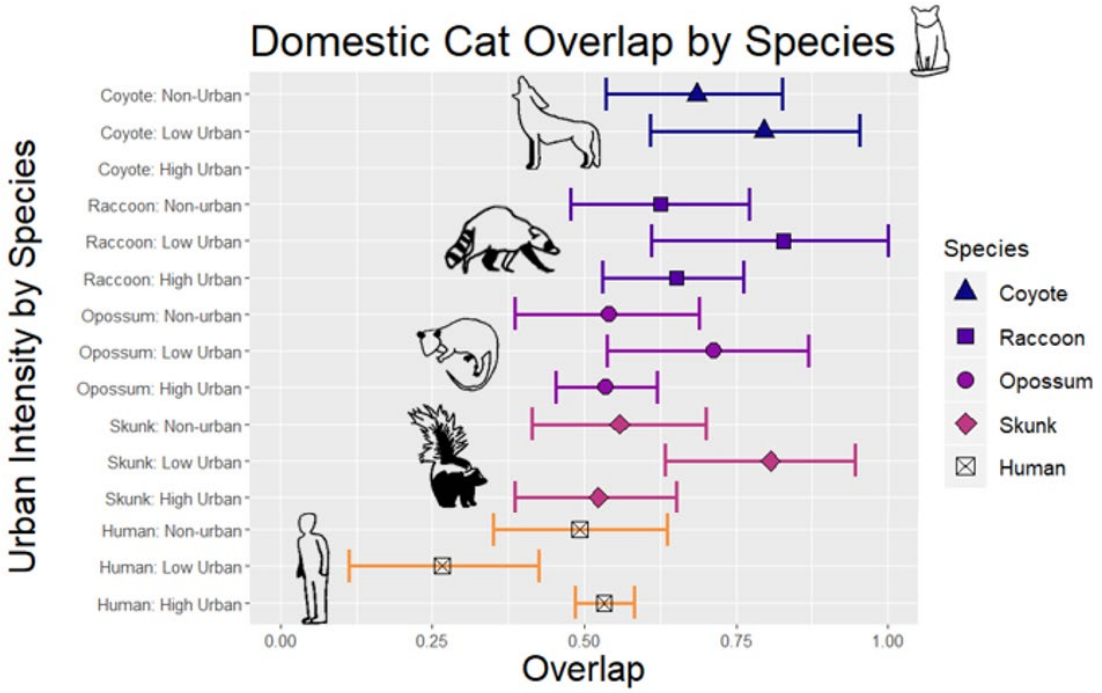

Figure 48. Temporal overlap between domestic cats and all other species across the three urban intensities (non-urban, low urban, and high urban).

Discussion

All mammalian mesopredators responded to increasing urban intensity at varying spatial scales in my study in the Sacramento Metropolitan Area and surrounding non-urban areas. I had hypothesized that spatiotemporal overlap of mesopredators would be highest in high intensity urban areas. I found evidence to suggest that small mesopredators were spatially attracted to urban areas, potentially increasing their overlap with each other and humans. Coyotes were not often found in high intensity urban areas, which could indirectly decrease spatial overlap of coyotes and small mesopredators in

these areas. Finally, I found support that while mesopredators may have higher spatial and temporal overlap with humans in urban areas, mesopredators may be avoiding humans across the urban gradient.

Mesopredators showed a combination of both spatial and temporal shifts in activity in urban areas compared to non-urban areas. While coyotes, opossums, striped skunks, and domestic cats had direct relationships between human presence and activity, opossums were the only species to have their relationship with humans change how they responded to urban intensity. This pattern of mesopredator attraction to urban resources while fearing human presence is well recorded and supported (Prange and Gehrt 2004, Wang et al. 2015, Nickel et al. 2020). Finally, while species did not respond to coyote presence at larger temporal scales, coyotes may be influencing mesopredator spatiotemporal activity differently across and urban intensity gradient at finer scales.

Mammalian Mesopredator Response to Urban Intensity

Mesopredators response to urban intensity was complex, as mesopredator land use, detection, and temporal activity were sensitive to changes in building density, imperviousness, and interactions with human presence at varying spatial scales as well as depending on the analysis used to evaluate mesopredator and urban intensity relationships. Therefore, it may be useful to visualize mesopredator response to urban intensity on a spectrum of most negatively impacted to most positively impacted (Figure 49).

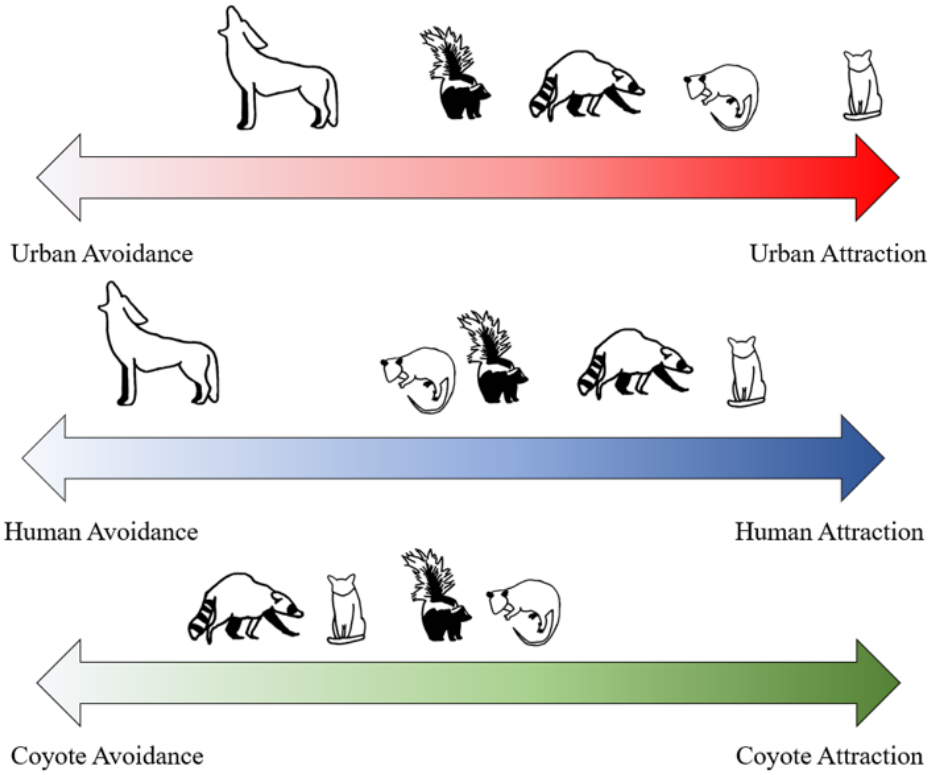

Figure 49. Mammalian mesopredator (coyote, raccoon, opossum, striped skunk, and domestic cat) responses to urban areas, humans, and coyotes. Species fall along a spectrum of either avoidance or attraction for each stressor, with area in the middle representing a neutral response.

Coyotes were the most negatively impacted by urban areas due to the combined effects of building density and increased human presence. Interestingly, coyotes displayed a negative relationship between building density and land use in both single species and two-species models; however, this relationship was only significant in two-species models excluding coyote-cat pairings. Coyote detection did drop significantly in residential backyards, and they were undetected in residential front yards, seeming to prefer camera sites in greenspaces to travel regardless of urban intensity (Tigas et al.

2002, Greenspan et al. 2018). Coyotes may be more stressed or wary of human residences, as often these are areas that represent increased potential conflict, unless they have been habituated due to feeding and provisioning (Hansen et al. 2005, White and Gehrt 2009, Poessel et al. 2013). Combined with evidence that coyotes avoided humans after a 2-day period across the urban gradient, coyotes were most likely avoiding high density human and building areas and restricting their urban presence to low intensity urban greenspaces such as parks and riparian corridors to reduce the risk of encountering humans. This avoidance of humans and buildings may allow for smaller mesopredators to use high intensity urban areas as refugia to avoid intraguild predation (Gosselink et al. 2003).

Wild mesopredators such as raccoons, striped skunks, and opossums, had varying tolerance to urban areas. Striped skunks and raccoons had opposite responses to building density and imperviousness. For instance, raccoon detection increased as building density increased and decreased as imperviousness increased. Additionally, opossums also were also positively influenced by building density, with opossum detection increasing as building density increases. This may be the result of raccoons and opossums being more tolerant of buildings than skunks, as arboreal species may benefit from using the network of fences and rooftops in urban areas compared to skunks which may not be able to navigate urban areas as easily (Gehrt 2004). Skunks may also be less tolerant of humans in urban areas, as skunks increased their temporal overlap with humans between non-urban and low intensity urban areas, while raccoons showed no change in temporal activity. Skunks may thus benefit from the resources of urban areas at a larger scale,

while trying to avoid humans at finer scales. Raccoons may be the boldest wild mesopredator compared to skunks and opossums (which had a negative relationship between detection and building density when humans were present; see also Bateman and Fleming 2012). Interestingly, raccoon detection was negatively influenced by building density in two-species models with coyotes, as imperviousness was not included as an important covariate for detection. This shows the importance of including multiple covariates to quantify urban intensity, as raccoons may be benefiting from urban areas by using buildings as links between greenspaces while avoiding areas of complete concrete coverage (Moll et al. 2019). Scale was also important to consider, as avoidance and attraction to urban areas may not be captured at too coarse or fine of a scale depending on the species (Fidino et al. 2020).

Domestic cats were unsurprisingly positively associated with high intensity urban areas at a coarse scale. Domestic cats were the only species to increase their habitat use as imperviousness increased, showing a general attraction to urban areas compared to non-urban habitat types. Domestic cats were also the only mesopredator to also respond strongly to anthropogenic food sources; however, this may be biased by residents of urban areas leaving out food specifically for both pet and feral cats. Cats were also positively associated with increased building density, as cat detection increased as building density increased. Unexpectedly, cats decreased their detection when humans were nearby in a 1-day period. This may be due to two reasons; first, pet cats were more likely to leave households when their owners were out and not nearby to put them inside, and second, feral cats were generally skittish around humans; however, they benefitted

from food being left out after humans had left the area (Clancy et al. 2003, Horn et al. 2011).

Mesopredators were generally more nocturnal in urban areas compared to non-urban areas, which is a common response to disturbance by humans (Gaynor et al. 2018), although in my study this trend varied. Wild mesopredators, including coyotes, tended to have high temporal overlap across all urban intensities in my study; therefore, temporal partitioning between mesopredator species is probably not occurring at the scale measured. In order to coexist, mesopredators may be exploiting different resources within urban areas even at the highest intensities, or resources may not be a limiting factor across the urban gradient, allowing species to occur together with reduced competition (Rosenzweig 1966, Gehrt 2004, Theimer et al. 2015).

Coyotes as Intraguild Predators

Coyotes may be influencing mammalian mesopredator spatiotemporal activity at a fine scale. While coyotes do not influence mesopredators at the one to three day scale in single species occupancy modeling, coyote presence was shown to influence certain mesopredators in two species occupancy models. Of the wild mesopredators, raccoons were most likely to respond to coyote presence and detection, while striped skunks and opossums did not respond to coyotes. Raccoon detection decreased when coyotes were present and detected, as well as when coyotes were assumed to be present but not detected. While previous studies of sympatric coyote and raccoon interactions suggests that intraguild predation is rare between raccoons and coyotes and that raccoons do not avoid coyotes (Gehrt and Prange 2007, Morey et al. 2007, Chitwood et al. 2020),

raccoons may be utilizing different habitat features such as trees and buildings when coyotes are in an area. However, raccoon response to coyotes may also be related to reproduction and seasonal effects, as raccoon detection decreased throughout the summer season while coyote detection increased. Juvenile raccoons may be most vulnerable to coyotes and thus, raccoons mothers with young may be avoiding coyotes during mid - summer (June/July), and late summer (August) dispersing males may no longer have the benefit of a family group to keep watch when coyotes are most active (Troyer et al. 2014, Chitwood et al. 2020). Skunks and opossums may avoid coyote predation through either defensive or deterrence behaviors, and thus may not have the same response as raccoons (Gabrielsen and Smith 1985, Larivière and Messier 1996).

Domestic cats were the only other species to be influenced by coyote presence and detection. Interestingly, coyote presence only negatively influenced cat detection when coyotes were assumed to be present but were not detected (rBa) compared to when coyotes were present and detected (rBA). This may be due to coyotes and cats only being detected together in the same day twice, while cats and coyotes only shared four camera sites in total. Of the four sites that coyotes and cats shared, two were in non-urban and low intensity urban areas where cats returned 4 to 5 days following coyotes, while at the other two sites (an exurban and high intensity urban site) cats returned within 1 day of coyote detection. Thus, feral and rural cats may be avoiding coyotes while pet cats that are close to homes may be naïve to the threat of coyotes (Grubbs and Krausman 2009, Breck et al. 2019). Cats can be a food source for coyotes in urban areas (Morey et al.

2007), and pet owners that know coyotes are in an area are more likely to keep their cats inside (Crooks and Soulé 1999).

While coyotes may be the defacto apex predator in the Central Valley, their role as an intraguild predator may be limited to pets and other wild canids rather than raccoons, skunks, and opossums (Gehrt and Clark 2003, Morey et al. 2007, Lesmeister et al. 2015, Breck et al. 2019). Coyotes may be limiting the distribution of two smaller canid mesopredators, the gray and red fox, which were both captured on cameras in the Central Valley. Gray foxes, were captured on cameras in parks within Sacramento and Stockton, and red foxes have been seen in urban Sacramento; therefore, urban areas may facilitate population increases of these foxes in absence of coyotes (Lewis et al. 1999, Lombardi et al. 2017, Mueller et al. 2018). Thus, mesopredator distributions and activity are most likely more influenced by the perceived risk of human presence.

Humans Risk across Urban Intensities

Human activity and presence in the Central Valley changed from non-urban areas to high intensity urban areas, impacting mesopredators across the urban gradient. In non-urban areas, human activity was mostly diurnal, meaning most mesopredators were able to avoid humans as they were mostly nocturnal. As urban intensity increased, human activity widened, with humans being active throughout the day at the highest urban intensities. This shift into more nocturnal activity increased striped skunk and human overlap in low intensity urban areas, potentially increasing the perceived risk of humans by striped skunk in these areas. However, striped skunks were still found to increase detection as imperviousness increases, and thus may increase activity in urban areas

while avoiding more human dense residential and city center areas (Rosatte et al. 1992, Gehrt 2004). Opossums were the only species to respond positively to building density when humans were not present in a 3-day period. Opossums likely avoided humans, but benefitted the most from urban features, as they were found to be ubiquitous across the urban gradient, and were captured on backyard, front yard, and greenspace cameras (Beatty et al. 2013, Wang et al. 2015, Greenspan et al. 2018). Raccoons likely benefit from the same features as opossums; however, they show less avoidance of humans. This may be because raccoons benefit the most from human trash and human structures, making urban raccoons more likely to aggregate and exploit these resources compared to other species (Gehrt et al. 2010, Theimer et al. 2015). Coyotes avoided humans across the urban intensity gradient, yet some individuals were able to use human backyards, especially in exurban and riparian corridors. Coyotes may shift from using more open areas to more densely vegetated areas in order to avoid humans while still benefiting from urban resources (Greenspan et al. 2018).

Increased human activity presents risk to all mesopredators within urban areas; however, urban lineages of species may modify their tolerance of humans over time via assortative mating of more human tolerant individuals in urban areas (Santini et al. 2019, Adducci et al. 2020). As my study captures mesopredator detections across varying levels of urban intensities, it is likely that certain behaviors and individual plasticity in response to urban areas and humans were captured and generalized together in my analyzes. For instance, while I was able to capture increases in human presence in the immediate camera area, I was unable to quantify how many humans were using the general area

around camera sites, especially in high intensity urban areas where cameras were placed in areas out of sight to reduce vandalism. Thus, the mesopredator responses to humans presented do not capture the magnitude of human tolerance (either increasing boldness or shyness to humans), and it is likely that individual mesopredators have varying levels of tolerance to human densities, especially if they have been repeatedly fed or habituated to humans (Poessel et al. 2017, Welch et al. 2017, Breck et al. 2019).

Management Implications

Many mammalian mesopredators have adapted to use anthropogenic resources across urban intensities (Bateman and Flemming 2012, Santini et al. 2019). While larger species like coyotes are less tolerant of humans and high intensity urban areas, bold individuals may still enter and persist in city centers (Breck et al. 2019). Additionally, while coyotes may alter the behavior of some species and individuals, mesopredators are likely responding to bottom-up effects of aggregated resources and usable movement corridors, allowing species to enter deeper into high intensity urban areas from lower intensity and non-urban areas. Thus, managers of urban ecosystems must consider urban areas as permeable landscapes, and should tailor conservation, ecosystem services, and human health projects objectives around the facilitation of wildlife presence and movement to areas that maximize both human and wildlife benefit over risk.

When it comes to mesopredator presence in cities, managers of wildlife are often tasked with preventing conflict (actual and perceived) between mesopredators and humans (Gehrt et al. 2010). Mammalian mesopredators can be labeled as pests for causing property damage by nesting in houses, rummaging through trash cans, killing and

eat pets, disturbing dogs and people walking along trails (e.g. skunks spraying), and being vectors for diseases (e.g., rabies, sarcoptic mange) and parasites (raccoon roundworm) that infect and kill humans and pets (Roussere et al. 2003, Gehrt et al. 2010, Murray et al. 2015). Trapping and lethal removal of individuals or targeted populations is often used to eliminate "problem animals"; however, lethal removal can often exacerbate human-wildlife conflict by increasing reproductive rates of target populations, being ineffective at large scales, and increasing movement and densities of species by destabilized social hierarchies if non-target individuals are removed (Treves and Karanth 2003). Non-lethal removal or discouragement of mesopredators can also have varying effects, and often more expensive methods of exclusion may work (Ratnaswamy et al. 1997). Managers of urban environments seeking to reduce conflict may have to try several methods before finding something that works, and hope that species do not quickly habituate and learn how to exploit expensive exclusions.

In addition to managing wildlife populations, managers may also seek to influence people's views of species in urban ecosystems, which are already changing to be less tolerant of lethal removal (Jackman and Rutberg 2015). As managers of urban ecosystems are often faced with the challenges of dealing with multiple nuisance mesopredators, managers should focus on measures that enhance ecosystem function and movement of mesopredators into more suitable habitat. By providing healthy and biodiverse greenspaces for both mesopredators and people, urban managers may be able to shift the public away from negative attitudes towards wildlife and predators, and rely less on short-term conflict prevention measures (Santini et al. 2019).

Restoring and maintaining greenspaces throughout high to low urban intensities may facilitate the movement of mesopredators through urban ecosystems. Creating larger interconnected greenspaces may allow for greater overlap of species, potentially reducing problem species (feral cats via coyotes), and increasing biodiversity of insects, birds, and for conservation goals (Goddard et al. 2010, Gallo et al. 2017). Increasing functioning urban greenspaces may also benefit human health by reducing heat island effects and improving access to nature (Lafortezza et al. 2009, Van den Berg et al. 2015), as well as indirectly benefit wildlife by increasing public awareness of local species and conservation goals (Budruk et al. 2009). Moreover, creating and maintaining greenspaces that facilitate wildlife movement and connectivity across urban areas may also provide more equitable access to nature by spreading out greenspaces throughout all socioeconomic areas (McKinney 2006, Schell et al. 2020).

Conclusions

Mammalian mesopredators change their spatiotemporal activity and behavior depending on the risks of urban intensity, intraguild predation, and resource distribution. Even so, mesopredators display high spatiotemporal overlap, suggesting that species can coexist by utilizing different features of their environments across human dominated landscapes. Humans both facilitate mesopredator communities while also being a constant source of risk throughout non-urban and urban landscapes (Tigas et al. 2002, Welch et al. 2017, Gaynor et al. 2018). Additionally, the scale and covariates urban ecologists use to investigate mammalian mesopredators can lead to different conclusions about how species are responding to urban features and each other (e.g. Moll et al. 2019).

Future research on mesopredator spatiotemporal activity should address whether fine scale microhabitat usage and behavioral plasticity towards intraguild predators and humans across urban gradients allow for mesopredator coexistence. Additionally, enhancing and connecting urban greenspaces across high intensity urban areas, including disadvantaged socioeconomic areas, has the potential to both facilitate wildlife movement and increase public health and connection to nature.

Literature Cited

Adducci, A., J. Jasperse, S. Riley, J. Brown, R. Honeycutt, and J. Monzón. 2020. Urban coyotes are genetically distinct from coyotes in natural habitats. Journal of Urban Ecology 6. Oxford Academic. <https://academic.oup.com/jue/article/6/1/juaa010/5828680>. Accessed 11 May 2020.

Anderson, D. R., and K. P. Burnham. 2002. Avoiding Pitfalls When Using Information-Theoretic Methods. The Journal of Wildlife Management 66:912–918. [Wiley, Wildlife Society].

Arnold, T. W. 2010. Uninformative Parameters and Model Selection Using Akaike's Information Criterion. The Journal of Wildlife Management 74:1175–1178.

Baker, A. D. 2016. Impacts of human disturbance on carnivores in protected areas of the American Southwest. University of Louisiana at Lafayette.

Baker, P. J., C. V. Dowding, S. E. Molony, P. C. L. White, and S. Harris. 2007. Activity patterns of urban red foxes (Vulpes vulpes) reduce the risk of traffic-induced mortality. Behavioral Ecology 18:716–724.

Bateman, P. W., and P. A. Fleming. 2012. Big city life: carnivores in urban environments. Journal of Zoology 287:1–23.

Beatty, W. S., J. C. Beasley, and O. E. Rhodes. 2013. Habitat selection by a generalist mesopredator near its historical range boundary. Canadian Journal of Zoology 92:41–48.

Bivand, R., T. Keitt, and B. Rowlingson (2020). rgdal: Bindings for the 'Geospatial' Data Abstraction Library. R package version 1.5-18. <https://CRAN.R-project.org/package=rgdal>.

Breck, S. W., S. A. Poessel, P. Mahoney, and J. K. Young. 2019. The intrepid urban coyote: a comparison of bold and exploratory behavior in coyotes from urban and rural environments. Scientific Reports 9:1–11.

Budruk, M., H. Thomas, and T. Tyrrell. 2009. Urban Green Spaces: A Study of Place Attachment and Environmental Attitudes in India. Society & Natural Resources 22:824–839. Routledge.

Cade, B. S. 2015. Model averaging and muddled multimodel inferences. Ecology 96:2370–2382.

Chitwood, M. C., M. A. Lashley, S. D. Higdon, C. S. DePerno, and C. E. Moorman. 2020. Raccoon Vigilance and Activity Patterns When Sympatric with Coyotes. Diversity 12:341. Multidisciplinary Digital Publishing Institute.

Clancy, E. A., A. S. Moore, and E. R. Bertone. 2003. Evaluation of cat and owner characteristics and their relationships to outdoor access of owned cats. Journal of the American Veterinary Medical Association 222:1541–1545. American Veterinary Medical Association.

Clinchy, M., L. Y. Zanette, D. Roberts, J. P. Suraci, C. D. Buesching, C. Newman, and D. W. Macdonald. 2016. Fear of the human "super predator" far exceeds the fear of large carnivores in a model mesocarnivore. Behavioral Ecology arw117.

Crooks, K. R., and M. E. Soulé. 1999. Mesopredator release and avifaunal extinctions in a fragmented system. Nature 400:563–566. Nature Publishing Group.

Ditchkoff, S. S., S. T. Saalfeld, and C. J. Gibson. 2006. Animal behavior in urban ecosystems: Modifications due to human-induced stress. Urban Ecosystems 9:5–12.

Durand, J. R., F. Bombardelli, W. E. Fleenor, Y. Henneberry, J. Herman, C. Jeffres, M. Leinfelder–Miles, J. R. Lund, R. Lusardi, A. D. Manfree, J. Medellín-Azuara, B. Milligan, and P. B. Moyle. 2020. Drought and the Sacramento-San Joaquin Delta, 2012–2016: Environmental Review and Lessons. San Francisco Estuary and Watershed Science 18. <https://escholarship.org/uc/item/6hq949t6>. Accessed 24 Nov 2020.

Elmqvist, T., M. Fragkias, J. Goodness, B. Güneralp, P. J. Marcotullio, R. I. McDonald, S. Parnell, M. Schewenius, M. Sendstad, K. C. Seto, and C. Wilkinson, editors.

2013. Urbanization, Biodiversity and Ecosystem Services: Challenges and Opportunities. Springer Netherlands, Dordrecht. <http://link.springer.com/10.1007/978-94-007-7088-1>. Accessed 28 Nov 2020.

Fidino, M., T. Gallo, E. W. Lehrer, M. H. Murray, C. Kay, H. A. Sander, B. MacDougall, C. M. Salsbury, T. J. Ryan, J. L. Angstmann, J. A. Belaire, B. Dugelby, C. Schell, T. Stankowich, M. Amaya, D. Drake, S. H. Hursh, A. A. Ahlers, J. Williamson, L. M. Hartley, A. J. Zellmer, K. Simon, and S. B. Magle. 2020. Landscape-scale differences among cities alter common species' responses to urbanization. Ecological Applications n/a:e2253.

Fiske, I., and R. Chandler. 2011. unmarked: An R Package for Fitting Hierarchical Models of Wildlife Occurrence and Abundance. Journal of Statistical Software 43:1–23.

Foley, J. A., R. DeFries, G. P. Asner, C. Barford, G. Bonan, S. R. Carpenter, F. S. Chapin, M. T. Coe, G. C. Daily, H. K. Gibbs, J. H. Helkowski, T. Holloway, E. A. Howard, C. J. Kucharik, C. Monfreda, J. A. Patz, I. C. Prentice, N. Ramankutty, and P. K. Snyder. 2005. Global Consequences of Land Use. Science 309:570–574.

Fox, C. H. 2006. Coyotes and Humans: Can We Coexist? Proceedings of the Vertebrate Pest Conference 22. <https://escholarship.org/uc/item/6mx0f9pf>. Accessed 24 Nov 2020.

Gabrielsen, G. W., and E. N. Smith. 1985. Physiological responses associated with feigned death in the American opossum. Acta Physiologica Scandinavica 123:393–398.

Gallo, T., M. Fidino, E. W. Lehrer, and S. B. Magle. 2017. Mammal diversity and metacommunity dynamics in urban green spaces: implications for urban wildlife conservation. Ecological Applications 27:2330–2341.

Gaynor, K. M., C. E. Hojnowski, N. H. Carter, and J. S. Brashares. 2018. The influence of human disturbance on wildlife nocturnality. Science 360:1232–1235.

Gehrt, S. D. 2004. Ecology and Management of Striped Skunks, Raccoons, and Coyotes in Urban Landscapes. Pages 81–104 *in*. People and Predators: From Conflict To Coexistence. Island Press.

Gehrt, S. D., and W. R. Clark. 2003. Raccoons, Coyotes, and Reflections on the Mesopredator Release Hypothesis. Wildlife Society Bulletin (1973-2006) 31:836–842.

Gehrt, S. D., and S. Prange. 2007. Interference competition between coyotes and raccoons: a test of the mesopredator release hypothesis. Behavioral Ecology 18:204–214.

Gehrt, S. D., S. P. D. Riley, and B. L. Cypher. 2010. Urban Carnivores: Ecology, Conflict, and Conservation. JHU Press.

Goddard, M. A., A. J. Dougill, and T. G. Benton. 2010. Scaling up from gardens: biodiversity conservation in urban environments. Trends in Ecology & Evolution 25:90–98.

Gompper, M. E. 2002. Top Carnivores in the Suburbs? Ecological and Conservation Issues Raised by Colonization of North-eastern North America by Coyotes: The expansion of the coyote's geographical range may broadly influence community structure, and rising coyote densities in the suburbs may alter how the general public views wildlife. BioScience 52:185–190.

Gosselink, T. E., T. R. Van Deelen, R. E. Warner, and M. G. Joselyn. 2003. Temporal Habitat Partitioning and Spatial Use of Coyotes and Red Foxes in East-Central Illinois. The Journal of Wildlife Management 67:90–103.

Greenspan, E., C. K. Nielsen, and K. W. Cassel. 2018. Potential distribution of coyotes (Canis latrans), Virginia opossums (Didelphis virginiana), striped skunks (Mephitis mephitis), and raccoons (Procyon lotor) in the Chicago Metropolitan Area. Urban Ecosystems 21:983–997.

Grubbs, S. E., and P. R. Krausman. 2009. Observations of Coyote-Cat Interactions. The Journal of Wildlife Management 73:683–685.

Hansen, A. J., R. L. Knight, J. M. Marzluff, S. Powell, K. Brown, P. H. Gude, and K. Jones. 2005. Effects of Exurban Development on Biodiversity: Patterns, Mechanisms, and Research Needs. Ecological Applications 15:1893–1905.

Hijmans R. J. (2020). raster: Geographic Data Analysis and Modeling. R package version 3.3-13. <https://CRAN.R-project.org/package=raster>.

Horn, J. A., N. Mateus-Pinilla, R. E. Warner, and E. J. Heske. 2011. Home range, habitat use, and activity patterns of free-roaming domestic cats. The Journal of Wildlife Management 75:1177–1185.

Jackman, J. L., and A. T. Rutberg. 2015. Shifts in Attitudes Toward Coyotes on the Urbanized East Coast: The Cape Cod Experience, 2005–2012. Human Dimensions of Wildlife 20:333–348. Routledge.

Kowalski, B., F. Watson, C. Garza, and B. Delgado. 2015. Effects of landscape covariates on the distribution and detection probabilities of mammalian carnivores. Journal of Mammalogy 96:511–521.

Lafortezza, R., G. Carrus, G. Sanesi, and C. Davies. 2009. Benefits and well-being perceived by people visiting green spaces in periods of heat stress. Urban Forestry & Urban Greening 8:97–108.

Larivière, S. 2004. Range expansion of raccoons in the Canadian prairies: review of hypotheses. Wildlife Society Bulletin 32:955–963.

Larivière, S., and F. Messier. 1996. Aposematic Behaviour in the Striped Skunk, Mephitis mephitis. Ethology 102:986–992.

Lesmeister, D. B., C. K. Nielsen, E. M. Schauber, and E. C. Hellgren. 2015. Spatial and temporal structure of a mesocarnivore guild in midwestern north America. Wildlife Monographs 191:1–61.

Leu, M., S. E. Hanser, and S. T. Knick. 2008. The human footprint in the west: a large-scale analysis of anthropogenic impacts. Ecological Applications 18:1119–1139.

Lewis, J. C., K. L. Sallee, and R. T. Golightly. 1999. Introduction and Range Expansion of Nonnative Red Foxes (Vulpes vulpes) in California. The American Midland Naturalist 142:372–381.

Lombardi, J. V., C. E. Comer, D. G. Scognamillo, and W. C. Conway. 2017. Coyote, fox, and bobcat response to anthropogenic and natural landscape features in a small urban area. Urban Ecosystems 20:1239–1248.

Longcore, T., and C. Rich. 2004. Ecological light pollution. Frontiers in Ecology and the Environment 2:191–198.

MacKenzie, D. I., and L. L. Bailey. 2004. Assessing the fit of site-occupancy models. Journal of Agricultural, Biological, and Environmental Statistics 9:300–318.

MacKenzie, D. I., J. D. Nichols, J. A. Royle, K. H. Pollock, L. Bailey, and J. E. Hines. 2017. Occupancy Estimation and Modeling: Inferring Patterns and Dynamics of Species Occurrence. Elsevier.

Magle, S. B., S. A. Poessel, K. R. Crooks, and S. W. Breck. 2014. More dogs less bite: The relationship between human–coyote conflict and prairie dog colonies in an urban landscape. Landscape and Urban Planning 127:146–153.

Markovchick-Nicholls, L., H. M. Regan, D. H. Deutschman, A. Widyanata, B. Martin, L. Noreke, and T. A. Hunt. 2008. Relationships between Human Disturbance and Wildlife Land Use in Urban Habitat Fragments. Conservation Biology 22:99–109.

Mazerolle MJ (2020). AICcmodavg: Model selection and multimodel inference based on (Q)AIC(c). R package version 2.3-1, <https://cran.r-project.org/package=AICcmodavg>.

McDonnell, M. J., and S. T. A. Pickett. 1990. Ecosystem Structure and Function along Urban-Rural Gradients: An Unexploited Opportunity for Ecology. Ecology 71:1232–1237.

McIntyre, N. E., K. Knowles-Yánez, and D. Hope. 2008. Urban Ecology as an Interdisciplinary Field: Differences in the use of "Urban" Between the Social and Natural Sciences. Pages 49–65 *in* J. M. Marzluff, E. Shulenberger, W. Endlicher, M. Alberti, G. Bradley, C. Ryan, U. Simon, and C. ZumBrunnen, editors. Urban Ecology: An International Perspective on the Interaction Between Humans and Nature. Springer US, Boston, MA. <https://doi.org/10.1007/978-0-387-73412-5_4>. Accessed 1 Nov 2018.

McKinney, M. L. 2002. Urbanization, Biodiversity, and ConservationThe impacts of urbanization on native species are poorly studied, but educating a highly urbanized human population about these impacts can greatly improve species conservation in all ecosystems. BioScience 52:883–890.

McKinney, M. L. 2006. Urbanization as a major cause of biotic homogenization. Biological Conservation 127:247–260. Urbanization.

McKinney, T., and T. W. Smith. 2007. Diets of sympatric bobcats and coyotes during years of varying rainfall in central Arizona. Western North American Naturalist 67:8–15. Monte L. Bean Life Science Museum, Brigham Young University.

Meredith, M., and M. Ridout. 2014. Overview of the overlap package. R. Proj. 1–9.

Moll, R. J., J. D. Cepek, P. D. Lorch, P. M. Dennis, E. Tans, T. Robison, J. J. Millspaugh, and R. A. Montgomery. 2019. What does urbanization actually mean? A framework for urban metrics in wildlife research. Journal of Applied Ecology 56:1289–1300.

Morey, P. S., E. M. Gese, and S. Gehrt. 2007. Spatial and Temporal Variation in the Diet of Coyotes in the Chicago Metropolitan Area. The American Midland Naturalist 158:147–161. University of Notre Dame.

Mueller, M. A., D. Drake, and M. L. Allen. 2018. Coexistence of coyotes (Canis latrans) and red foxes (Vulpes vulpes) in an urban landscape. PLOS ONE 13:e0190971.

Murray, M., M. A. Edwards, B. Abercrombie, and C. C. S. Clair. 2015. Poor health is associated with use of anthropogenic resources in an urban carnivore. Proc. R. Soc. B 282:20150009.

Nickel, B. A., J. P. Suraci, M. L. Allen, and C. C. Wilmers. 2020. Human presence and human footprint have non-equivalent effects on wildlife spatiotemporal habitat use. Biological Conservation 241:108383.

Niedballa, J., R. Sollmann, A. Courtiol, and A. Wilting. 2016. camtrapR: an R package for efficient camera trap data management. Methods in Ecology and Evolution 7:1457–1462.

Nouvellet, P., G. S. A. Rasmussen, D. W. Macdonald, and F. Courchamp. 2012. Noisy clocks and silent sunrises: measurement methods of daily activity pattern. Journal of Zoology 286:179–184.

Ordeñana, M. A., K. R. Crooks, E. E. Boydston, R. N. Fisher, L. M. Lyren, S. Siudyla, C. D. Haas, S. Harris, S. A. Hathaway, G. M. Turschak, A. K. Miles, and D. H. Van Vuren. 2010. Effects of urbanization on carnivore species distribution and richness. Journal of Mammalogy 91:1322–1331.

Parren, M. 2019. Drought and coyotes mediate the relationship between mesopredators and human disturbance in California. HSU theses and projects. <https://digitalcommons.humboldt.edu/etd/349>.

Poessel, S. A., S. W. Breck, T. L. Teel, S. Shwiff, K. R. Crooks, and L. Angeloni. 2013. Patterns of human–coyote conflicts in the Denver Metropolitan Area. The Journal of Wildlife Management 77:297–305.

Poessel, S. A., E. M. Gese, and J. K. Young. 2017. Environmental factors influencing the occurrence of coyotes and conflicts in urban areas. Landscape and Urban Planning 157:259–269.

Prange, S., and S. D. Gehrt. 2004. Changes in mesopredator-community structure in response to urbanization. Canadian Journal of Zoology 82:1804–1817.

Prange, S., S. D. Gehrt, and E. P. Wiggers. 2003. Demographic Factors Contributing to High Raccoon Densities in Urban Landscapes. The Journal of Wildlife Management 67:324.

Prange, S., S. D. Gehrt, and E. P. Wiggers. 2004. Influences of anthropogenic resources on raccoon (Procyon lotor) movements and spatial distribution. Journal of Mammalogy 85:483–490.

Price, C. J., and P. B. Banks. 2017. Habitat augmentation for introduced urban wildlife: the use of piles of railway sleepers as refuge for introduced black rats Rattus rattus. Australian Zoologist. <http://publications.rzsnsw.org.au/doi/abs/10.7882/AZ.2017.029>. Accessed 4 Sep 2018.

R Core Team (2014). R: A language and environment for statistical computing. R Foundation for Statistical Computing, Vienna, Austria. <http://www.R-project.org/>.

Ramalho, C. E., and R. J. Hobbs. 2012. Time for a change: dynamic urban ecology. Trends in Ecology & Evolution 27:179–188.

Ratnaswamy, M. J., R. J. Warren, M. T. Kramer, and M. D. Adam. 1997. Comparisons of Lethal and Nonlethal Techniques to Reduce Raccoon Depredation of Sea Turtle Nests. The Journal of Wildlife Management 61:368–376. [Wiley, Wildlife Society].

Rich, L. N., B. J. Furnas, J. S. Brashares, S. R. Beissinger, and C. A. Cordova. 2018. Evaluating mammalian diversity in the Mojave Desert and Great Valley ecoregions of California using camera trap surveys.

Richmond, O. M. W., J. E. Hines, and S. R. Beissinger. 2010. Two-species occupancy models: a new parameterization applied to co-occurrence of secretive rails. Ecological Applications 20:2036–2046.

Ridout, M. S., and M. Linkie. 2009. Estimating overlap of daily activity patterns from camera trap data. Journal of Agricultural, Biological, and Environmental Statistics 14:322–337.

Riley, S. P. D. 2006. Spatial Ecology of Bobcats and Gray Foxes in Urban and Rural Zones of a National Park. The Journal of Wildlife Management 70:1425–1435.

Rosatte, R. C., M. J. Power, and C. D. Macinnes. 1992. Density, Dispersion, Movements and Habitat Of Skunks (Mephitis mephitis) and Raccoons (Procyon Lotor) in Metropolitan Toronto. Pages 932–944 *in* D. R. McCullough and R. H. Barrett, editors. Wildlife 2001: Populations. Springer Netherlands, Dordrecht. <https://doi.org/10.1007/978-94-011-2868-1_71>. Accessed 20 Sep 2018.

Rosenzweig, M. L. 1966. Community Structure in Sympatric Carnivora. Journal of Mammalogy 47:602–612.

Roussere, G. P., W. J. Murray, C. B. Raudenbush, M. J. Kutilek, D. J. Levee, and K. R. Kazacos. 2003. Raccoon Roundworm Eggs near Homes and Risk for Larva Migrans Disease, California Communities. Emerging Infectious Diseases 9:1516–1522.

RStudio Team (2020). RStudio: Integrated Development for R. RStudio. PBC. Boston, MA <http://www.rstudio.com/>.

Šálek, M., L. Drahníková, and E. Tkadlec. 2014. Changes in home range sizes and population densities of carnivore species along the natural to urban habitat gradient: Carnivores along the natural-urban habitat gradient. Mammal Review n/a-n/a.

Santini, L., M. González-Suárez, D. Russo, A. Gonzalez-Voyer, A. von Hardenberg, and L. Ancillotto. 2019. One strategy does not fit all: determinants of urban adaptation in mammals. Ecology Letters 22:365–376.

Schell, C. J., K. Dyson, T. L. Fuentes, S. D. Roches, N. C. Harris, D. S. Miller, C. A. Woelfle-Erskine, and M. R. Lambert. 2020. The ecological and evolutionary consequences of systemic racism in urban environments. Science 369. American Association for the Advancement of Science. <https://science.sciencemag.org/content/369/6510/eaay4497>. Accessed 24 Nov 2020.

Schuette, P., A. P. Wagner, M. E. Wagner, and S. Creel. 2013. Occupancy patterns and niche partitioning within a diverse carnivore community exposed to anthropogenic pressures. Biological Conservation 158:301–312.

Shamoon, H., D. Saltz, and T. Dayan. 2017. Fine-scale temporal and spatial population fluctuations of medium sized carnivores in a Mediterranean agricultural matrix. Landscape Ecology 32:1243–1256.

Smith, J. A., A. C. Thomas, T. Levi, Y. Wang, and C. C. Wilmers. 2018. Human activity reduces niche partitioning among three widespread mesocarnivores. Oikos 127:890–901.

Soulard, C. E., and T. S. Wilson. 2015. Recent land-use/land-cover change in the Central California Valley. <https://pubag.nal.usda.gov/catalog/1229956>. Accessed 11 Nov 2020.

Stieger, C., D. Hegglin, G. Schwarzenbach, A. Mathis, and P. Deplazes. 2002. Spatial and temporal aspects of urban transmission of Echinococcus multilocularis. Parasitology 124:631–640.

Theimer, T. C., A. C. Clayton, A. Martinez, D. L. Peterson, and D. L. Bergman. 2015. Visitation rate and behavior of urban mesocarnivores differs in the presence of two common anthropogenic food sources. Urban Ecosystems 18:895–906.

Tigas, L. A., D. H. Van Vuren, and R. M. Sauvajot. 2002. Behavioral responses of bobcats and coyotes to habitat fragmentation and corridors in an urban environment. Biological Conservation 108:299–306.

Treves, A., and K. U. Karanth. 2003. Human-Carnivore Conflict and Perspectives on Carnivore Management Worldwide. Conservation Biology 17:1491–1499.

Troyer, E. M., S. E. C. Devitt, M. E. Sunquist, V. R. Goswami, and M. K. Oli. 2014. Survival, Recruitment, and Population Growth Rate of an Important Mesopredator: The Northern Raccoon. PLOS ONE 9:e98535. Public Library of Science.

Tylianakis, J. M., R. K. Didham, J. Bascompte, and D. A. Wardle. 2008. Global change and species interactions in terrestrial ecosystems. Ecology Letters 11:1351–1363.

U.S. Census Bureau (2019). City and Town Population Totals: 2010-2019. <https://www.census.gov/data/tables/time-series/demo/popest/2010s-total-cities-and-towns.html>. Accessed 28 Nov 2020.

Van den Berg, M., W. Wendel-Vos, M. van Poppel, H. Kemper, W. van Mechelen, and J. Maas. 2015. Health benefits of green spaces in the living environment: A systematic review of epidemiological studies. Urban Forestry & Urban Greening 14:806–816.

Venter, O., E. W. Sanderson, A. Magrach, J. R. Allan, J. Beher, K. R. Jones, H. P. Possingham, W. F. Laurance, P. Wood, B. M. Fekete, M. A. Levy, and J. E. M. Watson. 2016. Sixteen years of change in the global terrestrial human footprint and implications for biodiversity conservation. Nature Communications 7:12558.

Wang, Y., M. L. Allen, and C. C. Wilmers. 2015. Mesopredator spatial and temporal responses to large predators and human development in the Santa Cruz Mountains of California. Biological Conservation 190:23–33.

Wassmer, R. W. 2000. Urban Sprawl in a U.S. Metropolitan Area: Ways to Measure and a Comparison of the Sacramento Area to Similar Metropolitan Areas in California and the U.S. SSRN Scholarly Paper, Social Science Research Network,

Rochester, NY. <https://papers.ssrn.com/abstract=241975>. Accessed 22 Oct 2018.

Welch, R. J., S. Périquet, M. B. Petelle, and A. le Roux. 2017. Hunter or hunted? Perceptions of risk and reward in a small mesopredator. Journal of Mammalogy 98:1531–1537. Oxford Academic.

White, L. A., and S. D. Gehrt. 2009. Coyote Attacks on Humans in the United States and Canada. Human Dimensions of Wildlife 14:419–432. Routledge.

Appendix E

Appendix E. Camera placement between residential backyards (top left), residential front yards (top right), and urban (bottom left) and non-urban (bottom right) greenspaces in California's Central Valley and the Sacramento Metropolitan Area. Urban camera placement varied in height, attachment object (e.g. tree or fencepost), direction, and angle to reduce chances of vandalism, maximize resident privacy, and was limited by available attachment areas.

Appendix F

Appendix F. Covariates by urban intensity groups and Pearson correlation values for single-season single species and single-season two-species occupancy modeling.

Covariates across urban intensity groups. Camera placement (backyard, front yard, and greenspace) values are calculated from the number of camera sites that were considered backyard, front yard, or greenspace cameras. Average building density values are based on the average number of buildings/km^2 at a camera site within a 500 m kernel density search radius within a 500 m buffer size. Average imperviousness values are based on the average imperviousness coefficient/km^2 at a camera site within a 500 m buffer.

Urban Intensity	Backyard	Front yard	Greenspace	Avg. Building Density	Avg. Imperviousness
Non-urban (n = 60)	3	1	56	0.43	1.38
Low Intensity Urban (n = 16)	3	2	11	11.12	37.36
High Intensity Urban (n = 34)	19	9	6	24.07	61.19

Pearson correlation coefficients for detection covariates for single-season single species and two-species occupancy modeling. Building density is represented at the 500 m kernel density search radius and 500 m buffer scale and imperviousness is represented by the 500 m buffer scale. Pearson coefficient (r) values ≥ |0.70| are considered moderately correlated, and values ≥ |0.90| are considered highly correlated. *Building density and imperviousness, while highly correlated, were included for both modeling analyzes as they capture different types of urban intensity.

	Building Density	Imperviousness	Date	Backyard	Front yard	Greenspace	Food
Building Density		0.91*	-0.15	0.5	0.47	-0.75	0.33
Imperviousness			-0.07	0.5	0.38	-0.69	0.31
Date				0.02	-0.09	0.04	-0.1
Backyard					-0.19	-0.76	0.23
Front yard						-0.49	0.05
Greenspace							-0.24
Food							

Appendix G

Appendix G. Top single-season single species occupancy models for coyotes, raccoons, opossums, striped skunks, and domestic cats in California's Central Valley and Sacramento Metropolitan Area.

Top single species occupancy models for all species. Akaike's information criterion corrected for small sample sizes (AICc) is used for model selection for candidate model sets. Columns included for each model are AICc, change in AICc from the top model (Δ AICc), AICc weights (AICcWt), cumulative weights (Cum.Wt), and log-likelihood (LL). The top 10 models from each species candidate model set are included, as well as the global model for comparison. The top model used for model interpretation, highlighted in gray, is within the top 2 Δ AICc, has the least amount of uninformative beta estimates for all covariates, and is the most conservative (most parameterized). Goodness of fit testing is reported as the overdispersion parameter (c-hat) value given for 2000 bootstrap samples for the global model. If c-hat is greater than 1, QAICc is used to correct for overdispersion, otherwise a c-hat of 1 is used for models with c-hat's under 1.

Occupancy (psi or ψ) covariates used for modeling include **build –** building density at four kernel density search radii (100, 200, 500, and 1000 m) and at four buffer sizes (500, 1000, 2000, and 5000 m radii buffers); and **imperv** – imperviousness at four buffer sizes (500, 1000, 2000, and 5000 m radii). Detection (p) covariates include the top **build** and **imperv** combinations found for occupancy; camera **placement (**three factor levels, represented by the camera being placed either in a resident's backyard, front yard, or in a greenspace); Julian **date**; whether anthropogenic **food** was available at a site; **bait** age; a lag effect for whether a species was detected within the last 3 days if needed to improve goodness of fit (e.g. **opo3** for opossum); whether a coyote was detected after 1, 2, or 3 days (e.g. **coy3**); whether a human was detected after 1, 2 and 3 days (e.g. **hum2**); the interaction between human temporal activity and building density (e.g. **hum2*build**), as well as imperviousness (e.g. **hum2*imperv**)

Top single species occupancy models for coyotes. A total of 40 models were used to find the best combination of occupancy and detection covariates informing coyote spatial and temporal activity. The top model used for interpretation is highlighted in gray. The global model is ψ(build[200m; 500m buffer] + imperv[500m]) p(placement + food + bait + date + hum2 + build[200m; 500m buffer] + imperv[500m] + hum2*imperv[500m] + hum2* build[200m; 500m buffer]). The overdispersion parameter, c-hat, is 1.06.

Model	K	AICc	Δ AICc	AICc.Wt	Cum.Wt	LL
ψ(build[200m; 500m buffer]) p(placement + bait + date + hum2)	9	435.86	0	0.66	0.66	-208.03
ψ(build[200m; 500m buffer]) p(placement + date + hum2)	8	439.08	3.22	0.13	0.8	-210.83
ψ(build[200m; 500m buffer]) p(placement + date + hum1)	8	440.05	4.19	0.08	0.88	-211.31
ψ(build[200m; 500m buffer]) p(placement + date)	7	441.87	6.01	0.03	0.91	-213.39
ψ(build[200m; 500m buffer]) p(placement + date + hum2 + build[200m; 500m buffer] + hum*build[200m; 500m buffer])	10	442.98	7.12	0.02	0.93	-210.38
ψ(build[200m; 500m buffer]) p(placement + date + imperv[500m])	8	443.85	7.99	0.01	0.94	-213.21

Model	K	AICc	Δ AICc	AICc.Wt	Cum.Wt	LL
ψ(build[200m; 500m buffer]) p(placement +date + hum3)	8	444.00	8.13	0.01	0.95	-213.29
ψ(build[200m; 500m buffer]) p(placement + date + build[200m; 500m buffer])	8	444.15	8.29	0.01	0.96	-213.36
ψ(build[200m; 500m buffer]) p(placement + date + hum2 + build[200m; 500m buffer]+ imperv[500m] + hum2*imperv[500m])	11	444.17	8.3	0.01	0.97	-209.74
ψ(build[200m; 500m buffer]) p(placement + food + bait + date)	9	444.54	8.67	0.01	0.98	-212.37
Global Model	15	445.2	9.34	0.01	0.99	-205.05

Top single species occupancy models for raccoons. A total of 48 models were used to find the best combination of occupancy and detection covariates informing raccoon spatial and temporal activity. The top model used for interpretation is highlighted in gray. The global model is ψ(build[500m; 500m buffer] + imperv[500m]) p(placement + food + bait + date + coy2+ hum1 + build[500m; 500m buffer] + imperv[500m] + hum1*imperv[500m] + hum1* build[500m; 500m buffer]). The overdispersion parameter, c-hat, is 0.71.

Model	K	AICc	Δ AICc	AICc.Wt	Cum.Wt	LL
ψ(build[500m; 500m buffer]) p(placement + bait + date + build[500m; 500m buffer] + imperv[500m])	9	651.00	0	0.34	0.34	-315.6
ψ(build[500m; 500m buffer]) p(placement + date + build[500m; 500m buffer] + imperv[500m])	8	651.69	0.69	0.24	0.58	-317.13
ψ(build[500m; 500m buffer]) p(placement + date + hum1 + build[500m; 500m buffer] + imperv[500m])	9	652.64	1.65	0.15	0.73	-316.42
ψ(build[500m; 500m buffer]) p(placement + date + coy2 + hum1 + build[500m; 500m buffer]+imperv[500m])	9	653.28	2.29	0.11	0.84	-316.74

Model	K	AICc	Δ AICc	AICc.Wt	Cum.Wt	LL
ψ(build[500m; 500m buffer]) p(placement + date + coy2 + hum1+ build[500m; 500m buffer] + imperv[500m] + hum1*imperv[500m])	10	654.27	3.27	0.07	0.91	-316.02
ψ(build[500m; 500m buffer]) p(placement + date + coy2 + hum1+ build[500m; 500m buffer]+ imperv[500m] + hum1* build[500m; 500m buffer])	11	656.49	5.5	0.02	0.93	-315.9
Global Model	11	656.6	5.61	0.02	0.95	-315.95
ψ(build[500m; 500m buffer]) p(placement + date + coy2 + hum1+ build[500m; 500m buffer]+ imperv[500m] + hum1* build[500m; 500m buffer] + hum1*imperv[500m])	15	657.72	6.73	0.01	0.96	-311.31
ψ(build[500m; 500m buffer]) p(placement + date)	12	658.91	7.92	0.01	0.97	-315.85
ψ(build[500m; 500m buffer]) p(placement + date + coy2)	6	659.69	8.69	0	0.97	-323.44

Model	K	AICc	Δ AICc	AICc.Wt	Cum.Wt	LL
ψ(build[500m; 500m buffer]) p(placement + date + hum1 + build[500m; 500m buffer] + imperv[500m])	7	659.99	9	0	0.98	-322.45

Top single species occupancy models for opossums. A total of 48 models were used to find the best combination of occupancy and detection covariates informing opossum spatial and temporal activity. The detection covariate **opo3** was used as a lag effect for opossums appearing within the last 3 days. The top model used for interpretation is highlighted in gray. The global model is ψ(build[100m; 1000m buffer] + imperv[5000m]) p(placement + food + date + coy1+ hum3 + opo3 + build[100m; 1000m buffer] + imperv[5000m] + hum3*imperv[5000m] + hum3* build[100m; 1000m buffer]). The overdispersion parameter, c-hat, is 0.86.

Model	K	AICc	Δ AICc	AICc.Wt	Cum.Wt	LL
ψ(.) p(date + bait + hum3 + opo3 + build[100m; 1000m buffer] + hum3* build[100m; 1000m buffer])	9	337.49	0	0.22	0.22	-158.85
ψ(.) p(date + coy1 + hum3 + opo3 + build[100m; 1000m buffer] + hum3* build[100m; 1000m buffer])	9	337.57	0.07	0.21	0.42	-158.88
ψ(.) p(date + hum3 + opo3 + build[100m; 1000m buffer] + hum3* build[100m; 1000m buffer])	8	337.99	0.5	0.17	0.59	-160.28
ψ(.) p(date + coy1 + hum3 + opo3 + build[100m; 1000m buffer] + hum3* build[100m; 1000m buffer])	10	339.99	2.49	0.06	0.65	-158.88

Model	K	AICc	Δ AICc	AICc.Wt	Cum.Wt	LL
ψ(.) p(date + hum2 + opo3)	6	340.59	3.1	0.05	0.7	-163.89
ψ(.) p(date + bait + coy1 + hum3 + opo3)	8	340.8	3.31	0.04	0.74	-161.69
ψ(.) p(date + coy1 + hum3 + opo3)	7	341.29	3.79	0.03	0.77	-163.09
ψ(.) p(date + hum3 + opo3)	6	341.59	4.1	0.03	0.8	-164.39
ψ(.) p(date + hum3 + opo3 + imperv[5000m] + hum3*imperv[5000m])	8	341.8	4.31	0.03	0.83	-162.19
ψ(.) p(bait + opo3)	5	342.28	4.79	0.02	0.85	-165.85
Global Model	17	354	16.51	0	1	-156.67

Top single species occupancy models for skunks. A total of 48 models were used to find the best combination of occupancy and detection covariates informing skunk spatial and temporal activity. The top model used for interpretation is highlighted in gray. The global model is ψ(build[200m; 500m buffer] + imperv[500m]) p(placement + food + bait + date + coy1+ hum1 + build[200m; 500m buffer] + imperv[500m] + hum1*imperv[500m] + hum1* build[200m; 500m buffer]). The overdispersion parameter, c-hat, is 1.39.

Model	K	AICc	Δ AICc	AICc.Wt	Cum.Wt	LL
ψ(build[200m; 500m buffer]) p(date + build[200m; 500m buffer] + imperv[500m])	7	429.87	0	0.21	0.21	-207.39
ψ(build[200m; 500m buffer]) p(date + hum1 + build[200m; 500m buffer] + imperv[500m])	8	430.67	0.8	0.14	0.36	-206.62
ψ(build[200m; 500m buffer]) p(placement + date + build[200m; 500m buffer] + imperv[500m])	9	431.66	1.79	0.09	0.44	-205.93
ψ(build[200m; 500m buffer]) p(date + hum1 + build[200m; 500m buffer] + imperv[500m] + hum1* build[200m; 500m buffer] + hum1* imperv[500m])	10	432.81	2.94	0.05	0.49	-205.29

Model	K	AICc	Δ AICc	AICc.Wt	Cum.Wt	LL
ψ(build[200m; 500m buffer]) p(date)	5	433.6	3.73	0.03	0.53	-211.51
ψ(build[200m; 500m buffer]) p(placement + date)	7	433.91	4.04	0.03	0.55	-209.4
ψ(build[200m; 500m buffer]) p(food + date)	6	434.13	4.26	0.03	0.58	-210.66
ψ(build[200m; 500m buffer]) p(date + hum1)	6	434.49	4.62	0.02	0.6	-210.84
ψ(build[200m; 500m buffer]) p(.)	4	434.5	4.63	0.02	0.62	-213.06
ψ(build[500m; 500m buffer]) p(.)	4	434.51	4.64	0.02	0.64	-213.06
Global Model	16	445.13	15.26	0	1	-203.64

Top single species occupancy models for domestic cats. A total of 48 models were used to find the best combination of occupancy and detection covariates informing domestic cat spatial and temporal activity. The top model used for interpretation is highlighted in gray. The global model is ψ(build[500m; 500m buffer] + imperv[500m]) p(placement + food + bait + date + coy2+ hum1 + build[500m; 500m buffer] + imperv[500m] + hum1*imperv[500m] + hum1* build[500m; 500m buffer]). The overdispersion parameter, c-hat, is 0.75.

Model	K	AICc	Δ AICc	AICc.Wt	Cum.Wt	LL
ψ(imperv[500m]) p(placement + food + bait + hum1 + build[500m; 500m buffer])	9	847.63	0	0.27	0.27	-413.91
ψ(imperv[500m]) p(placement + food + date + bait + hum1 + build[500m; 500m buffer])	10	847.84	0.21	0.24	0.51	-412.81
ψ(imperv[500m]) p(placement + food + bait + hum1 + build[500m; 500m buffer]+ hum1* build[500m; 500m buffer])	10	848.4	0.78	0.18	0.7	-413.09
ψ(imperv[500m]) p(placement + food + bait + hum1 + build[500m; 500m buffer]+ imperv[500m])	10	849.3	1.67	0.12	0.82	-413.54
ψ(imperv[500m]) p(placement + food + bait + hum1 + imperv[500m])	9	850.77	3.14	0.06	0.87	-415.48

Model	K	AICc	Δ AICc	AICc.Wt	Cum.Wt	LL
ψ(build[500m; 500m buffer] + imperv[500m]) p(placement + food + bait + hum1 + coy2 + build[500m; 500m buffer]+ imperv[500m])	11	850.95	3.32	0.05	0.92	-413.13
ψ(imperv[500m]) p(placement + food + bait + hum1 + imperv[500m] + hum1*imperv[500m])	10	851.13	3.5	0.05	0.97	-414.45
ψ(imperv[500m]) p(placement + food + bait + hum1 + imperv[500m] + build[500m; 500m buffer] + hum1*imperv[500m] + hum1*build[500m; 500m buffer])	12	852.31	4.69	0.03	1	-412.55
Global Model	15	856.36	8.74	0	1	-410.63
ψ(imperv[500m]) p(placement + food + bait + hum1)	8	866.02	18.39	0	1	-424.3
ψ(imperv[500m]) p(placement + food + bait + coy2 + hum1)	9	868.00	20.38	0	1	-424.1

Appendix H

Appendix H. Top single-season two species conditional detection and occupancy models for coyote-mesopredator pairs (coyote-raccoon, coyote-opossum, coyote-skunk, and coyote-cat) in California's Central Valley and Sacramento Metropolitan Area.

Candidate model sets were created using two-species conditional modeling in program PRESENCE (Hines 2006). Akaike's information criterion corrected for small sample sizes (AICc) is used for model selection for candidate model sets. Columns included for each model are AICc, change in AICc from the top model (Δ AICc), AICc weights (AICcWt), cumulative weights (Cum.Wt), and log-likelihood (LL). Top detection model covariates and conditional configuration were used to inform top occupancy model. The top model used for model interpretation, highlighted in gray, is within the top 2 Δ AICc, has the least amount of uninformative beta estimates for all covariates, and is the most conservative (most parameterized). Goodness of fit testing is currently unavailable for two-species occupancy modeling, so goodness of fit is assumed based off of single-season single-species occupancy modeling for both species.

Occupancy and detection covariates for two-species occupancy modeling are the same as those used for single-species models. Coyote detection covariates (pA) are the same for all detection and occupancy models. Occupancy (psi or ψ) covariates used for modeling include **build –** building density at four kernel density search radii (100, 200, 500, and 1000 m) and at four buffer sizes (500, 1,000, 2,000, and 5,000 m radii buffers); and **imperv** – imperviousness at four buffer sizes (500, 1000, 2000, and 5000 m radii). Detection (p) covariates include the top **build** and **imperv** combinations found for occupancy; camera **placement (**three factor levels, represented by the camera being placed either in a resident's backyard, frontyard, or in a greenspace); Julian **date**; whether anthropogenic **food** was available at a site; **bait** age; a lag effect for whether a species was detected within the last 3 days if needed to improve goodness of fit (e.g. **opo3** for opossum); whether a coyote was detected after 1, 2, or 3 days (e.g. **coy3**); whether a human was detected after 1, 2 and 3 days (e.g. **hum2**); the interaction between human temporal activity and building density (e.g. **hum2*build**), as well as imperviousness (e.g. **hum2*imperv).**

Coyote-raccoon:

Candidate model set for coyote and raccoon two-species conditional detection models. Top detection model is highlighted in gray. Global model for raccoon detection is pB(placement + date + bait + build[500m; 500m buffer] + imperv[500m buffer]), rBA(.), rBa(.).

Detection Models	K	AICc	Δ AICc	AICc.Wt	Model Likelihood	LL
ψA(.), ψBA(.), ψBa(.), pA(coy) = rA, pB(date+build), rBA(.), rBa(.)	13	1140.86	0	0.6706	1	1111.07
ψA(.), ψBA(.), ψBa(.), pA(coy) = rA, pB(placement+date+build), rBA(.), rBa(.)	14	1143.49	2.63	0.18	0.2685	1111.07
ψA(.), ψBA(.), ψBa(.), pA(coy) = rA, pB(placement+date+build+imperv), rBA(.), rBa(.)	15	1146.12	5.26	0.0483	0.0721	1111.01
ψA(.), ψBA(.), ψBa(.), pA(coy) = rA, pB(date+build), rBA(.) = rBa(.)	12	1146.16	5.3	0.0474	0.0707	1118.94
ψA(.), ψBA(.), ψBa(.), pA(coy) = rA, pB(date+build) = rBA(.) = rBa(.)	11	1147.37	6.51	0.0259	0.0386	1122.68
ψA(.), ψBA(.), ψBa(.), pA(coy) = rA, pB(date+build+imperv), rBA(.), rBa(.)	14	1148.17	7.31	0.0173	0.0259	1115.75
ψA(.), ψBA(.), ψBa(.), pA(coy) = rA, pB(placement+date+imperv), rBA(.), rBa(.)	14	1150.31	9.45	0.0059	0.0089	1117.89

Detection Models	K	AICc	Δ AICc	AICc.Wt	Model Likelihood	LL
ψA(.), ψBA(.), ψBa(.), pA(coy) = rA, pB(global), rBA(.), rBa(.)	16	1150.87	10.01	0.0045	0.0067	1113.02
ψA, ψBA, ψBa, pA, pB, rA, rBA, rBa	8	1165.72	24.86	0	0	1148.29

Candidate model set for coyote and raccoon two-species conditional occupancy models. Top occupancy model is highlighted in gray. Top model for raccoon detection is pB(date + build[500m; 500m buffer]), rBA(.), rBa(.).

Occupancy Models	K	AICc	Δ AICc	AICc.Wt	Model Likelihood	LL
ψA(build200_500), ψBA = ψBa(build500_500), pA(coy) = rA, pB(date+build), rBA(.), rBa(.)	14	1124.48	0	0.5084	1	1092.06
ψA(build200_500), ψBA(.), ψBa(build500_500), pA(coy) = rA, pB(date+build), rBA(.), rBa(.)	15	1124.59	0.11	0.4812	0.9465	1089.48
ψA(build200_500), ψBA(.) = ψBa(.), pA(coy) = rA, pB(date+build), rBA(.), rBa(.)	13	1133.23	8.75	0.0064	0.0126	1103.44
ψA(build200_500), ψBA(.), ψBa(.), pA(coy) = rA, pB(date+build), rBA(.), rBa(.)	14	1135.44	10.96	0.0021	0.0042	1103.02

Occupancy Models	K	AICc	Δ AICc	AICc.Wt	Model Likelihood	LL
ψA(build200_500), ψBA(build500_500), ψBa(.), pA(coy) = rA, pB(date+build), rBA(.), rBa(.)	15	1136.59	12.11	0.0012	0.0023	1101.48
ψA(build200_500), ψBA(build500_500), ψBa(build500_500), pA(coy) = rA, pB(date+build), rBA(.), rBa(.)	16	1138.4	13.92	0.0005	0.0009	1100.55
ψA(.), ψBA(.), ψBa(.), pA(coy) = rA, pB(date+build), rBA(.), rBa(.)	13	1140.86	16.38	0.0001	0.0003	1111.07

Coyote-opossum:

Candidate model set for coyote and opossum two-species conditional detection models. Top detection model is highlighted in gray. Top model for opossum detection is pB(date + bait + opo3 + hum3 + build[100m; 1000m buffer] + hum3*build[100m; 1000m buffer]) = rBA(.) = rBa(.).

Detection Models	K	AICc	Δ AICc	AICc.Wt	Model Likelihood	LL
ψA(.), ψBA(.), ψBa(.), pA(coy) = rA, pB(opo3+hum3:build) = rBA(.) = rBa(.)	13	826.96	0	1	1	797.17
ψA(.), ψBA(.), ψBa(.), pA(coy) = rA, pB(opo3+hum3:build), rBA(.) = rBa(.)	14	925.16	98.2	0	0	892.74
ψA(.), ψBA(.), ψBa(.), pA(coy) = rA, pB(opo3+hum3:build), rBA(.), rBa(.)	15	927.73	100.77	0	0	892.62
ψA(.), ψBA(.), ψBa(.), pA(coy) = rA, pB(date+opo3+hum3:build), rBA(.), rBa(.)	16	929.7	102.74	0	0	891.85
ψA(.), ψBA(.), ψBa(.), pA(coy) = rA, pB(global), rBA(.), rBa(.)	17	930.41	103.45	0	0	889.76
ψA(.), ψBA(.), ψBa(.); pA(coy) = rA, pB(opo3+hum3+build), rBA(.), rBa(.)	14	931.07	104.11	0	0	898.65
ψA, ψBA, ψBa, pA, pB, rA, rBA, rBa	8	1209.34	382.38	0	0	1191.91

Candidate model set for coyote and opossum two-species conditional occupancy models. Top occupancy model is highlighted in gray. Global model for opossum detection is pB(opo3 + hum3 + build[100m; 1000m buffer]+hum3*build), rBA(.), rBa(.).

Occupancy Models	K	AICc	Δ AICc	AICc.Wt	Model Likelihood	LL
ψA(build200_500), ψBA(.) = ψBa(.), pA(coy) = rA, pB(opo3+hum3:build) = rBA(.) = rBa(.)	13	810.45	0	0.7099	1	780.66
ψA(build200_500), ψBA(.), ψBa(.), pA(coy) = rA, pB(opo3+hum3:build) = rBA(.) = rBa(.)	14	813.08	2.63	0.1906	0.2685	780.66
ψA(build200_500), ψBA(.), ψBa(build100_1000), pA(coy) = rA, pB(opo3+hum3:build) = rBA(.) = rBa(.)	15	815.77	5.32	0.0497	0.0699	780.66
ψA(build200_500), ψBA(build100_1000), ψBa(.), pA(coy) = rA, pB(opo3+hum3:build) = rBA(.) = rBa(.)	15	815.77	5.32	0.0497	0.0699	780.66
ψA(.), ψBA(.), ψBa(.), pA(coy) = rA, pB(opo3+hum3:build) = rBA(.) = rBa(.)	13	826.96	16.51	0.0002	0.0003	797.17

Coyote-skunk:

Candidate model set for coyote and striped skunk two-species conditional detection models. Top detection model is highlighted in gray. Global model for skunk detection is pB(placement + date + imperv[500m buffer] + build[200m; 500m buffer]), rBA(.), rBa(.).

Detection Models	K	AICc	Δ AICc	AICc.Wt	Model Likelihood	LL
ψA(.), ψBA(.), ψBa(.), pA(coy) = rA, pB(date+build+imperv) = rBA(.) = rBa(.)	12	1073.61	0	0.7904	1	1046.39
ψA(.), ψBA(.), ψBa(.), pA(coy) = rA, pB(date+build+imperv), rBA(.) = rBa(.)	13	1078.04	4.43	0.0863	0.1092	1048.25
ψA(.), ψBA(.), ψBa(.), pA(coy) = rA, pB(date+build+imperv), rBA(.), rBa(.)	14	1078.44	4.83	0.0706	0.0894	1046.02
ψA(.), ψBA(.), ψBa(.), pA(coy) = rA, pB(build+imperv), rBA(.), rBa(.)	13	1080.54	6.93	0.0247	0.0313	1050.75
ψA(.), ψBA(.), ψBa(.), pA(coy) = rA, pB(date+build), rBA(.), rBa(.)	13	1081.12	7.51	0.0185	0.0234	1051.33
ψA(.), ψBA(.), ψBa(.), pA(coy) = rA, pB(date+imperv), rBA(.), rBa(.)	13	1082.47	8.86	0.0094	0.0119	1052.68
ψA(.), ψBA(.), ψBa(.), pA(coy) = rA, pB(placement+build+imperv), rBA(.), rBa(.)	14	1105.74	32.13	0	0	1073.32

Detection Models	K	AICc	Δ AICc	AICc.Wt	Model Likelihood	LL
ψA, ψBA, ψBa, pA, pB, rA, rBA, rBa	8	1109.21	35.6	0	0	1091.78
ψA(.), ψBA(.), ψBa(.); pA(coy) = rA, pB(placement+date+build), rBA(.), rBa(.)	14	1125.79	52.18	0	0	1093.37
ψA(.), ψBA(.), ψBa(.); pA(coy) = rA, pB(placement+date+imperv), rBA(.), rBa(.)	14	1126.82	53.21	0	0	1094.4
ψA(.), ψBA(.), ψBa(.); pA(coy) = rA, pB(global), rBA(.), rBa(.)	15	1127.53	53.92	0	0	1092.42

Candidate model set for coyote and striped skunk two-species conditional occupancy models. Top occupancy model is highlighted in gray. Top model for skunk detection is pB(date + imperv[500m buffer] + build[200m; 500m buffer]) = rBA(.) = rBa(.).

Occupancy Models	K	AICc	Δ AICc	AICc.Wt	Model Likelihood	LL
ψA(build), ψBA(build) = ψBa(build); pA(coy) = rA, pB(date+build+imperv) = rBA(.) = rBa(.)	13	1056.94	0	0.3347	1	1027.15
ψA(build), ψBA(.), ψBa(build); pA(coy) = rA, pB(date+build+imperv) = rBA(.) = rBa(.)	14	1057.06	0.12	0.3153	0.9418	1024.64

Occupancy Models	K	AICc	Δ AICc	AICc.Wt	Model Likelihood	LL
ψA(build), ψBA(.) = ψBa(.); pA(coy) = rA, pB(date+build+imperv) = rBA(.) = rBa(.)	12	1058.77	1.83	0.1341	0.4005	1031.55
ψA(build), ψBA(.), ψBa(.); pA(coy) = rA, pB(date+build+imperv) = rBA(.) = rBa(.)	13	1059.09	2.15	0.1142	0.3413	1029.3
ψA(build), ψBA(build), ψBa(build); pA(coy) = rA, pB(date+build+imperv) = rBA(.) = rBa(.)	15	1059.33	2.39	0.1013	0.3027	1024.22
ψA(.), ψBA(.), ψBa(build); pA(coy) = rA, pB(date+build+imperv) = rBA(.) = rBa(.)	13	1071.72	14.78	0.0002	0.0006	1041.93
ψA(.), ψBA(.), ψBa(.); pA(coy) = rA, pB(date+build+imperv) = rBA(.) = rBa(.)	12	1073.61	16.67	0.0001	0.0002	1046.39
ψA(.), ψBA(build), ψBa(build); pA(coy) = rA, pB(date+build+imperv) = rBA(.) = rBa(.)	14	1074.31	17.37	0.0001	0.0002	1041.89

Coyote-cat:

Candidate model set for coyote and domestic cat two-species conditional detection models. Top detection model is highlighted in gray. Global model for cat detection is pB(placement + food + bait + hum1 + build[500m; 500m buffer] + hum1*build) [500m; 500m buffer], rBA(.), rBa(.).

Detection Models	K	AICc	Δ AICc	AICc.Wt	Model Likelihood	LL
ψA(.), ψBA(.), ψBa(.), pA(coy) = rA, pB(place+food+bait+hum1+build), rBA(.), rBa(.)	16	1358.39	0	0.7385	1	1320.54
ψA(.), ψBA(.), ψBa(.), pA(coy) = rA, pB(global), rBA(.), rBa(.)	17	1361.16	2.77	0.1849	0.2503	1320.51
ψA(.), ψBA(.), ψBa(.), pA(coy) = rA, pB(place+food+bait+hum1+build) = rBA(.) = rBa(.)	14	1363.02	4.63	0.0729	0.0988	1330.6
ψA(.), ψBA(.), ψBa(.), pA(coy) = rA, pB(place+food+hum1+build), rBA(.), rBa(.)	15	1368.97	10.58	0.0037	0.005	1333.86
ψA(.), ψBA(.), ψBa(.), pA(coy) = rA, pB(food+bait+hum1+build), rBA(.), rBa(.)	15	1397.2	38.81	0	0	1362.09
ψA(.), ψBA(.), ψBa(.), pA(coy) = rA, pB(place+food+bait+build), rBA(.), rBa(.)	15	1397.74	39.35	0	0	1362.63
ψA(.), ψBA(.), ψBa(.), pA(coy) = rA, pB(place+bait+hum1+build), rBA(.), rBa(.)	15	1397.91	39.52	0	0	1362.8

Detection Models	K	AICc	Δ AICc	AICc.Wt	Model Likelihood	LL
ψA(.), ψBA(.), ψBa(.), pA(coy) = rA, pB(place+food+bait+hum1+build), rBA(.) = rBa(.)	15	1397.98	39.59	0	0	1362.87
ψA, ψBA, ψBa, pA, pB, rA, rBA, rBa	8	1398.52	40.13	0	0	1381.09
ψA(.), ψBA(.), ψBa(.), pA(coy) = rA, pB(place+food+bait+hum1), rBA(.), rBa(.)	15	1401.58	43.19	0	0	1366.47

Candidate model set for coyote and domestic cat two-species conditional occupancy models. Top occupancy model is highlighted in gray. Top model for cat detection is pB(placement + food + bait + hum1 + build[500m; 500m buffer]), rBA(.), rBa(.).

Occupancy Models	K	AICc	Δ AICc	AICc.Wt	Model Likelihood	LL
ψA(build), ψBA(imperv) = ψBa(.), pA(coy) = rA, pB(place+food+bait+hum1+build), rBA(.), rBa(.)	17	1323.55	0	0.853	1	1282.9
ψA(build), ψBA(build), ψBa(imperv), pA(coy) = rA, pB(place+food+bait+hum1+build), rBA(.), rBa(.)	19	1327.07	3.52	0.1468	0.172	1280.63
ψA(build), ψBA(.), ψBa(imperv), pA(coy) = rA,	18	1340.22	16.67	0.0002	0.0002	1296.7

Occupancy Models	K	AICc	Δ AICc	AICc.Wt	Model Likelihood	LL
pB(place+food+bait+hum1+build), rBA(.), rBa(.)						
ψA(build), ψBA(.), ψBa(.), pA(coy) = rA, pB(place+food+bait+hum1+build), rBA(.), rBa(.)	17	1356.69	33.14	0	0	1316.04
ψA(build), ψBA(imperv), ψBa(imperv500), pA(coy) = rA, pB(place+food+bait+hum1+build), rBA(.), rBa(.)	19	1358.39	34.84	0	0	1311.95
ψA(.), ψBA(.), ψBa(.), pA(coy) = rA, pB(place+food+bait+hum1+build), rBA(.), rBa(.)	16	1358.39	34.84	0	0	1320.54
ψA(.), ψBA(build), ψBa(imperv), pA(coy) = rA, pB(place+food+bait+hum1+build), rBA(.), rBa(.)	18	1358.76	35.21	0	0	1315.24
ψA(build), ψBA(.) = ψBa(.), pA(coy) = rA, pB(place+food+bait+hum1+build), rBA(.), rBa(.)	16	1362.22	38.67	0	0	1324.37
ψA(build), ψBA(build) = ψBa(.), pA(coy) = rA, pB(place+food+bait+hum1+build), rBA(.), rBa(.)	17	1366.82	43.27	0	0	1326.17

Occupancy Models	K	AICc	Δ AICc	AICc.Wt	Model Likelihood	LL
ψA(build), ψBA(build), ψBa(.), pA(coy) = rA, pB(place+food+bait+hum1+build), rBA(.), rBa(.)	18	1372.72	49.17	0	0	1329.2

Appendix I

Appendix I. Temporal activity patterns for species across urban intensity groups (non-urban, low intensity urban, high intensity urban). Plots are scaled from a 24-hour clock to sun-time to account for daylight from sunrise to sunset. Rug at the bottom of the plots indicate when species were detected.